UCLouvain

epl

École polytechnique de Louvain

Control strategies on islanded low-voltage microgrids

Master/slave & droop control: study and comparison

Authors: **Gaetan Dujardin, Félix Lambilliotte**
Supervisor: **Emmanuel De Jaeger**
Readers: **Bruno Dehez, Henri Laloyaux**
Academic year 2018–2019
Master [120] in Electro-mechanical Engineering

Abstract

Distributed generation appears as the eco-friendly[1] solution to a growing demand of electricity. Within the same idea, microgrids have become one of the most attractive sources of attention since they integrate local supply sources both with cleanliness and robustness.
These microgrids can operate either connected to the utility grid, or on their own, namely the *islanded mode*. As it is the case for conventional grids, they need to be controlled, allowing electrical load and supply management on one hand, synchronisation with the main grid on the other.

Different diversified methods of control have emerged over the last years, each suited to specific applications. This paper aims to take a closer look at numerous existing solutions by analysing their working principle and ensured functions into the grid.
Further on, two of them are selected for a deeper analysis of their features: the *Master/Slave control strategy* and *droop control*.
The major difference dissociating the control methods is the use of communications links in the first case, enabling smart power sharing, but implying communication delays and low expandability, while the second is based on local control and allows more precise regulation.

Both control strategies are implemented on a proposed microgird benchmark. Each case demonstrates, as per expected, fundamentally different behaviours and reactions to robustness testing experiments conducted on *SIMULINK* simulation software; an observation section has been established so as to compare each of them. The idea is to determine the pros and cons of each and figure some general guidelines clarifying which method of control is best suited for some basic layouts of microgrid.

[1] not harmful to the environment

Acknowledgements

We would first like to thank our thesis advisor De Jaeger Emmanuel of the Institute of Mechanics, Materials and Civil Engineering (IMMC) at Université Catholique de Louvain. The door to Professor De Jaeger office was always open whenever we ran into a brick wall or had a question about our simulations or writing. He consistently allowed this paper to be our own work, but steered us in the right direction whenever he thought we needed it. All the key information he was able to provide us were essential in the understanding of the subject.

We would also like warmly thank Guy Wanlongo Ndiwulu who was involved since the beginning and throughout the research project. Without his participation and dedicated time, the present thesis could not have been successfully conducted.

Finally, we must express our very sincere gratitude to our parents and siblings for providing us with unfailing support and continuous encouragement throughout our student years as well as the research and writing of this thesis. This accomplishment would not have been possible without them. Thank you so much.

Dujardin Gaëtan and Lambilliotte Félix

Contents

List of symbols

Symbols/ Abbreviations	Meaning
I_d - I_q	Current [A]
V_d - V_q	Voltage [V]
P	Active power [W]
Q	Reactive power [VAr]
ω	Pulsation [rad/s]
f	Frequency [Hz]
AC	Alternating current
DC	Direct current
MG	Microgrid
DG	Distributed generation
DER	Distributed energy resource
RES	Renewable energy source
LV	Low voltage
MS	Microsource
PCC	Point of common coupling
MGCC	Microgrid central controller
MC	Microsource controller
LC	Load controller
PEI	Power electronic interface
UPS	Uninterruptible power supply
VSI	Voltage source inverter
CSI	Current source inverter
IGBT	Insulated Gate Bipolar Transistor
EMS	Energy management system
PLL	Phase-locked loop
CLC	Central control unit
M/S	Master/Slave
PWM	Pulse-width modulation
CCU	Central control unit

Introduction

Environmental concerns and the constantly increasing demand for electricity, among other things, have over the recent years, forced some countries to consider their resilience to fossil fuel energy sources and the liberalisation of the energy sector.
A direct result of those findings was the emergence of domestic renewable sources of energy, allowing a reduction of environmental impact, while satisfying future demands.
The concept of microgrid composed of local energy sources feeding nearby loads has consequently appeared as the most robust, efficient and clean evolution of the conventional grid, leading the energy transition. The core idea this new generation grid tends to incorporate is getting generators and loads closer to each other, allowing for the use of smaller supply units.
The microgrid can either be connected to the main grid or operate independently, giving it a dimension of resilience when a fault occurs on the upper level, or when the quality of supply doesn't meet the standards.

As it is for the conventional grid, those microgrids need to implement a control structure, enabling the stability and reliability of the network. Adjustment, supervision and optimisation are other criteria the global control aims to deal with. This control simply manages the production process of power from energy sources. In other words, by commanding their voltage and frequency as well as ensuring an efficient power sharing.
Each distributed generation (DG) unit is made out of an inverter whose PWM signal is activated, in combination with a LCL filter so as to create a smooth signal at its output. The mentioned inverter can actually act either as a *grid-forming* which theoretically means acting like an ideal controlled voltage source, or conduct itself as a *grid-following*, in other words as a controlled current source referring to a sent command.

In this paper, two main proceedings of effectuating the control task are investigated. The first one, the *Master/Slave strategy*, makes use of communication channels between the components of the grid, allowing fast and rigorous power

sharing. The unique master unit is grid-forming and takes care of voltage regulation (acting as a V/f controller), while other slave units adapt, through the received command, their power generation (P/Q controllers). The system is globally directed by a central control unit observed as the operating brain of the system.
The second structure, more widely used, gets rid of these communications links and favours local control instead (using P/V - Q/f controllers), making it both more robust and expandable: *the droop control*.

As a first step, the present report describes the most likely scenarios for the global energetic evolution in more details. The second chapter describes the several aspects of the microgrid itself (structure, sources and loads characterisation, etc.) and the various control possibilities existing nowadays, with and without communication.

After testing/simulating both chosen methods, a comparison between them (their several limitations and respective assets) is established. By pushing each control structure towards their limit of robustness, the aim is to get a clearer idea of how they are able to deal with a transient situation and what perks/defects can be extracted from a particular configuration.

Chapter 1

Evolution of the energetic landscape

1 Energy transition: context and state

1.1 Consumption on the rise

With the expected growth in the world population (an additional 1 to 2 billion) and the expansion of urbanisation, electricity needs will increase significantly: an 60% increase of the total electric energy needed according to the International Energy Agency (IEA), and this, taking into account the reduction in consumption demanded by the countries to reach the goal of energy efficiency. It would account for more than one-fourth of total energy use, compared to 19% today. This explains why experts keep claiming the future is undoubtedly electrical energy oriented.

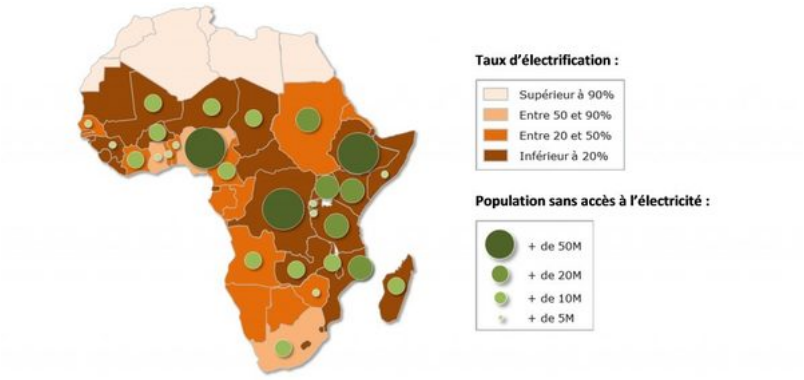

Figure 1.1: Africa's electric situation and expected evolution [1]

Electricity consumption is expected to slightly increase in developing countries but to jump in emerging countries. In 2016, only 42% of the African population had access to electricity and there were large disparities between countries (some whose rate was below 10%, see Figure 1.1). Even within a same country, difference between cities and rural households is noticeable. [2]

1.2 Decentralised renewables as a major actor

Alongside the steady growing demand of electric power, ecological issues and economical matters encountered over the last decade have led to the rise of the fuel cost. Considered as the largest energy importer in the world, the EU[1] is strongly concerned by this rapidly changing sector.

The direct consequence of this has been the drastic increase of use of small-scale and decentralised renewable power sources into modern electric grids, surpassing all expectations.
Indeed, the idea of getting rid of polluting fossil fuels while increasing the use of inexhaustible and free to exploit energy sources seems extremely appealing for both private and public sectors: *"Conventionally, operators have relied on diesel generators. But they are now turning to renewables and especially solar photo-voltaic (PV) installations to reduce their reliance on diesel fuel."*[3]
Distributed energy resources (DER) so appear as a real opportunity to meet some of our energetic needs, respecting environmental, social and economic imperatives as well as strategic and ethical aspects.

Among them, photovoltaic and wind energies are the most developed and exploited ones. Economically not viable a few years ago, rapid technological evolution has today made them affordable and efficient enough to be competitive. The development of the early 2000s showed an upward trend in terms of global renewable interests of integrating such energy sources in all sectors. Since then, it has witnessed an extraordinary expansion that was to unfold in the upcoming decade. From the end of 2004, the worldwide renewable energy capacity grew at rates of 10–60 % annually for many technologies. The part of the global energetic consumption it covers has more than doubled over a twelve-year period, going from 8.5 % to 17,2 % between 2004 and 2016.

In terms of installed capacity, global wind power capacity expanded to about 370 gigawatts (GW) in 2014 while in 2015, worldwide installed photovoltaics capacity increased to 227 GW, sufficient to supply 1 percent of global electricity demands. According to Bloomberg [4], the world even reached, end June 2018, the symbolic

[1]European Union

step of 1 terawatt (1000 GW) of installed wind and solar power with a homogeneous division between the two of them (54% and 46 % respectively). A second terawatt of these same energies is expected to be reached in 2023 and will cost 46% less than the first one.

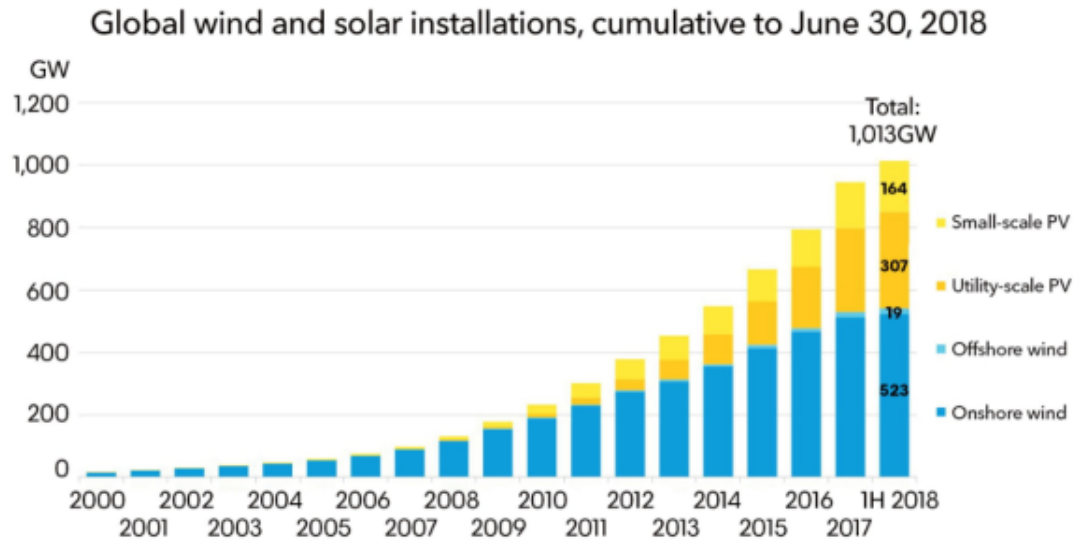

Figure 1.2: Global wind and solar installations accumulated [4]

Our model of the world energy system up to 2050 demonstrates that a cleaner, more electrified world is within our reach. By mid-century, the world will run much more on electricity as its share in total energy supply rises to 40% compared with 19% today. [5]
The idea is to reach a peak in global emissions at the end of this decade, a return to 1990 levels in 2030, a 60% reduction by 2040 and near zero emissions in 2050.

As previously stated, the increase in the use of these renewables is correlated to the massive drop in their cost. The WT and especially PV auction has dramatically declined the last ten years and is trending downward for the coming years with by a quarter for utility scale PV and by respectively almost 15 % and 30 % for onshore and offshore windturbines. [6]

Incorporating renewables to the energetic model through solar or wind generation is obviously an increasingly attractive option. The decrease in cost of solar and wind energy per kilowatt-hour makes it more attractive on a financial aspect than diesel generators. But the main issue of these renewables remains their intermittent behaviour, and storage appears as the best and necessary solution to overcome this challenge.

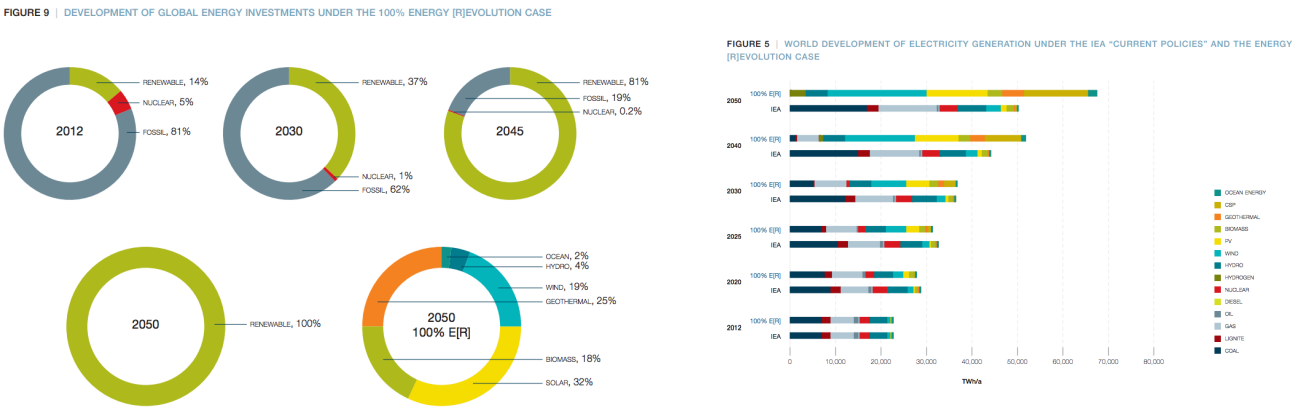

Figure 1.3: Predicted evolution of renewable shares [6]

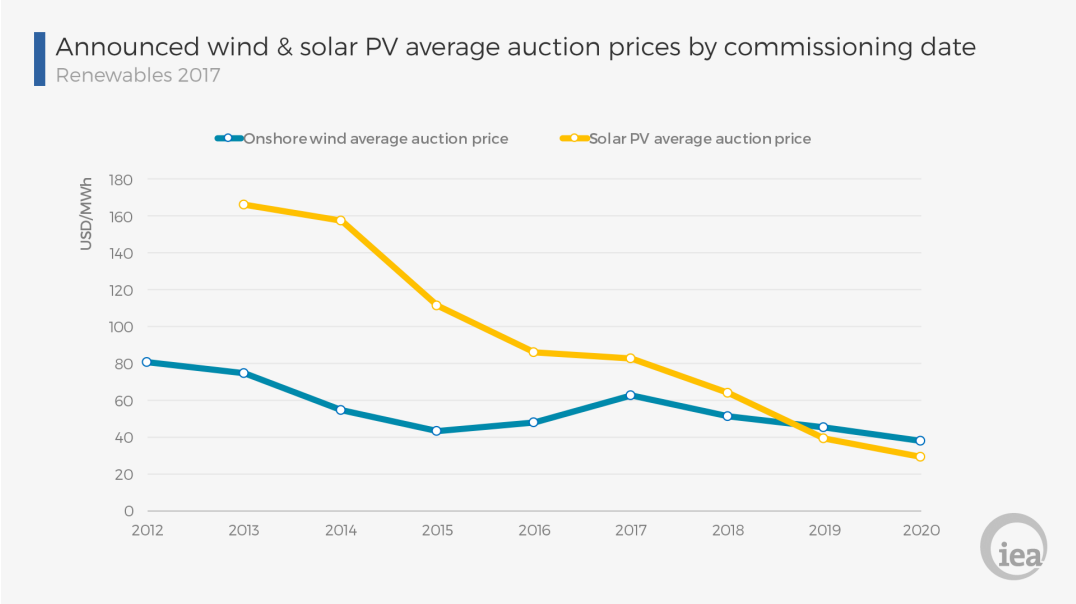

Figure 1.4: Evolution of PV & WT costs between 2012 and 2020 [6]

1.3 Necessity of storage

The main purpose of the grid is to connect power supply and consumption, which are theoretically supposed to be equal at any time. Energy storage plays a key role in this balancing process and helps to move towards a more flexible and reliable grid system.
The idea behind it is to store excess power during low-consumption periods where the electrical generation exceeds the needs so as to restore it to the grid over high-demand peaks and allow to smoothen the consumption profile. "Energy storage is

also valued for its rapid response – most storage technologies can begin discharging power to the grid very quickly, while fossil fuel sources tend to take longer to ramp up." [7]
Finally, when it comes to decentralised generation, storage is key to autonomy as it will be explained further in more details.

Among all the existing techniques, hydroelectric storage[2] is the most developed one. The installed capacity of pumped storage plants reached 153 MW in 2017 [8], accounting for more than 90 % of the worldwide storage capacity. Such pumped-storage plants are known for being highly efficient with round-trip efficiencies reaching more than 80 %. They have demonstrated practically their usefulness for quickly adjusting to small changes in demand or supply too. However, this technology remains limited to restrained topographical situations.

Chemical storage with batteries appears as one of the best alternatives given their performance and the possibility to integrate them on a domestic scale to interact with dispersed generation. Thanks to their typically small size and high energy density, they can be located anywhere and are so often seen as storage for distribution, i.e. located near consumers to provide power stability.

Figure 1.5: Evolution of the price of battery storage between 2010 and 2017 [4]

Another main advantage of these batteries is their reasonable acquisition cost which happens to be in constant decrease since these past years. Their price has lowered for Li-ion batteries at a rate of 14% per year from 2007 to 2014 ; from $ 1,000/kWh to about $ 410/kWh. The reduction has been even greater since then,

[2]Water is pumped from a lower level reservoir to a higher altitude.

as depicted on Figure 1.5, mainly caused by their integration in the electric vehicles (EV) industry.

Spreading the use of electrical vehicles by making them more and more affordable and reliable could, however, lead to a big increase in electricity demand, especially in the low voltage (LV) network. LV grid may not be able to satisfy the whole transition and would, consequently, need to be modified. The solution is to develop and build *microgrids*.

2 Microgrid: the future of the electric grid

Over the last years, a growing worldwide trend concerning microgrids has arose, as it appears as the solution to defective or even non-existent power supply grid, especially in rural areas for instance. As already mentioned, even today around one-fifth of the population around the world still lives with no access to electricity.

A microgrid can be defined as a down-scaled power system composed of distributed energy resources (DER) such as renewable (PV systems, wind turbines or biomass) and non-renewable (internal combustion engine, micro-turbine and fuel cells) resources and energy storage systems (flywheels, batteries,...), both feeding local loads. Energy storage systems aim to support the microgrid and to increase the system reliability and efficiency, as they are traditionally designed to be self-sufficient energetically.
In fact, the microgrid can either be connected to the utility grid or operate autonomously. In the first case, market production is taken into account with the optimised production of local DERs participating in power exchanges with the utility grid. Active and reactive powers exchanges are then considered following the balance between the microgrid and the main system.
On the other hand, allowing it to function on its own is essential to ensure electricity supply while power outage or failure on the line, especially in high-risked zones. To illustrate these words, in September 2017, Hurricane Maria devastated the territory of Puerto Rico, causing a massive blackout. More than 5 months later, in February 2018, approximately 400,000 customers (more than 10% of the island's population) still did not have access to grid electricity.
The disconnection process is thus mainly adopted for independence and robustness matters. As a result, sensitive loads such as medical equipments or core industrial processes are able to run without critical interruptions.

A system defect can case an unintentional disconnection between the utility and the microgrid harming momentary the power quality at PCC. In case of failure, the black start capability (process of recovering from a partial shutdown by restoring an

electric power station/grid) is vital for microgrids, which can potentially improve the reliability of the power grid.

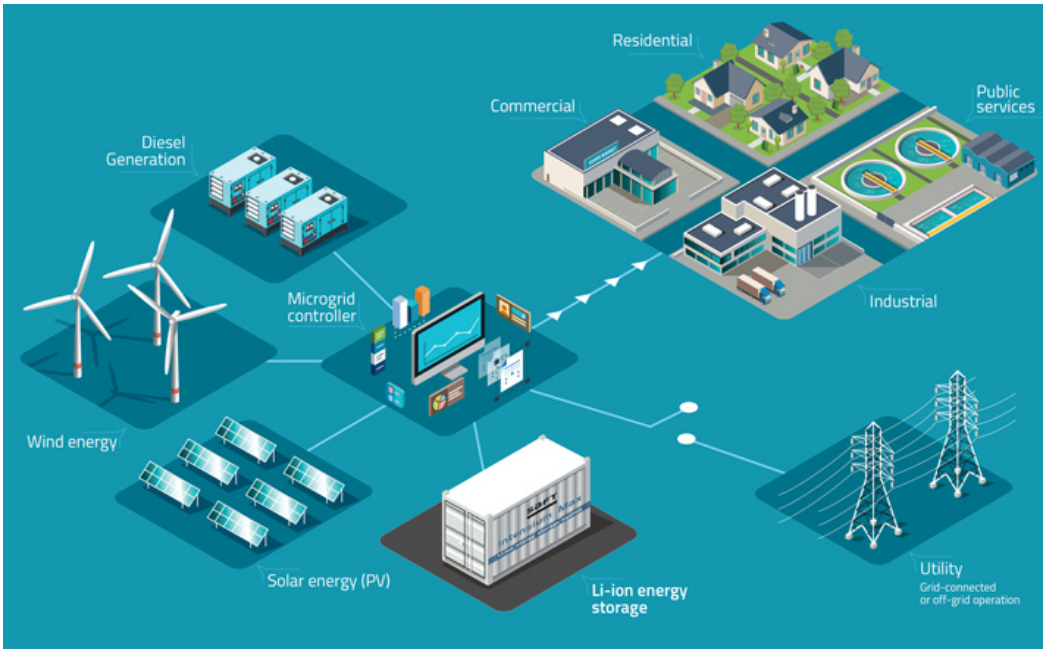

Figure 1.6: Classical representation of a MG and its various components [9]

Developing a *"smart grid"* in which energy is automatically used at the moment it is produced represents another factor capable of reducing costs of renewable energy integration in the grid.
Indeed, beyond facilitating the use of renewable energy resources, the use of microgrids in distribution networks enhances its power quality and reduces losses, thus increasing the performance of the electrical system.

The microgrid topology consequently offers many advantages enumerated as follows:

- Ability to disconnect from the main grid when a fault occurs and to operate on its own, avoiding any abrupt disconnection of the loads
- Optimisation of the operation system on different aspects (see later) & local use of energy, encouraging RES development
- Enhance the quality of power delivered to Microgrid loads

Despite these, some challenges still remain and need to be faced:

- Necessity to implement control and protection systems
- Transition from islanded to grid-tied mode: difference of phase angles between the two grids causing voltage disturbance
- Errors in voltage set-point can lead to a circulating current between distributed sources, causing voltage and reactive power oscillations

As mentioned, microgrids appear vital in some applications requiring constant energy supply (hospitals, servers, etc.). Its use can also be interesting in the case of not robust main grid caused by several factors such as long distance coverage. In highly expanded countries like Canada or Japan, major research is being made to exploit these technologies.
In Europe, many projects are also currently being studied: those projects, as they are all from different countries and universities, need standardisation at first and then the use of an universal benchmark to be able to accurately compare the results of the proposed technologies of control.

The "More microgrids" project includes several aims such as standardisation and benchmarking, study of the impact on the operation of power system, alternative network designs,etc.
In the same way,the European Technology Platform for Electricity Networks of the Future, also called SmartGrids ETP, was created in 2005 with the general objective of providing a bold programme of research, development and demonstration to meet Europe's future electricity needs." [10]

3 Thesis scope

The control of an **islanded AC low voltage microgrid** will be the main focus of this thesis. It includes frequency and voltage regulation with local improvement of delivered electricity's quality. The time scale varies from milliseconds to seconds and does not comprise the optimisation of the operation of microgrids (see Figure 1.7), which is based on many higher level aspects (economic, technical, or environmental), which won't be discussed in this work.

First, the *islandable* microgrid offers several features and services. Primarily, the resilience of the microgrid: in the event of a power/line failure, the microgrid is isolated from the main grid and is able to serve its users thanks to local production and via a *"black start"* restart in just a few seconds, taking into account the network's automatisms. The flexibility provided by energy storage allows to smoothen

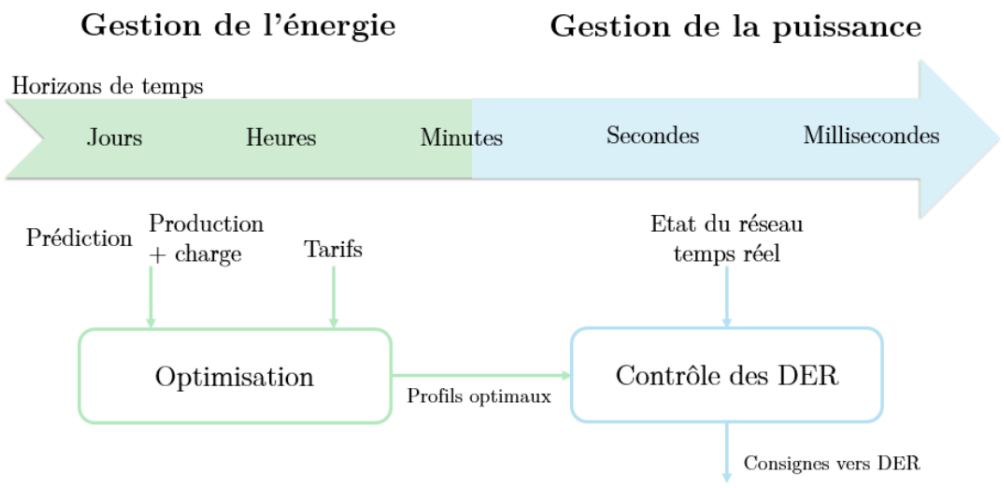

Figure 1.7: Time scale operation of the microgrid

peaks of consumption and cover the variability of renewables.

Alternating current *(AC)*, direct current(DC) and mixed AC/DC microgrids exist. AC distribution systems are the main focus of this thesis as they present many advantages in comparison to DC systems. In fact, AC voltage can be easily adjusted through the use of electrical transformers, which are quite easier to implement in regards to DC-DC converters. Moreover, AC system protection is way more developed compared to the DC case.

Chapter 2

Microgrid: characterisation

1 Definition

According to the U. S. Department of Energy (DOE), the definition of a microgrid is as follows:

"A Microgrid, a local energy network, offers integration of distributed energy resources (DER) with local variable loads, which can operate in parallel with the grid or in an intentional island mode to provide a customized level of high reliability and resilience to grid disturbances. This advanced, integrated distribution system addresses the need for application in locations with electric supply and/or delivery constraints, in remote sites, and for protection of critical loads and economically sensitive development. (Myles, et al. 2011)"

From an European viewpoint, Sébastien Vilbois, head and research engineer in automation and protection of networks at the R&D section of the French group EDF, has declared:

"The islandable microgrids offer several features and services. First the resilience of the microgrid: in the event of a break in current, the microgrid is isolated from main network and is able to recharge its users thanks to local productions and via a restart "black start" in a few seconds only or minutes if automatisms are taken into account network. Then, the flexibility provided by storage that allows particular to smooth the peaks of consumption and /or production, to mitigate the variability of renewable energies and that can be a solution alternative to strengthening networks (lines / cables, transformers, etc.) made necessary by production development decentralised. Finally, microgrids can provide so-called "system" services at the interface with the main network as of the regulation of frequency, regulation of

tension and more locally a improvement of the quality of electricity delivered by "absorbing" the transient disturbances."

Considering the previous definitions and regarding what has been said in the previous chapter, one assumes a Microgrid to be a local distribution grid made of controllable microsources (MS), storage units and loads. The global capacity of the microgrid is assumed to range between a few kW to approximately 10 MW. It tends to optimise the energetic couple generation-consumption on a local scale. Those microgrids aim to feed specific sites such as industrial areas, islands or even University Campuses. These sites can be isolated (island areas, isolated industrial sites such as mines, military bases in operation or rural electrification in developing countries for example) or be otherwise connected to an existing distribution network. In connected areas, a microgrid is characterised by its ability to isolate itself from the network and operate autonomously ("islanded mode") for at least several hours.

As it is for the main grid, the microgrid needs to be controlled in order to ensure both stability and power quality into it. Of course, the control process might differ from the islanded mode of the non-isolated microgrid and will be described later on in this chapter.

2 Structure

The microgrid is expected to be a strategic entity at the LV side of the distribution network, connected or not to the main grid via a single bus called point of common coupling (PCC) through a circuit breaker or a static transfer switch. A central controller manages this connection, it is named the Microgrids Central Controller (MGCC) as illustrated on Figure 2.1. In grid-connected mode, the PCC is closed and the microgrid is connected with the main grid, making it able to exchange active and reactive power in both ways with the utility grid. Should a default or disturbance occur on the upstream network, the connection is opened and the reliability of the microgrid is preserved.

Various types of microsources (MS) and storage units (flywheel, battery and super capacitors) are connected to LV radial feeders through power electronics interfacing (PEI), mostly DC-AC or AC-DC-AC converters, and MS controllers (MC). The loads are also distributed along the feeders via load controllers (LCs) for individual or grouped loads. [11]

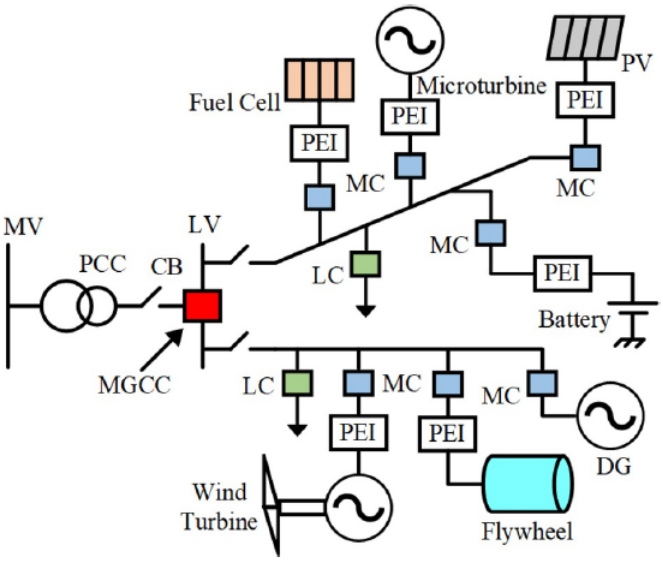

Figure 2.1: General structure of a microgrid [11]

3 Components of the microgrid: description and modelling

3.1 Uninterruptible Power Supply (UPS)

Renewable energy sources like solar photovoltaic or wind turbines are undoubtedly the major sources for DGs in microgrid. However, the power generated from these RESs is in DC form for PV power and in AC at variable frequency for wind generators. Hence, these RES are interfaced through power electronic inverters (PEI) to the grid. The roles ensured by these inverters are multiple[12]:

- Control voltage and frequency variation on a local scale
- Track the load demand using the energy storage devices
- Link central control unit and DG for load sharing

Distributed renewable sources are working together with energy storage devices able to be charged with the power excess and discharge to cover the power deficit. Most of the storage units present fast response devices, allowing them to handle transient situations by balancing energy consumption and generation on short time intervals. DGs can run at a constant and stable output or follow control reference in case of load fluctuations.

Each DG will be modelled by a DC source, a converter and a LC(L) filter. The DC source of each DG is assumed to model a RES standing together with a battery energy storage system. The LCL filter of all DG is acting as a low pass filter and aims to filter out the higher order harmonics generated by the voltage source converter (VSC) [13]. The general representation of the 3 components making up the DER is given on Figure 2.2, with the filter being an LC filter.

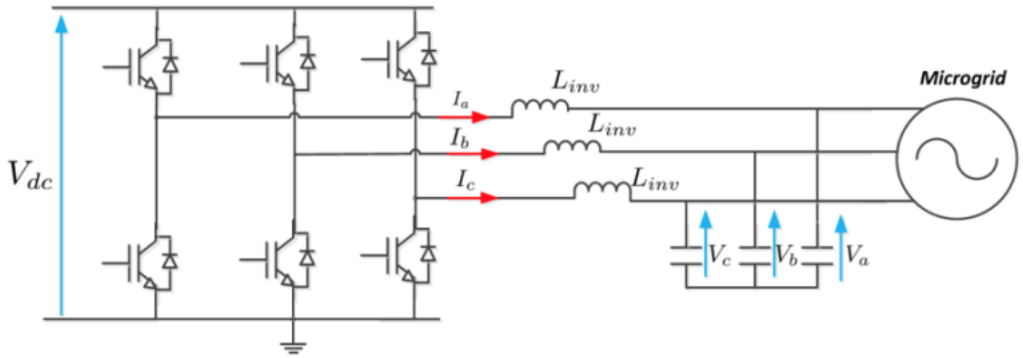

Figure 2.2: DC source, VSC and LC filter [14]

A control device dictates to the DG unit which signal to generate. To do so, a feedback loop comparing the values measured at the output of the coupling inductance (v_a, v_b, v_c) and reference values (v_a^*, v_b^*, v_c^*) is used. A corresponding PWM signal is created and injected into the command of the inverter using an Insulated Gate Bipolar Transistor (IGBT) as switch (see Figure 2.3).

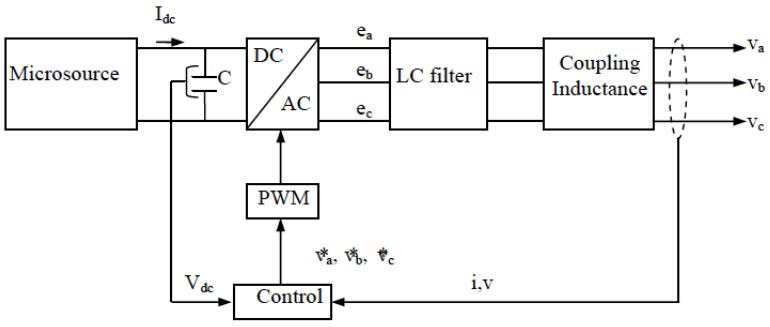

Figure 2.3: Control on microsource [14]

Power converters are classified among three categories: *grid-forming*,*grid-following* or *grid-supporting*.

Grid-forming converters are designed for autonomous operations and are controlled through their voltage. They are usually represented by an ideal AC controlled voltage source with a fixed frequency f. In islanded mode, at least one of the converters must operate this way in order to provide voltage reference to the system.
On the control scheme provided on Figure 2.4, active component and reactive component are decoupled to ensure the independent voltage regulation, imposing the frequency reference.
Current i_d has control over the active component while the current i_q has control over the reactive component.

Grid-following converters, on the other hand, are controlled in current and can be modelled as an ideal current sources interfaced through the grid by a high parallel impedance. Their role is to deliver to the MG a specified but variable amount of active and reactive power. This group of converters, which comprises the biggest majority of them, can either contribute to power balancing or not, depending on the control mode and the source type (as it will be shown in later simulations). Grid-following converters cannot operate in islanded mode without a grid-forming converter establishing a reference voltage amplitude and frequency on the AC grid.
Also called grid-feeding, it has to be perfectly synchronised with the AC voltage at the connection point, in order to regulate precisely the active and reactive power exchanged with the grid. To achieve that, a phase locked loop (PLL) is used. Currents i_d and i_q respectively results from the active and reactive power command [15].

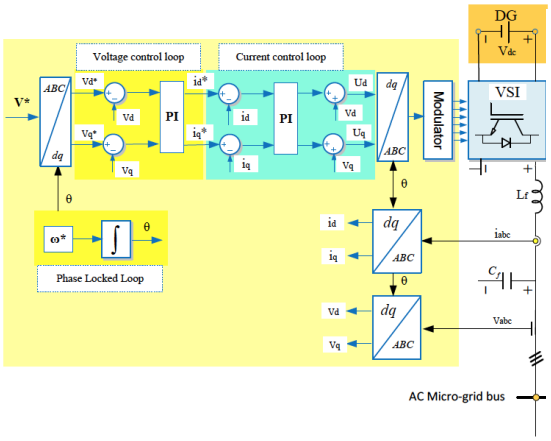

Figure 2.4: Control scheme of a grid-forming voltage source inverter [15]

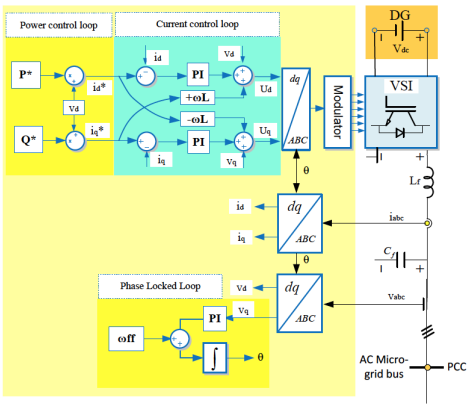

Figure 2.5: Control scheme of a grid-following voltage source inverter [15]

Grid-supporting converters, finally, are made liable by controlling the AC grid voltage amplitude and frequency of the microgrid in either the grid-tied or islanded mode. Some are controlled as voltage sources, others as current ones. A summary of all kind of inverters is proposed in Figure 2.6, showing each time the source type, output impedance, frequency and its used modes.

Contribution to the grid.	Classification of Grid-Connected		
	Grid-forming	***Grid-feeding***	***Grid-supporting***
Source type	Ideal voltage source	Ideal current source	Non-ideal voltage or current source
Control type	Constant frequency/voltage control	PQ control	Droop control
Combination	Series	Parallel	Parallel or series
Output impedance	$Z_d = 0$	$Z_d = \infty$	Finite, nonzero
Output frequency	Fixed frequency	Grid synchronized	Frequency droop
Application	Isolated	Grid-connected	Grid-connected or Isolated

Figure 2.6: Classification of grid-connected components according to their electrical behaviour and their contribution to the grid [15]

3.2 Behaviour of the loads

Microgrids can supply electrical energy to different kinds of loads such as: industrial, residential, medical, etc. Load sharing among DGs in the MG can differ from conventional power systems, and is different depending on the control strategy.

The load model can be divided in two types: the static and dynamic model. In the static load model, presented as constant power, constant current or constant impedance characteristic. In this thesis, the load model is assumed to be characterised by a constant active and reactive power. [16]

Finally, each load is classified according a certain degree of criticality including aspects like priority service.

4 Energy management system (EMS)

One challenge the microgrid faces is to reduce energy imbalances possibly caused by intermittent supply of renewable energy source based DGs and the dynamic nature of electrical consumption. Energy management aims to ensure that the

power demand can be covered according to the power supply from utility grid or local sources through (in)direct load control strategy.

When the microgrid is composed of a plural number of energy generation units, the energy management system optimizes the power sharing among the DERs to meet specified criteria:

- Maximizing system efficiency
- Maximization of renewables sources usage
- Minimization of operating costs
- Minimization of produced emissions

To do so, the mentioned system takes into account several parameters as input such as load, generation and price of the energy on the market forecasts for the next day. The considered case is an islanded Microgrid, no power exchanges with the utility grid will be considered. However, global costs and emission will be predicted.

One should keep in mind that, as it was mentioned in the introduction (see Figure 1.7), that this whole energy management level is on a different layer than the control matters, with time scale ranging from minutes to hours, not covered in this work.

5 Control methods

The control of a microgrid is considered as one of the most important challenges for facing the implementation of microgrids and to ensure a quality supply to the customers in islanded mode.

Control of the microgrid implies several points. The main ones are in fact, the voltage amplitude and the frequency, which deviation form the desired reference have to respect a certain gap to match compliance, of domestic instruments for instance. Proper communication among DERs is necessary for efficient load sharing, i.e. active P and reactive Q power balance. Even if not taken into account in this work, seamless transition between two modes of operation, in other words grid synchronisation and island mode detection is also required. Same for the economic dispatch of the DERs units trying to lower operating costs.

Different control strategies have been reported in the literature. Four global types are identified: centralised, decentralised, distributed and hierarchical strategies. Each one of them is presented in the following section. The choice will

depend on different criteria like financial or structural aspects, but also on types of generation units and on the desire or not to expand the microgrid in the near future.

In the **centralised control** scheme, all the information is sent to the MGCC through high speed communication channels. This central unit processes the received components and acts on the different units in operation. Set-points for each LCs are sent through the same two-way communication link. Small-scale microgrids are the biggest use made out of this type of control as exchange of information between different units is essential to its operation and with short distance between each component of the MG it is reasonable to implement physical communication to each of them.

The **decentralised control** architecture performs measurements on a local scale and executes control algorithms in function on each DER. This kind of control is the best suitable for up-sized and high-rated microgrids with a large number of components, and multi-agent system (MAS).
n the case of this control method, each LCs communicate with its neighbours through low-bandwidth channels in a collaborative manner. The control algorithm is performed on a local level, taking into account the behaviour of nearby devices. The substructure thus enables optimisation of system operations while ensuring autonomy, especially for MAS.

But the most exploited control strategy in the literature is the **hierarchical** one, based upon the difference in time scales of various control requirements as it is composed of primary, secondary and even tertiary control methods imitating the behaviour of the main grid. It combines both centralised and decentralised control. The first layer aims at regulating $V - f$ on a nearly instantaneous time scale (milliseconds to second). In the meantime, the slower (in the range of a minute) secondary layer of control eliminates steady-state deviations by adjusting the system set-points. Finally, the third layer manages the power exchange with the main grid in a much larger time scale ranging from a couple of minutes to hours. Of course, in case the of the islanded microgrid, this third layer of control is ineffective. [12]

The target of the first level of control is to adjust the voltage and either the frequency or the phase references which feed the inner current and voltage-control loops, depending on the operating mode. It is sometimes considered as "level 0" of control and designed to avoid circulating currents among the DERs.

Controllers aim to regulate frequency and voltage especially while transient operations such as load or generation variation (as the switching from connected to islanded mode is not taken into account here).

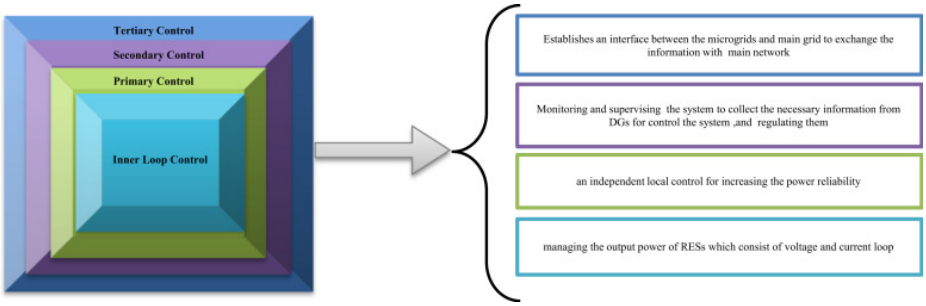

Figure 2.7: Hierarchical control levels [19]

DERs controllers allow power sharing between different sources within the microgrid. The control will be operated on the electronic converters which links DERs to the network by retro-action loop depending on the control strategy. In grid-tied mode, the main power, voltage and frequency of the microgrid are dictated by the main grid. In our case, another solution needs to be found in order to characterise voltage and frequency references.

On top of that, the microgrid can be operated in a centralised or decentralised way. In the centralised control, a central controller handles the optimisation of its operation by managing power exchanges with the main grid and local production/consumption on the microgrid. In other words, the following parameters are depending on its behalf:

- Load & generation forecast
- Units monitoring
- Security enquiries
- Economic dispatching

Of course, these parameters will not be identical depending on the mode of operation.

Two distinct ways of effectuating primary control are distinguished.

- With communication: The algorithm of control easier to implement but requiring communications between modules, making it more vulnerable.
- Without communication: Achieving accurate power sharing and voltage adjustment. The grid-forming control techniques are further classified on their communication requirements.

The main communication-based controller is the master/slave control. Without communication, the concept of droop control is usually adopted.

A review of the multiple primary control methods is proposed on Figure 2.8.

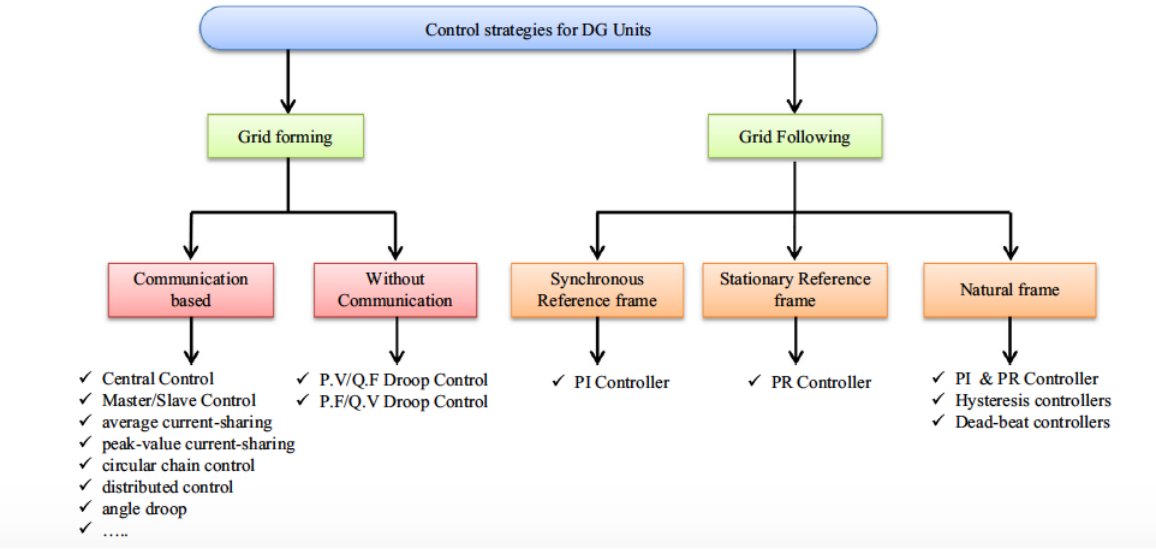

Figure 2.8: Review of primary control methods [19]

5.1 With communication

The key points which characterise the control with communication are good voltage regulation and power sharing. Voltage deviations are also narrower in comparison to the droop control method described later. Despite these, the used communication lines imply a vulnerable and expensive way of operating, reducing system flexibility and reliability.

Central control

Inverters are commanded by a central controller that determines different required generations so as to satisfy an active and reactive power balance in steady-state conditions. The information is sent through communication cables linking DERs and the mentioned controller. Despite being an easy algorithm of control to implement, the communication lines it uses are known to be vulnerable and expensive to install, making it complicated to cover large systems and to expand them.

The central control unit is responsible of the load power sharing by measuring the total load power and divide it among the generation units with weighted values

according to their ratings. One main unit, called the master, is considered to be grid-forming and acts as a voltage source. The others follow the generated voltage and change their output power in function of the received signal. The synchronisation is ensured by a Phase-Locked-Loop (PLL)[1].

The *central-limit control (CLC)* working principle is presented on Figure 2.9. First, the total load current i_{load} is computed. Starting from it, a set of current reference values is determined by the central controller and sent to each modules thanks to the communication lines. For instance, in case of N identical modules, one obtains $i_{ref} = i_{load}/N$.
The produced current of the sources are analysed and re-adapted through the inner control loop.

The voltage is regulated with the computation of the correction term v_e obtained by comparing the load voltage v_o to the reference one v_{ref}. This voltage deviation is communicated once again through communication lines to all the different modules. The output v_c of the current controller is added to v_e. The output voltage of each module is generated from the sum of these two, by using a pulse-width modulation(PWM).

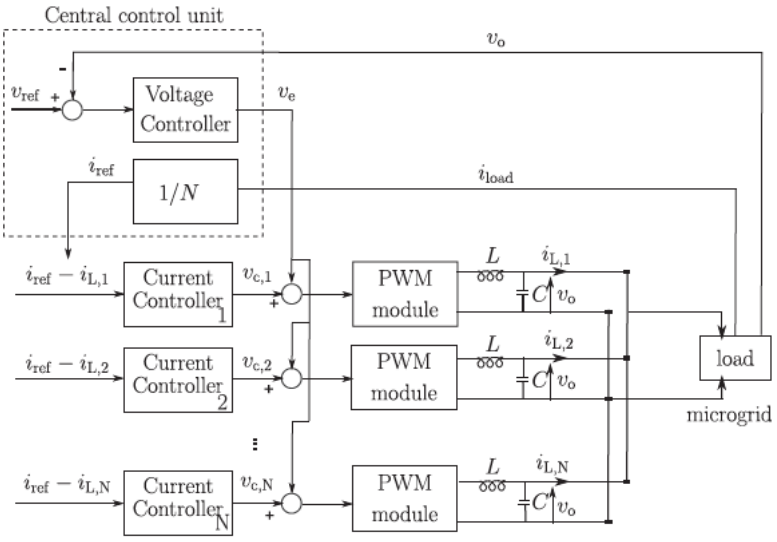

Figure 2.9: CLC working principle [18]

Its key advantage is an accurate power sharing (current sharing ensured at any time, even during transients).

[1] "A control system that generates an output signal whose phase is related to the phase of an input signal."

The *power deviation method* is shown in Figure 2.10. The active and reactive powers are determined separately by phase angle and amplitude of each module output voltage. Once again, the total load current i_{load} is computed and shared among the different converters using a weighting factor to compute i_{ref}. Together with the load voltage v_o, these two elements are forwarded to all generation modules using communication lines. Using the difference between the reference current and the generated one, i.e. $i_{ref} - i_{L,i}$, and the voltage signal v_o, the power components ΔP and ΔQ, here called the power deviations, are computed. In case of a mainly inductive network as it is shown in Figure 2.10, the reactive power deviation ΔQ, the common grid voltage reference v_{ref} and inverter output voltage v_o determine the set value v_g^* of the inverters. The active power deviation ΔP and the frequency reference both determine the new frequency set-value. [18]

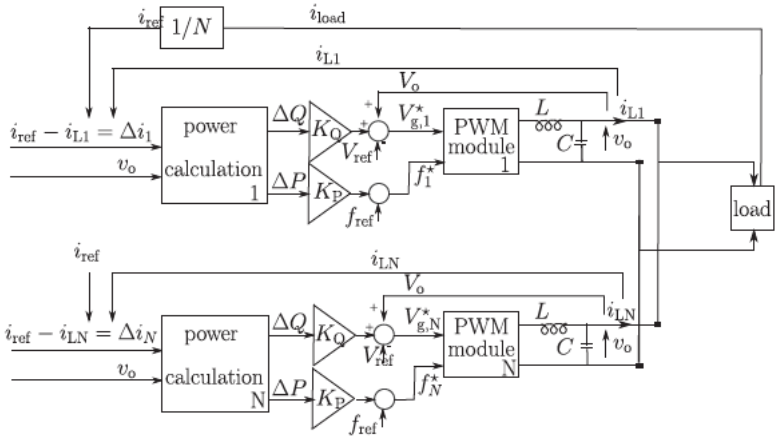

Figure 2.10: Power deviation working principle [18]

Master-Slave

This control strategy relies on both voltage and current controllers. Control of system voltage and frequency is made by only one unique generation unit, considered as the master, but the current control mode is treated by the rest of the generation systems. In other words, Master UPS behaves as a voltage source, while slaves UPS as current sources.

Hence, these units compensate current variations during transients operations, which was not the case for the central control previously described. Indeed, slave inverters track the current command provided to adapt their current generation. Contrary to the droop control method explained later, the Master-Slave technique

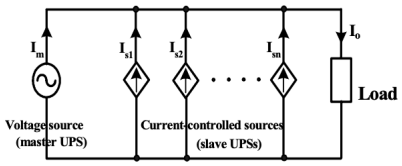

Figure 2.11: The proposed equivalent circuit [19]

avoids circulating currents among the DERs and exerts excellent current sharing between them. The used algorithm of implementation is simple and works for non-identical modules as well. The Master/slave control strategy does however does not allow redundancy, explained by the fact that slave units rely on the master. As mentioned, the output current of the master unit isn't controlled. It can lead to a high current overshoot during transient operations. *The slave units react slower to the transient current demand, so much so that the master needs to provide the compensation current.* Different strategies exist to assign the master unit[16]:

- Master is a fixed module, often the one with the highest rating or the one with highest peak current capability
- Master unit is unfixed and depends on the encountered situation

Inside the global master/slave strategy, one can find a different procedure differentiating on whether they use a central controller or not.

The master/slave control can operate *without central controller* as illustrated on Figure 2.12. In this case, load voltage variations and currents are sent to the master unit.

Depending on it, a set of N reference currents is computed and communicated to the slave units through the communication links. These slave units, acting as controlled current sources, adapt their generation to match the received command. The inverters interfacing the DER to the grid are so-called current source inverters (CSI). In the master/slave topology proposed in Figure 2.12, the reference current of the slaves equals the master output current with $i_m = i_{ref}$. Each slave module is composed of a current controller adapting the generated current $i_{L,i}$ in function of the received command through a pulse-width modulation (PWM) block. This PWM block takes, as input, the sum of the master voltage v_e and current controller output voltage $v_{c,i}$. The voltage v_e comes from the master voltage controller comparing both the reference voltage v_{ref} and the load output voltage v_o.

Advantages of this method are, first, a good voltage regulation obtained by both the voltage controller of the master and the current controllers of the slaves,

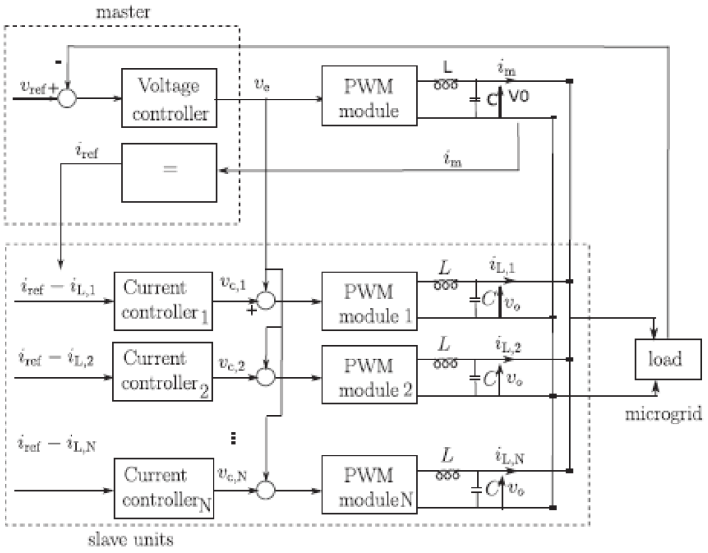

Figure 2.12: Master-Slave control principle without the central controller [18]

and then a good current sharing in steady-state operation.

However, high bandwidth communication cables are used to forward v_e and i_{ref} to the slave units (instantaneous values are communicated). Moreover, big current peaks on the master side during transients must be dealt with.

A wide array of implementation possibilities exists. In a first one, the master unit sends its signals to every other unit. It results in a large number of interconnection cables but robustness and redundancy in case of failure of one of the auxiliary units. In a second case, generation units are arranged in circular shape so that the signal is only sent to the first and the last modules. The observations made are opposite to the previously described case. Anyway, in both configurations, the problem of modularity[2] arises.

With the use of a *central controller*, the layout is slightly different and presented on Figure 2.13. Once again, the master unit operates as a VSI and is made liable of voltage regulation, while the slaves units behave as a CSI and a predetermined amount of current. The total load current i_{load} is first measured, sent to the central control unit, which considers the computation of the reference current i_{ref}, communicated to the DERs.
For instance, in the case of N equal modules, one would obtain $i_{ref} = i_{load}/N$.

The major differences with the previous case are that, at first, the load current

[2]Extent to which the components of a system can be separated and recombined.

is not communicated to the master unit. Secondly, the voltage reference value is not shared so that the reference current is the only value transmitted through high-bandwidth communication links.

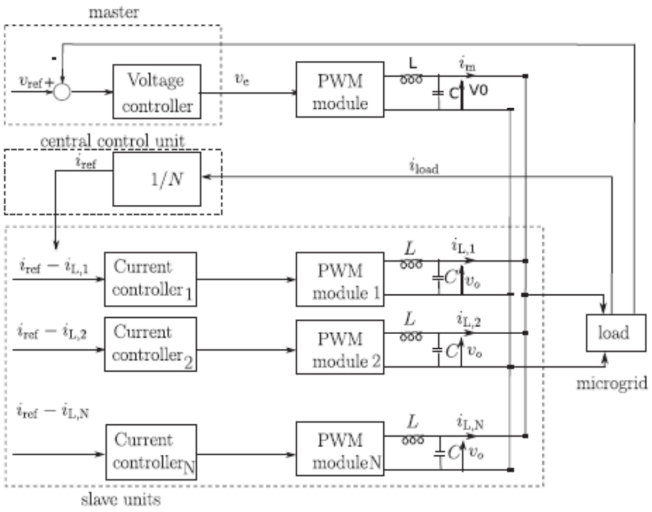

Figure 2.13: Master-Slave control archetype with a central controller [18]

Advantages noticed are globally the same as the previous case. Nevertheless, only one information is communicated through communication links. In grid-tied mode, the grid can be considered as the master.

The master tries to recover the output voltage during transients, which may lead to large master current overshoots. In addition to this, a phase delay between slave units and loads currents always arises. Finally, the system is not redundant.

The required communication speed is, however, limited and can be attained by commercial power line communication devices. Naturally, it all depends on the distance between the units but should never exceeds the 0.2 second time scale for a microgrid.[20] This assertion will be verified with simulations presented into the next chapter.

Instantaneous current sharing

This third control strategy with communication does not require a master to operate but a current sharing bus and a reference synchronisation for the voltage. Two variables are communicated: the voltage and reference current i_{ref}. The idea behind it is to characterise the difference between this reference current and the injected one at every inverter. Each of these inverters are interconnected to ensure the good operation of this control technique as depicted in Figure 2.14.
Inverters are linked to loads through an impedance Z_i. Considering this impedance,

no common voltage reference of the DG units equal to the load voltage v_o is treated. Indeed, each voltage-feedback loop is synchronised to make the output voltages of all inverters in phase. In order to achieve it, a common voltage reference is needed for the whole set of modules.
The taken voltage reference is the one of the inner voltage control loop added to the outer current-sharing loop output. The reference current i_{ref} is determined by measuring the output power at each inverter. The value of the current sharing loop is the difference between this reference current and the terminal currents of the DGs. There are three ways of choosing the reference current i_{ref}: highest output current, current of the inverter with the highest frequency or average of the output currents. The last option is often what is selected.

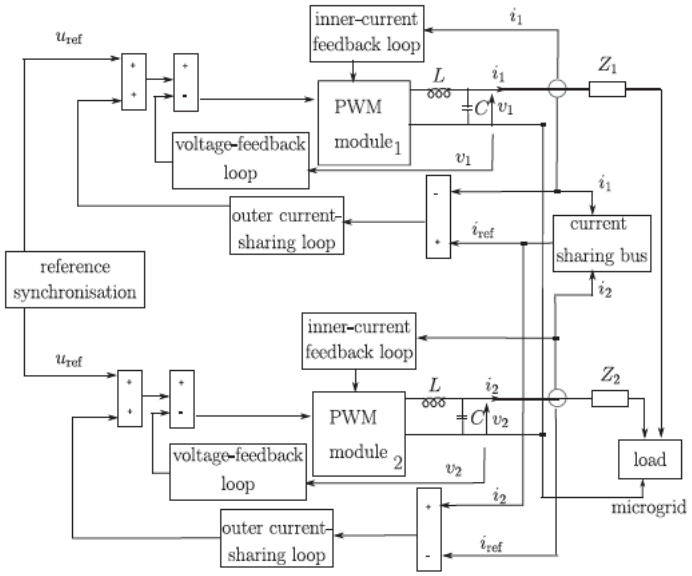

Figure 2.14: Instantaneous Current sharing schematic representation [18]

Even though good current sharing and voltage regulation are observed for this method, output currents contain many harmonics which show a clear lack of flexibility and redundancy.

5.2 Without communication

The main advantage of using a control method without communication is the non existing need of implementing a communication channel between the sources and the loads. As already mentioned, these lines may be a source of weakness within

the network. By suppressing them, it enables a high reduction of cost and makes a real profit in bigger microgrids, useful in rural regions where the components of the MG are far away from each others. Moreover, adopting a droop control method induces redundancy, thus avoiding the need for high cost material and for a supervisor.
Another advantage of adopting a control without communication is the simplification of the network's future expansion, also improving the building of the grid by developing "plug and play" inverters.

However, the droop control has also some downsides such as allowing current circulation between loads, possible current harmonics and the necessity to have a trade-off between the voltage deviation and the power sharing.

In the following development, only the primary control is considered, because secondary and tertiary control are usually computed using communication requirements, as presented in the previous section. A method to ensure a secondary control using the droop technique as presented in [21].
Of course, there are several methods of control without communication [22]. Yet, only the droop control adapted to a microgrid will be studied here. It is derived from the well-known control method applied on the synchronous machine.

Droop control P/f

In short, the principle is quite simple: two quantities depend linearly from each other, here for example the frequency and the active power and the voltage and reactive power as illustrated in Figure 2.15. The relation, as shown in the following equations, is simply linear.

$$\omega = \omega_0 - m_i * (P_i - P_{0i}) \tag{2.1}$$

$$E^* = E_0 - n_i * (Q_i - Q_{i0}) \tag{2.2}$$

In the classical P/f droop method control applied on generators, the control of the motor is regulated by measuring its AC electrical power and comparing it to its mechanical one. If it is greater, the rotor speed will slow down because of its inertia, leading to a decreased frequency. Doing so, the system is capable to regulate itself on its own.

The droop control method adopted depends on the type of generators and power system which mainly depends on the characteristics of the line composing

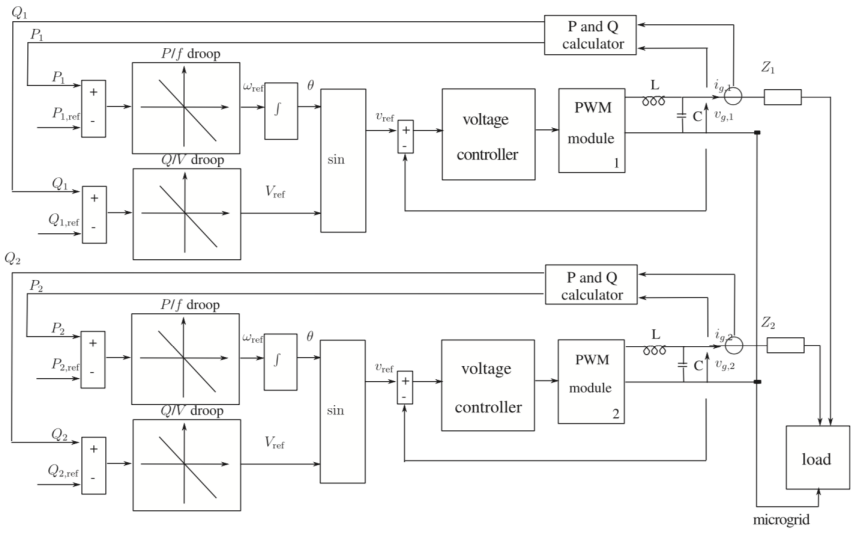

Figure 2.15: Conventional droop control method [18]

the network because of the crucial lack of inertia encountered in MG due to the use of electrical converter/inverter instead of synchronous generators.

There are three main cases:

Firstly, in high voltage systems (typically large size grids), the lines are mainly inductive. In fact, the resistive part of the impedance is negligible. Secondly, in mid size systems, the resistive part of the impedance becomes less and less negligible and needs to be considered. One advantage of the resistive part is the ability to maintain the amount of voltage from each of the DGs. Thirdly, in small scale systems, the inductance part of the impedance becomes negligible, the microgrid having an almost purely resistive characteristic.

From these line characteristics, the method of droop control is exactly the same in HV and MV networks than the one developed above for the synchronous machine.

Variants of the P/f droop control method

Variant techniques of the P/f droop control methods are briefly described in the following section, such as the virtual output impedance, virtual inertia and harmonic power sharing.

One way to avoid coupling between active (P) and reactive (Q) power is to introduce a virtual output impedance like an output inductor [23, 24]. The scheme of the modified droop method is presented in Figure 2.16.

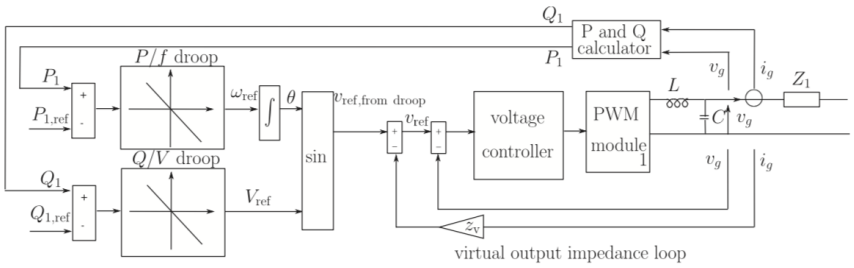

Figure 2.16: P/V droop with a virtual output impedance [18]

The idea is to introduce a mostly inductive impedance, avoiding the need for the line impedance characteristics. This technique is useful to prevent power coupling but may induce a reactive power sharing error because of the inevitably increased voltage fall.

In addition to the introduction of a virtual impedance, a frame transformation of the virtual P and Q is proposed in the literature, achieving a decoupling of power when the lines are not mainly but purely inductive.

Another technique is virtual inertia. After an event in the network, the frequency is not limited within the standardised values. Generators and loads begin to couple to the grid, as a result the amount of inertia available will decrease because the network inertia itself is increasing with unstable components. This phenomenon is worse in islanded mode of the MG.

To counteract the increase in frequency variation, a solution is to simulate inertia by emulating rotating inertia. To do so, the microsources will act as a virtual synchronous generators, using for instance synchroconverters.[3] Those devices are composed of two parts, one for the power control, the other for electronic control.

A last technique to improve the classic droop control method is to implement distribution of the harmonic power sharing between each controller. To do so, the usage of a G/H droops is introduced, with G being the harmonic conductance and H the reactive harmonic. The circuit is depicted in Figure 2.17.

[3]Synchronverters are inverters which imitate synchronous generators to create "synthetic inertia" for ancillary services in electric power systems

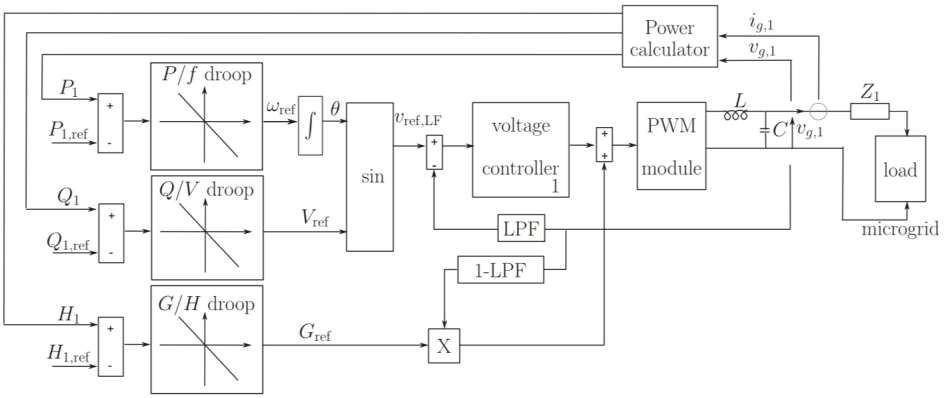

Figure 2.17: Harmonic power sharing technique [18]

Droop control P/V

When in the case of a microgrid, the small amount of inertia induced by its limited size and the absence of synchronous generator leads to a control strategy of the active and reactive power based on the line characteristics.

Also, in an islanded MG based on converters, having them being able to measure the frequency is not so easy,whereas the measurement of power is rather easier. So active power P influences the voltage, and the frequency is influenced by the reactive power Q. Thereby, the active power is controlled by the voltage amplitude variations and the reactive one by the frequency. A P/V and Q/f control is used as depicted in Figure 2.18, in opposition with the conventional P/f and Q/V droop control method presented above.

Some studies have conducted a comparison between P/f and P/V droop, and observe a more damped response for the second one in the case of a resistive network, i.e. in the case of a MG. [25, 26]

Choosing droop coefficients has a major influence on the network stability. Adopting a large droop coefficient can benefit the rapidity in power sharing, but will possibly lead to instabilities. As expected, a smaller coefficient will slower the control process.

Another thing to keep in mind is the load dependency of the frequency and voltage, simply because the droop method itself does not implement an integral term. Indeed, a proportional term is used in the droop control method.
In order to slightly regulate the dynamic, a low-pass filter is required before calculating the power P and Q used to influence the droop control.

Finally, other variants can complete the droop control model, such as virtual output impedance, frequency-based signal injection taking into account the resistance of the line, etc. Those variants are similar from the one developed previously for the P/f droop method. The frequency-based signal injection is the one developed in the following section.

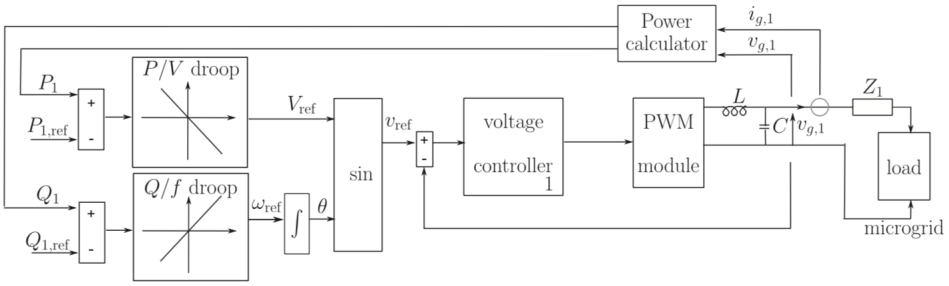

Figure 2.18: P/V droop for microgrids [18]

Variants of the P/V droop control method

To decouple the power P and Q, as it is the case in the P/f droop method, one can introduce a virtual output impedance, which will be resistive. Another technique is to control the current sharing by using the power line to superpose a little AC signal in order to control the power sharing. The layout of this device is presented in Figure 2.19.

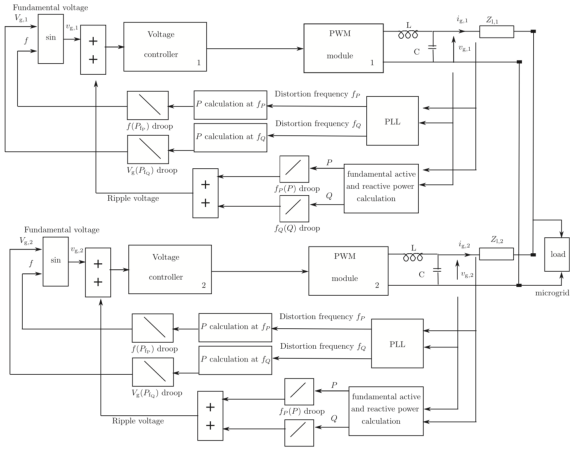

Figure 2.19: Frequency signal injection [18]

As depicted, a cosinusoidal signal is summed up to the reference voltage with a constant amplitude. In each load, the reactive power Q is measured, and taken

into account with a coefficient $K_{ripple,i}$ to compute $f_{Q_i} = f_{Q_0} + K_{ripple,i} * Q_i$. For two generation units, their frequency will be almost the same, but when comparing them, one notices an increase in power demand and needs to automatically adapt the frequency.

In this technique, a Q/V control is possible, not directly but by using the frequency f_Q as the controlling variable.

6 Features summary

To conclude this chapter, with all the information gathered until now, one can establish a tree-shaped frame comprising all the key features of the microgrid, proposed in Figure 2.20.

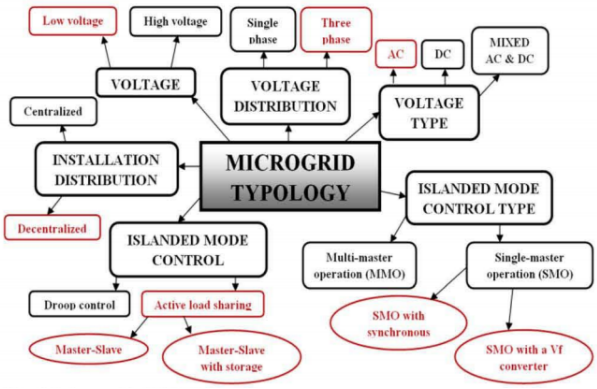

Figure 2.20: Summary of all the important features related, by near or far, to a microgrid [27]

Chapter 3

Master-Slave *vs.* droop control: practical application and comparative analysis

This chapter concentrates more deeply on two chosen relatively different local control methods: the *Master-Slave control* & *Droop control*. A specific grid topology is proposed, comprising loads and generators of different ratings. The idea is to compare performances for both control techniques on basic cases and test their abilities to handle disturbances.

1 General characteristics of the LV network

Before the studied models, some technical descriptions of the LV distribution network and its structure are introduced. The configuration is illustrated in Figure 3.1. As the majority of LV public distribution networks, it has a radial layout, with a number of LV feeders and loads (three of each) connected to a main LV busbar (see orange line in Figure 3.1).

Symmetry of the system:
Loads are considered to be three-phase, no unbalance situations are simulated at this level. In regards to PV suppliers, these are interfaced to the grid through inverters so three-phase AC power is generated.

Line types:
The line type varies in function of its use. LV network lines are either underground cable lines, encountered mainly in urban areas with a high load density, or most commonly overhead lines, traditionally constructed by Al (or Cu) bare conductors.

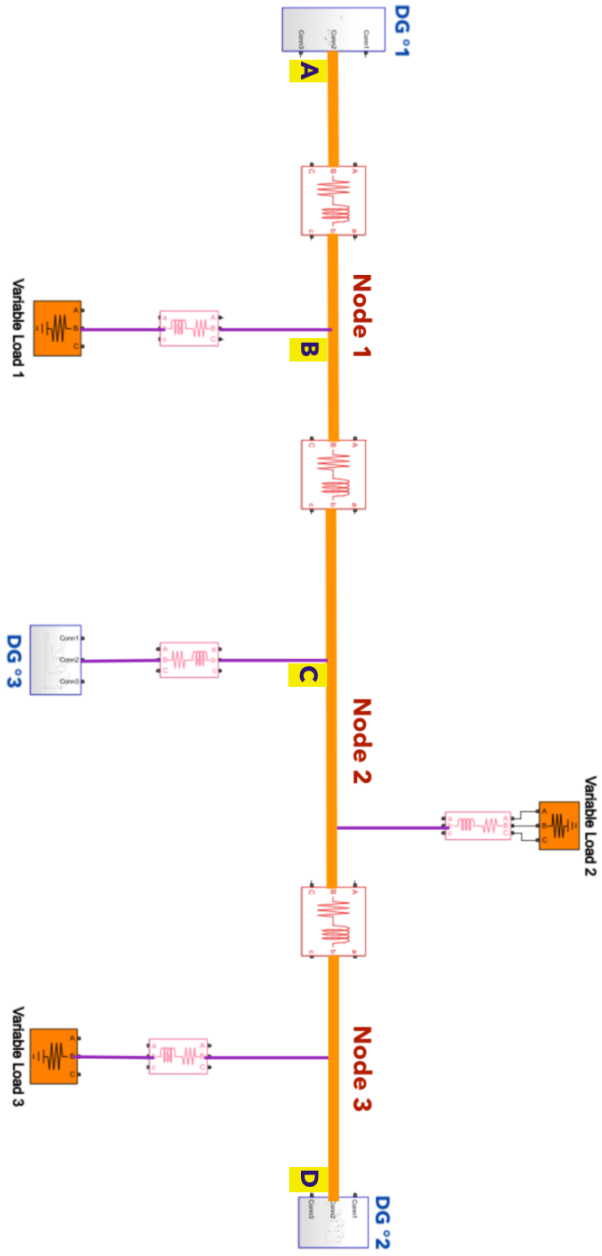

Figure 3.1: Benchmark of the considered model

The main connection of the presented circuit linking the first distributed generation unit to the second one (in other words, between point A and D), is an overhead line (OL) *Twisted cable* $4 \times 120mm^2$ *Al* with characteristics given in table 3.1. Be aware that initial lengths are fixed but will be modified in the coming sections to test system's robustness:

A $\rightarrow$ B: 55 m
B $\rightarrow$ C: 55 m
C $\rightarrow$ D: 110 m

Other lines, arising from this main one perpendicularly to it, are *service connection (SC)* cables with different features, presented in table 3.1 as well.
Line type 2 connects the loads to the main three-phase line, while line type 3 (SC - $4 \times 25mm^2$) ensures link to the third generation unit DG3. These line choices are taken from benchmark configuration [28] and are justified by the maximum current each one is supposed to handle, depicted later on in this chapter.

	Line type	$R_{ph}[\Omega/km]$	$X_{ph}[\Omega/km]$	$R_0[\Omega/km]$	$X_0[\Omega/km]$
1	Twisted cable $4 \times 120mm^2$ Al	0.284	0.083	1.136	0.417
2	SC - $4 \times 16mm^2$Cu	1.380	0.082	5.52	0.418
3	SC - $4 \times 25mm^2$ Cu	0.871	0.081	3.48	0.409

Table 3.1: Impedance data for the benchmark network lines [28]

One can observe the different lines being essentially resistive ($R >> X$), which is common for LV systems. Here, a nominal value of 400 V is considered. Finally, each line is theoretically supposed to be made out of 5 conductor cables: 3 phases, 1 neutral and 1 protective earth.

Demand analysis:
Each consumer of the feeder is characterised by a maximum permissible current, I_s, which corresponds to the rated current of the overcurrent protection element. The maximum demand P_{max} is given for each one. The actual consumption of loads is considered to be resistive only at first, and will range between 0 and this provided maximum power. Total load power $P_{L|tot}$ is then equal to 45 kW and needs to be

Load number	Load 1	Load 2	Load 3
Max. active power [kW]	15	20	10

supported autonomously by the three local generation units.

When considering the reactive load case, a 0.9 leading or lagging power factor will be assumed. Reactive power is bounded to 22.3 kVAr.

Load number	Load 1	Load 2	Load 3
Max. reactive power [kVAr]	7.262	10.292	4.842

Total resulting apparent power is thus $|S| = 50.26$ kVA.

DER characterisation:
As introduced in the first chapter, the considered microgrid is expected to operate autonomously with renewable suppliers. Therefore, each DER will be constituted of either a PV or windturbine installation working together with a Li-ion battery storage system, an inverter and a LCL filter. This whole package tends to be considered as a "black box" with specified characteristics, such as maximal current I_{max} and output power S_{max}. The zero level of control is considered as ideal, as the primary control is the main focus of the present report.

This being said, sizing ought to be dependent on the control type as these can lead to different needs in output current.

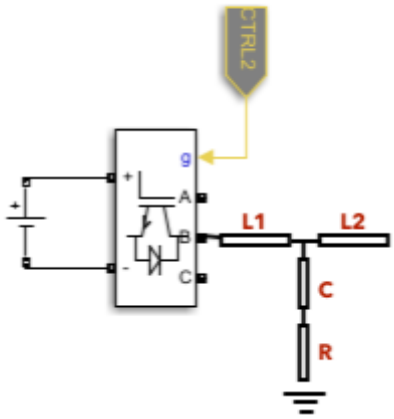

Figure 3.2: Global representation of a DG

The harmonics caused by the use of the inverter are the main factor-causing problems in regards to sensitive equipment or the connected loads.
A LCL filter is placed at the output of the power electronic device. Stability problems could be caused due to the undesired resonance induced by low impedance

at certain frequencies. "To avoid this resonance from contaminating the system, several damping techniques have been proposed. One way is to incorporate a physical passive element, such as, a resistor in series with the filter capacitor." [29]

Parameters of the inverters and the LCL filter characteristics it implies are listed in table 3.2. Those values were computed knowing the grid voltage and frequency, in order to reduce harmonic distortion generated by the IGBT.

Parameter	**Value**
Grid voltage	400 V
Grid frequency	50 Hz
DC-link voltage	800 V
Switching frequency	10 kHz
L_1	1.5 mH
L_2	0.5 mH
C	15 µF
R	50 µΩ

Table 3.2: Parameters of inverters

2 Master-Slave

The system is, as shown, composed of multiple inverters connected in parallel. For the master/slave strategy of operation, *one of them plays a master unit and act as a controlled voltage source (VSI), regulating the voltage and frequency whereas the other units keep the constant power, behaving like current controlled sources (CSI).* In other words, the master unit act as a V/f controller, while the remaining ones act as P/Q controllers.
The master unit is named grid-forming and plays the role of utility grid replacement. The slaves support the master considering a dictated command and take place as grid-following units.

Through communication channels, the instantaneous and varying load demand and the generation of the several DGs connected to micro-grid are communicated to the centralised control unit. With all the mentioned data taken into account, the centralised control unit will generate a reference signal and send it to all the slave inverters.
On the other side, the master DG will control the system voltage. It also is responsible for handling the transients caused disturbances and ensuring the balance between generated power and load demand.

A brief reminder of the master/slave topology is provided below. In this configuration of the master/slave, the master unit is regulating the grid voltage all by itself.

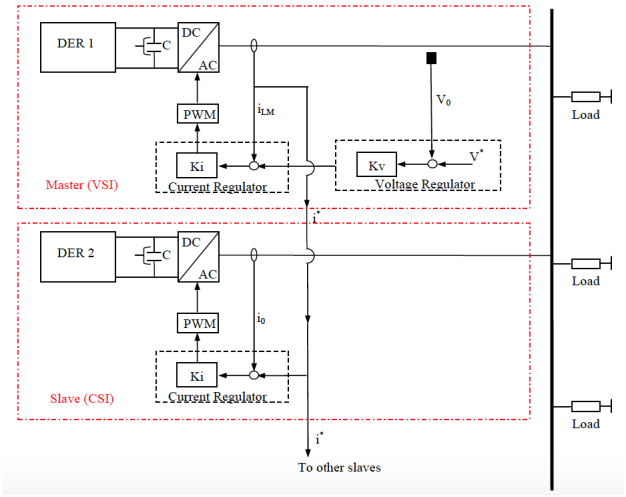

Figure 3.3: Reminder of master-slave control [30]

Nonetheless, as level-0 of control is not considered here, a simplified model of the generation units is used. The master is modelled as a voltage controlled source, slaves as current controlled sources, without treating the inverters and the PWM generator. The full simulated master-slave model (i.e. the Simulink frame) is depicted in Appendix A.

• **Voltage control:** Voltage is measured at load 2, seen as the reference node (because of its central position in the grid). The value is sent to the central control unit, which adapts the voltage generation of the master according to the difference between voltage at this node and the reference voltage $U_{ref} = 400$V (see Figure A.1). The idea is the get the smallest voltage deviation at each load. The phase of the voltage is continuously adapted to reach the desired power factor ($cos(\phi_M) = 0$; $cos(\phi_S) = 1$). [1] In practice, as shown on Figure A.1 in Appendix A, a unity sinusoidal signal is generated with desired phase and is multiplied by the desired amplitude value.

• **Current control:** DG2 and DG3 thereby both operate as slaves units. The RMS current feeding the three varying loads (I_{load}) is added up and then divided

[1] Ideally, the aim would be to have a power factor close to 1 for both. However, the simplified model leads to a lack of degrees of freedom causing the slave power factor to decrease when the master power factor increases. The two slaves are privileged.

by the number of slaves, namely 2 in the presented case, to determine the reference current norm I_{ref}. The injected current is adjusted at each time step in function of the reference (see Figure 3.5). Contrarily to the slaves, the master voltage phase is fixed and is used as reference for the slaves' current phase.

• **Central control unit (CCU):** This unit is the operating brain of the system responsible for analysing every state of it and react in function. Here are computed reference value for the voltage and the currents. One should notice that voltage difference between reference value and voltage at load 2 is multiplied by a modifiable gain K. This gain will have to be small ($\approx 1-2$) at a system initiation for a quick system voltage stabilisation and will be increased after that ($\approx 5-6$) to enhance regulation performance.
The CCU developed in this model comprises a load management system trying to respect, among other things, the physical constraints of it by disconnecting/reconnecting loads in function of power capacity of the system.

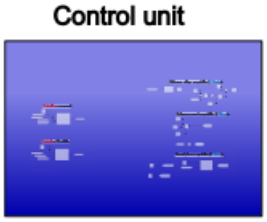

Figure 3.4: CCU

1) Voltage deviation: As explained earlier, for voltage quality matters, voltage across loads is expected to range in the $[360; 440]$V interval.

2) Over-current: Lines connecting the master and the slaves to the grid have been designed to accept a maximum current of 110 A and 90 A, respectively. The master is susceptible to suffer from high transient peak currents. As it was for voltage deviation matters, the choice was made to disconnect load 3 in priority in case of disfunctionment.

The proposed microgrid system shown in Appendix A is simulated using MATLAB/Simulink. The simulation time is 1.5 seconds and various load changes are effectuated every 0.5 second time steps to observe the behaviour of the microgrid against them. At first, loads are supposed to be purely resistive.

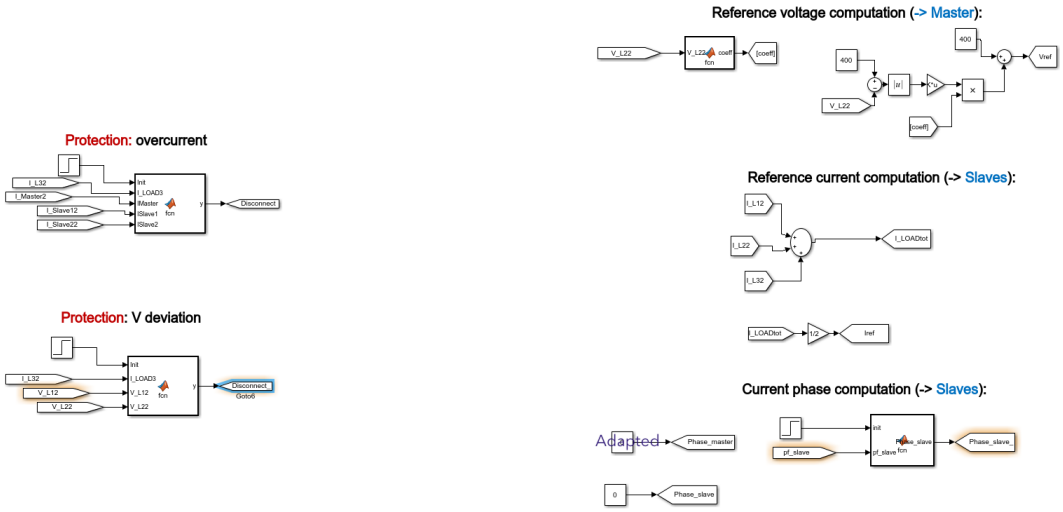

Figure 3.5: Inside look at the CCU

2.1 Simulations

A. During t_0 to t_1

The microgrid is operated in islanded mode during the whole simulation. The total load demand is 23 kW divided as follows during $t_0 = 0$ and $t_1 = 0.5$ sec.:

$$\begin{aligned} &P_{L1} : 12 \text{ kW} \\ &P_{L2} : 7 \text{ kW} \\ &P_{L3} : 4 \text{ kW} \end{aligned}$$

B. During t_1 to t_2

At $t_1 = 0.5$ sec., the first load is modified, dividing its consumption by 2 to reach 6 kW:

$$\begin{aligned} &P_{L1} : 12 \text{ kW} \rightarrow 6 \text{ kW} \\ &P_{L2} : 7 \text{ kW} \\ &P_{L3} : 4 \text{ kW} \end{aligned}$$

The total consumption is down-rated. Variation of the total load current should be taken care of by the central control devices redefining reference currents for the slave generation devices.

C. During t_2 to t_3

At $t_1 = 1$ sec., load 2 and 3 are disturbed.

$$\left|\begin{array}{l} P_{L1} : 6 \text{ kW} \\ P_{L2} : 7 \text{ kW} \rightarrow 17 \text{ kW} \\ P_{L3} : 4 \text{ kW} \rightarrow 8 \text{ kW} \end{array}\right.$$

D. Illustrations

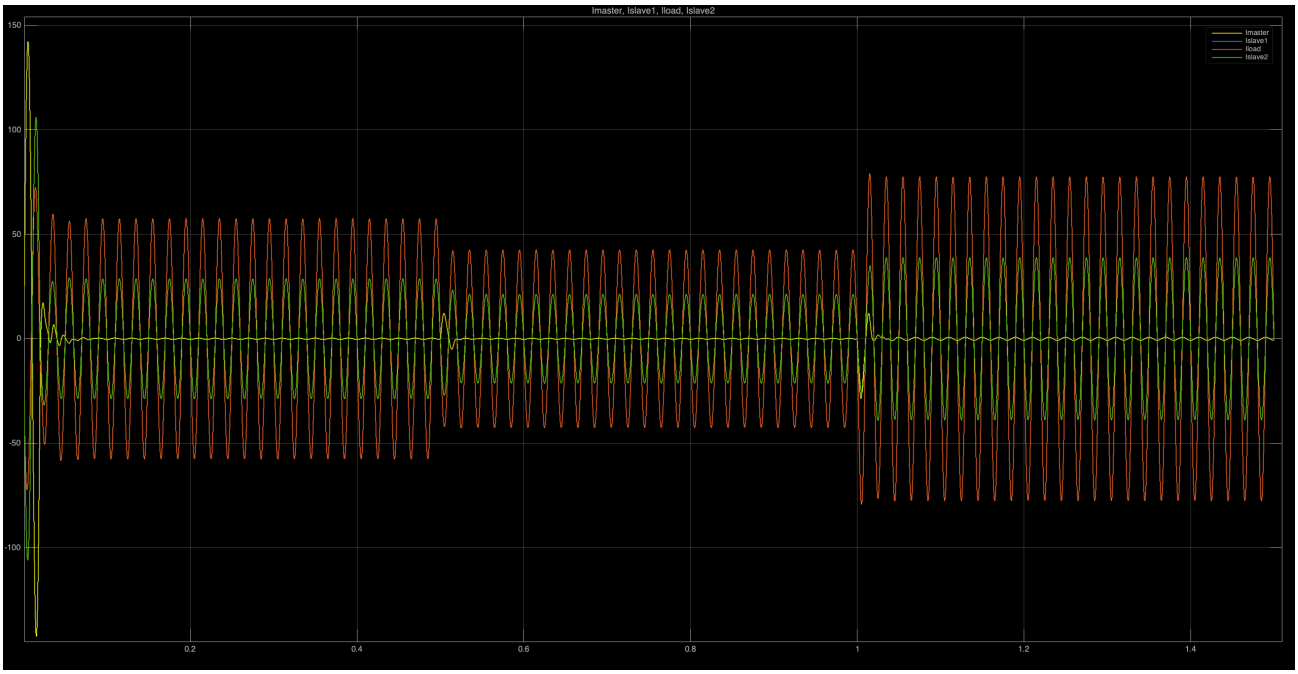

Figure 3.6: Comparison of one-phase current of I_{Load} summed up (red), I_{master} (yellow) and both I_{slave} (blue and green)

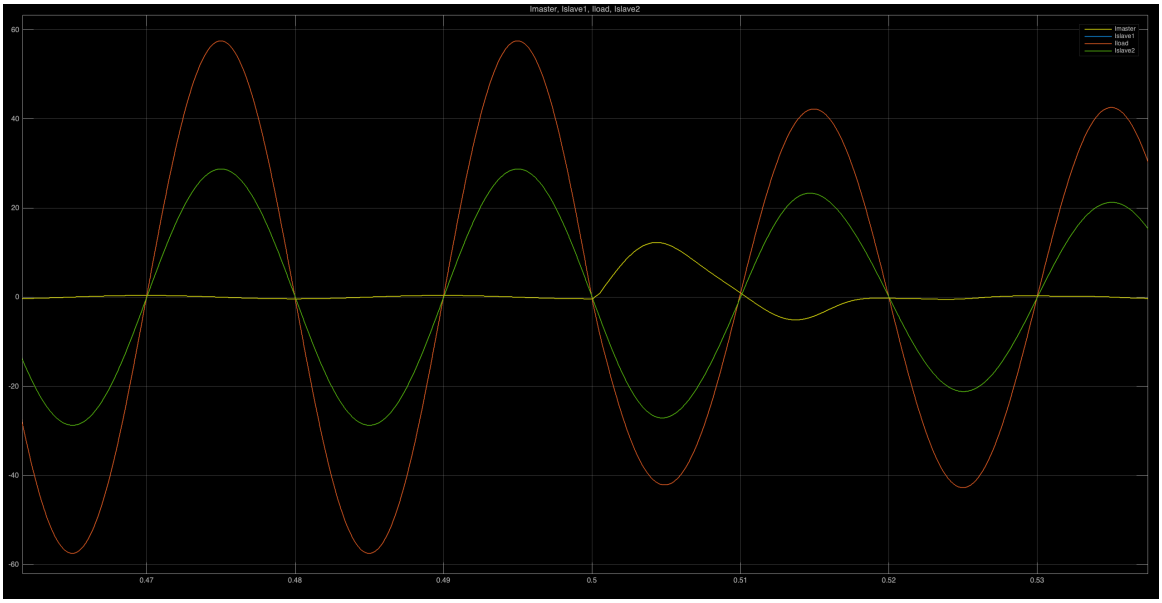

Figure 3.7: Comparison of one-phase current of I_{Load} (red), I_{master} (yellow) and both I_{slave} (green and blue) during the first transition (total load decreases)

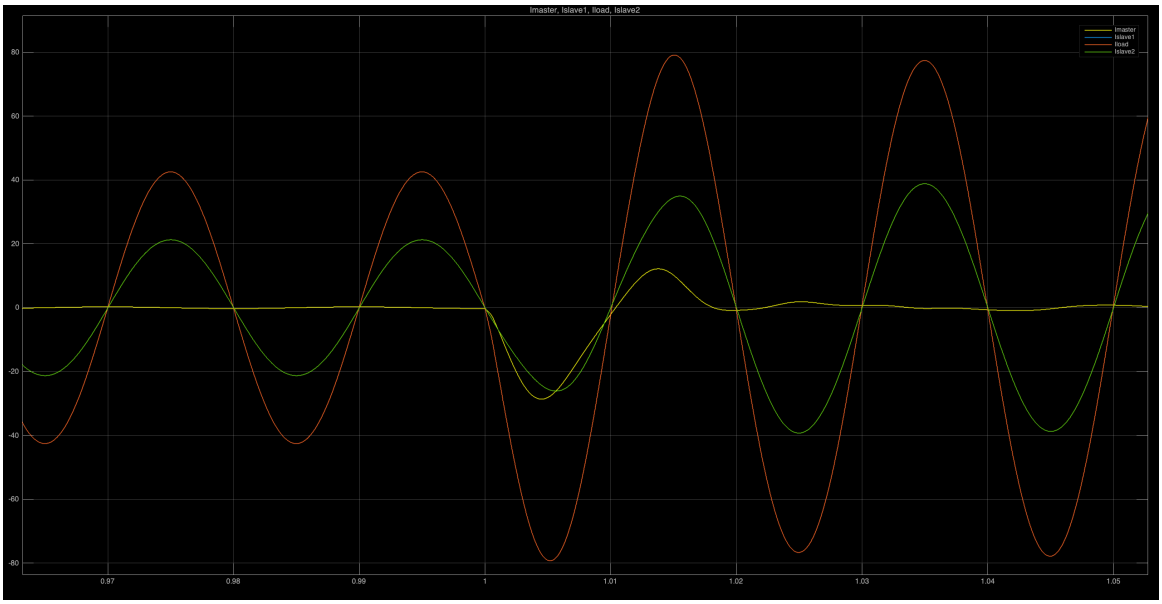

Figure 3.8: Comparison of one-phase current of I_{Load} (red), I_{master} (yellow) and both I_{slave} (blue and green) during the second transition (total load increases)

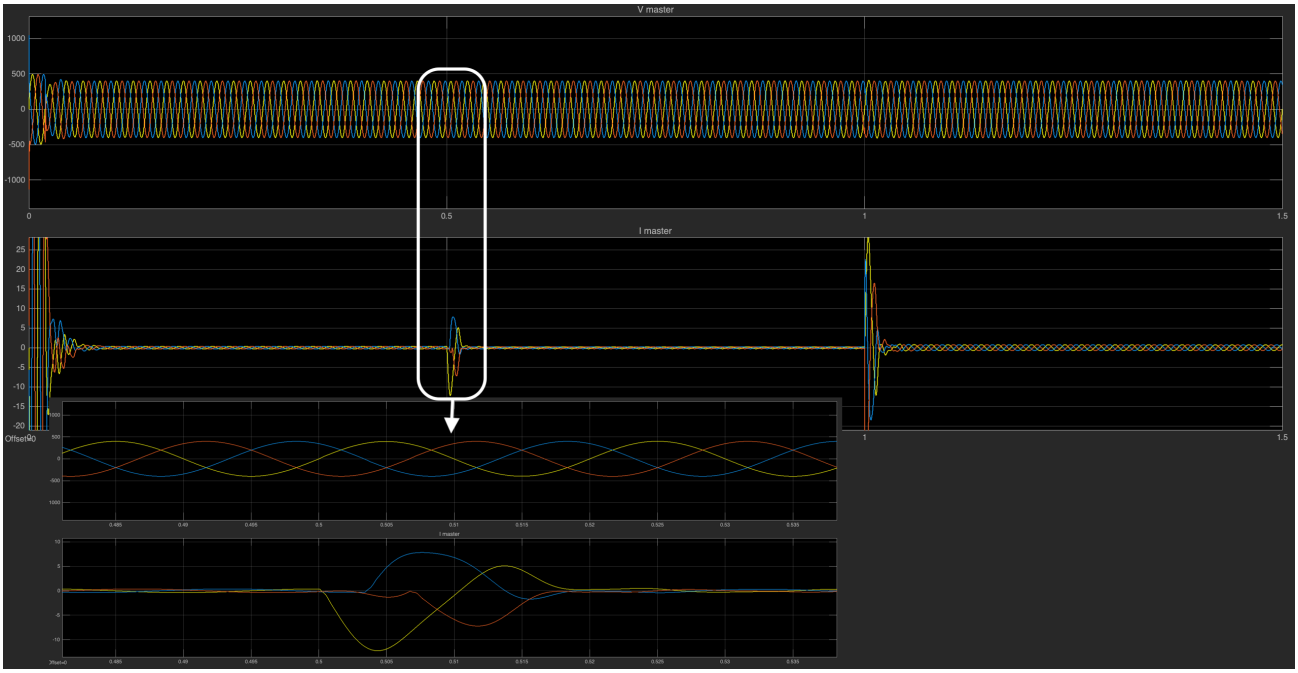

Figure 3.9: Evolution of the 3-phase voltage and current at the master DG

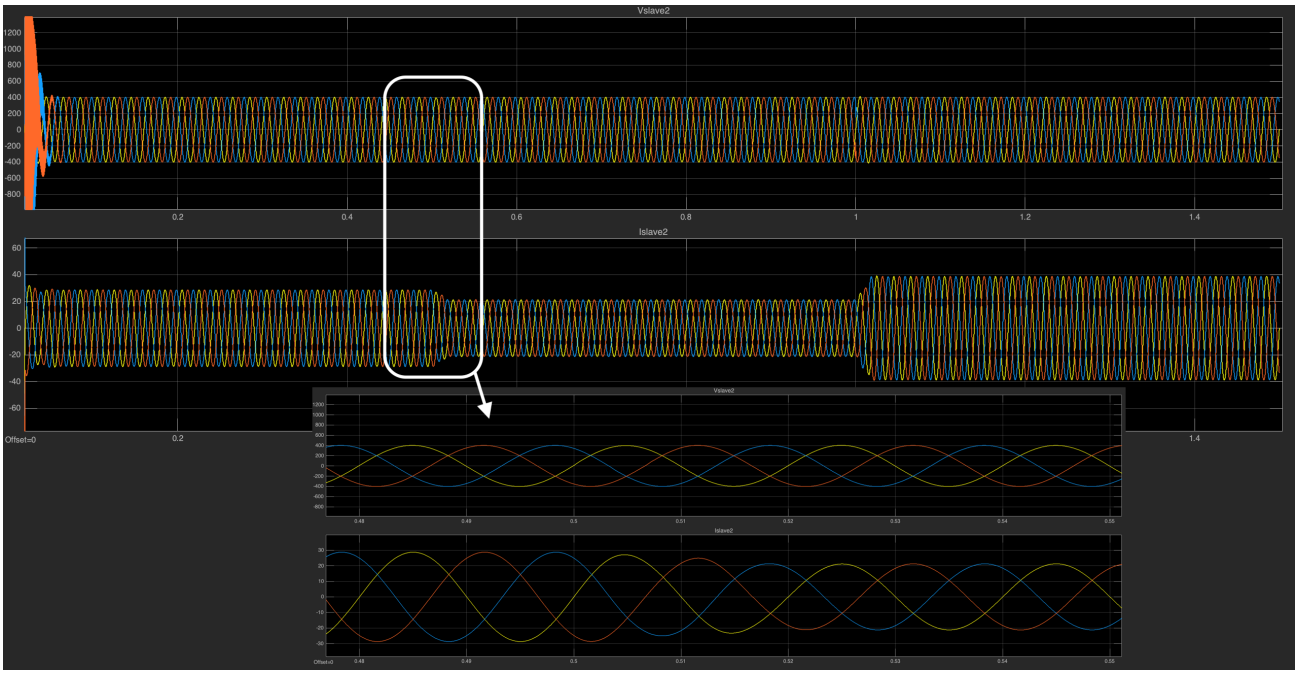

Figure 3.10: Evolution of the 3-phase voltage and current at the Slave1 DG

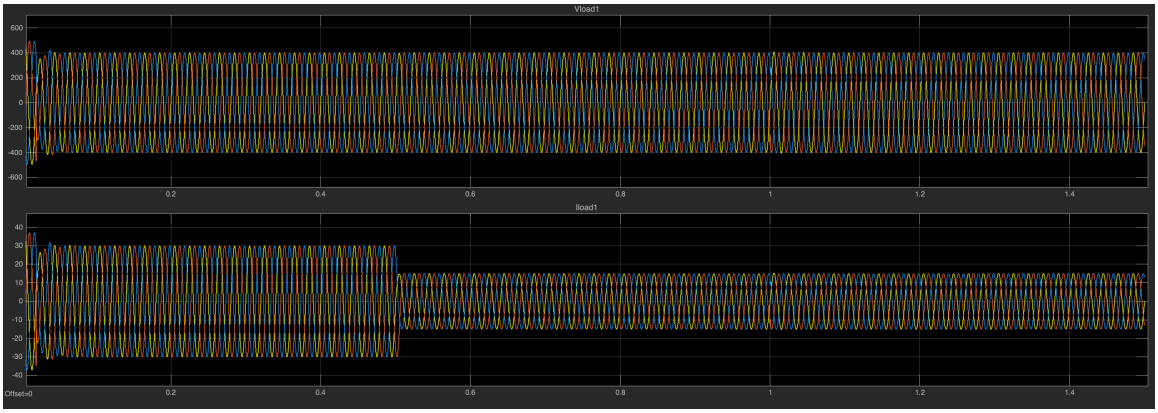

Figure 3.11: Evolution of the 3-phase voltage and current at load 1

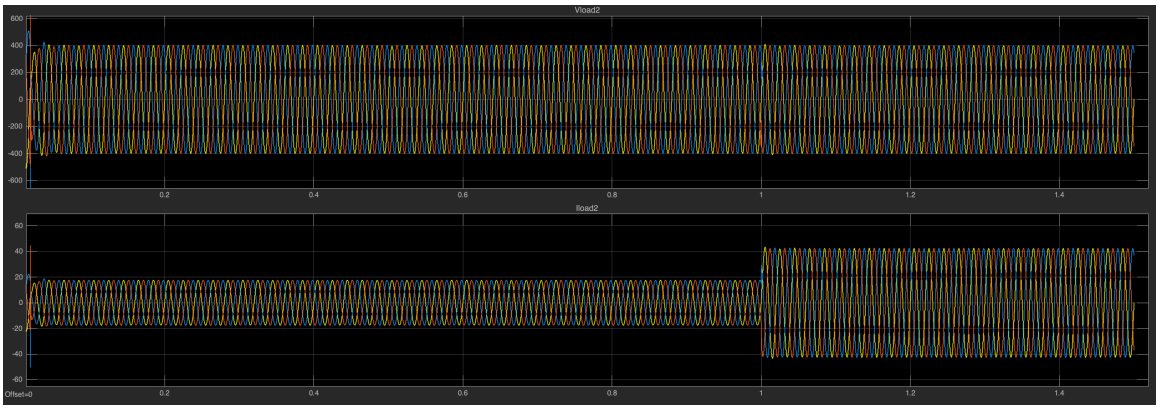

Figure 3.12: Evolution of the 3-phase voltage and current at load 2

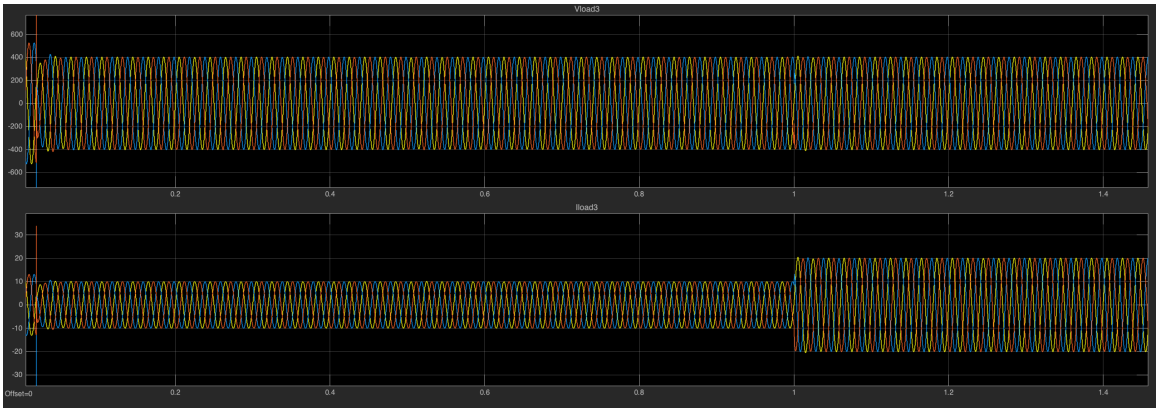

Figure 3.13: Evolution of the 3-phase voltage and current at load 3

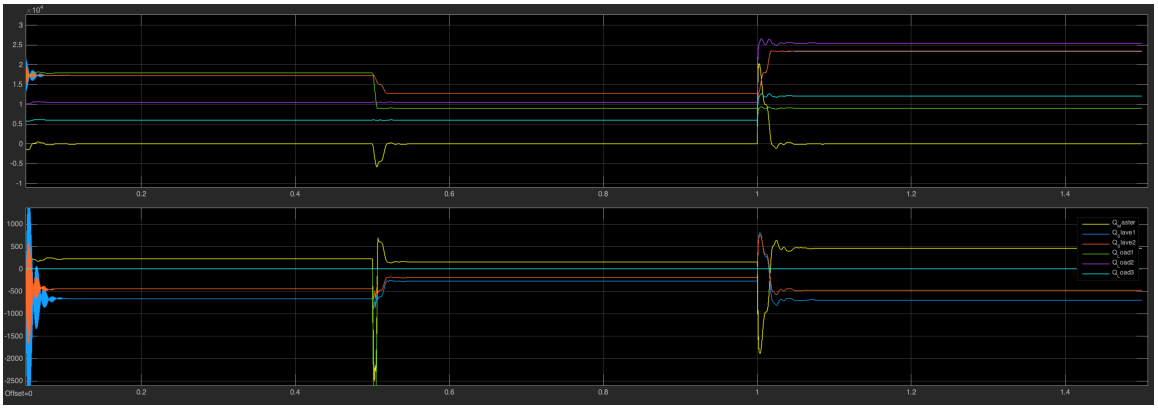

Figure 3.14: Evolution of the power production/consumption: yellow= master, blue = slave1, ref = slave2, green = load1, purple = load2, cyan = load3

2.2 Results analysis

As both slaves are supposed to have the same ratings and are communicated the same reference current (amplitude and phase), their current and voltage ought to reach same values and will so be described by the same wave shapes in Figure 3.10.

A first set of load is connected to the system start at the of the operation ($P_{L1} = 12$ kW, $P_{L2} = 7$ kW, $P_{L1} = 4$ kW). After an initial stabilisation of a couple of milliseconds, the various peak values for currents and voltages of the system are:

Variable	V_{ma}	I_{ma}	V_{sl}	I_{sl}
Value	399.5 V	0.37 A	402.1 V	28.76 A

Variable	V_{L1}	I_{L1}	V_{L2}	I_{L2}	V_{L3}	I_{L3}
Value	399.3 V	29.94 A	400.5 V	17.52 A	401.7 V	10.04 A

The smart voltage regulator situated in the central controller aims for the minimisation of voltage gaps in the system. It thus provides a computed command to the master, which supplies a constant voltage amplitude of 399.5 V to the system, instead of the initial 400 V imposed.
It does lead to insignificant voltage deviations at loads (naturally inside the tolerated limits), with the greatest deviation for Load3, + 1.7 V compared to reference voltage, while load 1 is around 0.7 V below it. It explains the excessively small current provided by the master module.

It is clearly observed in Figures 3.9 and 3.10 that voltages and current phasors are in phase for the slaves and 90° outphased for the master, as predicted for this model.

At **t=0.5 s**, the first load is downscaled to half its value ($P_{L1} = 6$ kW, $P_{L2} = 7$ kW, $P_{L3} = 4$ kW).
This load's decrease leads to even smaller voltage deviations, globally:

Variable	V_{ma}	I_{ma}	V_{sl}	I_{sl}
Value	399.7 V	0.26 A	401.6 V	21.27 A

Variable	V_{L1}	I_{L1}	V_{L2}	I_{L2}	V_{L3}	I_{L3}
Value	400.1 V	15 A	400.3 V	17.52 A	401 V	10.04 A

Current I_{L1} is logically decreasing as an aftereffect, similarly to total the load current. As depicted in Figures 3.6, 3.7 and 3.8, the sharp change of I_{load} is not immediately handled by the slaves, waiting for a readjustment of the reference current. The master compensates for the short-time transition by injecting high-value current into the system to ensure power balance. Its peak current reaches 7.5 A, in other words an expansion of nearly 20 times compared to before load transition! This stabilisation procedure is however quite short (less than 0.03 s) and the system was designed to accept these peak currents.
The slaves command is afterwards adjusted and the master current goes back to normal with a low value of 0.26 A.

At **t=1 s**, load 2 and 3 increase their values ($P_{L1} = 6$ kW, $P_{L2} = 17$ kW, $P_{L1} = 8$ kW), boosting back the total load power. I_{load3} rises to a value 42.49 A, while I_{load} (sum of the three load currents) is now reaching 77.5 A. A Reference current is thus equal to 38.75 A and is sent to the slaves.

Variable name	V_{ma}	I_{ma}	V_{sl}	I_{sl}
Value	400 V	0.76 A	402.8 V	38.8 A

Voltage gaps remain negligible as they do not even outrun 3 V each, reason why current at the slave stays extremely low during the whole simulation. The same buffering phenomenon, however negative this time, as the one previously described is observed for I_{master}, with a stronger difference though, as currents rise unequally for different phases to approximately 22, 29 and 35 A. After less than 0.02 s, the system regulation is operated and a new reference state is established.

Variable name	V_{L1}	I_{L1}	V_{L2}	I_{L2}	V_{L3}	I_{L3}
Value	400.7 V	15.05 A	400 V	42.49 A	401.7 V	20.08 A

V/f controlled master is only taking care of voltage regulation and only injects extremely small amount of active power as the phase between voltage and current is at 90 °. On the other side, a power factor close to unity is observed for slave units with a mainly active injected power. A jump of phase for the master current is also clearly noticed on 3.6, 3.7 and 3.8.

Globally, for the considered distances of the microgrid, the voltage deviations are well handled and never exceed the restricted range. The further the load, the greater the error on nominal voltage as the distance with the reference voltage bus increases and the more line impedance has to be taken into account, even if the difference is negligible as load 2, central to the grid, is the reference node.

The loads being resistive only in this first case, the phase of the slaves does not require important changes and remains more or less constant during the process.

Concerning power consumption/generation, Figure 3.14 shows that active power of the master is fixed at 0, although some short valleys are observed when the global load is reduced and peaks when it is increased, confirming the buffering effect deduced earlier. The opposite effects is observed for its reactive power. In terms of frequency, deviations are extremely narrow, never exceeding 0.5 Hz during transitions, probably due to the fact that sources are ideal.

One can finally notice high transition currents during the initialisation procedure of the system for both master and slaves. The same observation can be made for voltages, surpassing 500 V on a really short time interval.
One way to prevent it and keep them below the desired limit would be a smooth and progressive connection of the loads, avoiding abrupt changes in consumed power (compensated by sources to respect power balance).

2.3 Robustness: distance

The performance of the system operating with master-slave control technique was analysed on a standard configuration in the above section.

The objective is to now try to observe the behaviour of the system while varying the distance between units (i.e. increasing line impedance values), assuming the loads will stay in the same range of values.

Increasing the size of the system to 1km, keeping the same proportion for the reference node to remain central to the grid, means:

$$\overline{AB} : 55m \rightarrow 250m \qquad \overline{BC} : 55m \rightarrow 250m \qquad \overline{CD} : 110m \rightarrow 500m$$

For this simulation, the duration time is 1 second with one load variation taken into account. Initially, loads 1, 2 and 3 are connected to the microgrid with the following ratings: $P_{L1} = 15kW$, $P_{L2} = 6kW$, $P_{L3} = 7kW$.

At t = 0.5 s, each load is pushed to its limits with $P_{L1} = 15kW$, $P_{L2} = 10kW$, $P_{L3} = 20kW$. Four important plots are proposed on Figures 3.15, 3.16, 3.17 and 3.18, while the rest of them are grouped in Appendix B.

Despite a short stabilisation period when the system is initiated at t=0s, a stable state is observed before the load transition with a voltage across load close enough to the reference nominal value as $V_{L1} = 390.1$V, $V_{L2} = 403.4$V and $V_{L3} = 425.5$V. The current amplitude have increased compared to previous case, especially in the master with $I_{master} = 9.95$A, way below the imposed limit though.

When load 2 and 3 are changed to their maximal value at t=0.5 s, one can observe on the different graphs of Appendix B a rise in voltage deviations at each load, as expected: $V_{L1} = 380$V, $V_{L2} = 405.1$V and $V_{L3} = 440.4$V.
The voltage gap to 400 V is at the limit for load 3. A further increase of line impedances or load rating would mean a step out of voltage quality criteria and would force the central control unit to disconnect load 3 (which is considered as the one with less priority). At that limit state, current amplitudes are divided as follows:

$$I_{master} = 19.5A \qquad I_{slave} = 56.9A \qquad I_{L1} = 35.8A \qquad I_{L2} = 50.4A \qquad I_{L3} = 27.62A$$

Voltage V_{L2}, at the reference node stay relatively close to the reference value. The voltage amplitude injected by the master drops to 370 V after load transition. Its phase is adapted after t=0.5s. The longer the lines, the more important phase adjustment becomes to keep the desired power factor at the sources. Like it was the case previously, the master also handles current changes during the transition period and its current shows a noticeable peak during a short term period with a phase jump in it, explaining the noisy shape of I_{master} between t=0.5s and t=0.55s. Globally, at a transition, the phase and the amplitude of all modules are adapted leading to an inconstant active and reactive power.

As observation, one could state that the longer the line, the greater their impedance, leading to higher voltage deviations from nominal value, i.e. meaning deterioration of power quality. Of course, load power consumption impacts the amplitude of these voltage deviations. They must be restricted below a certain value

depending on the line lengths. A length of 1 km is obtained for $P_{Load|tot}$ at 100% of its maximal value. It has been simulated that restricting those loads to 80% of their maximal rating allows greater line lengths before reaching the same voltage deviation limit (40V), with total length of 1.3 km ($\overline{AB} = 330m; \overline{BC} = 330m; \overline{CD} = 660m$).

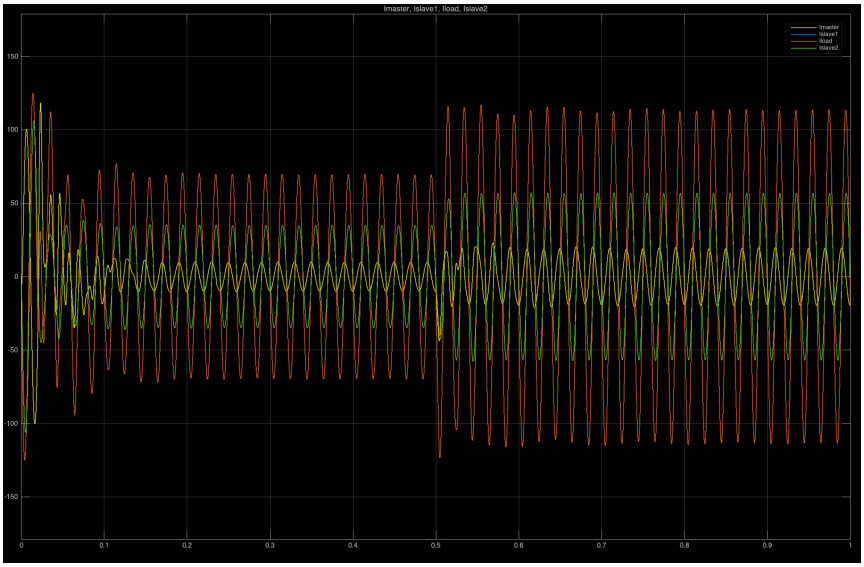

Figure 3.15: Representation of Phase A currents during transition (yellow = master; red= sum of loads; green = slave 1; blue = slave 2)

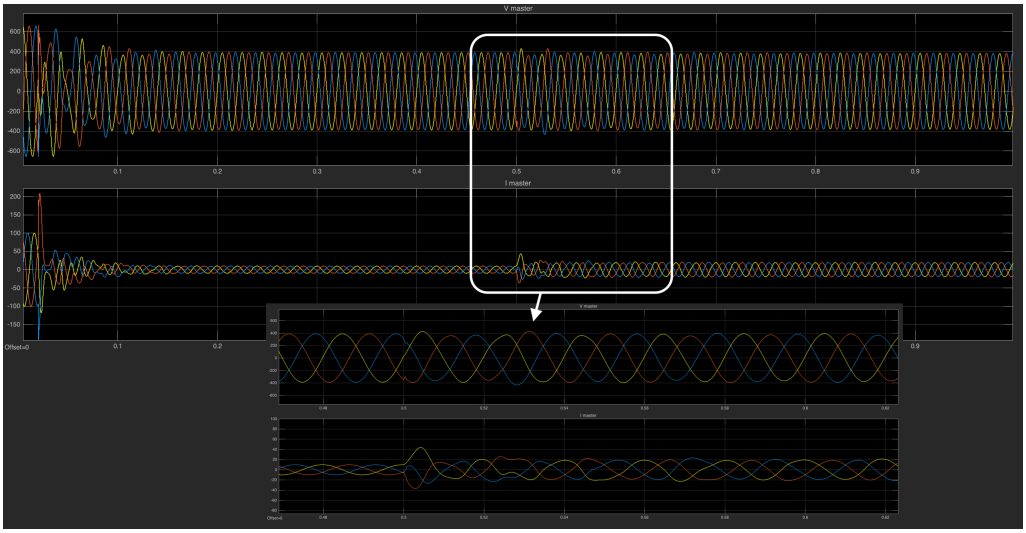

Figure 3.16: Representation of the 3-phase voltage and current for the master

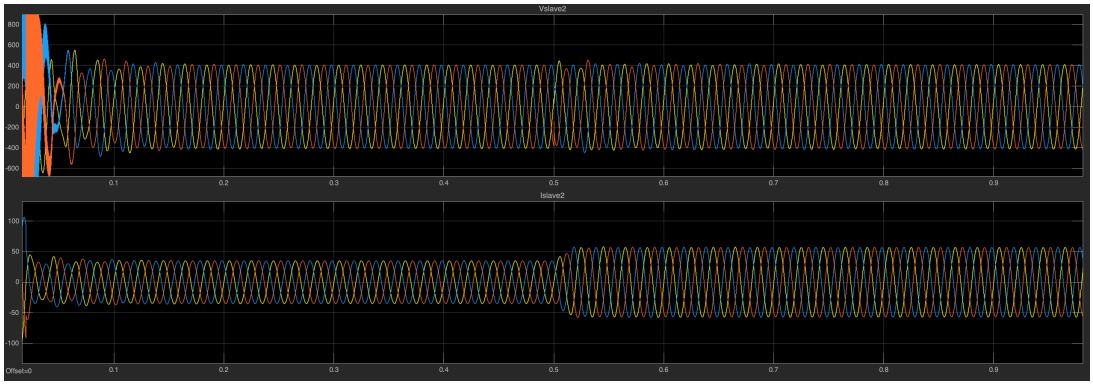

Figure 3.17: Representation of the 3-phase voltage and current for the slaves

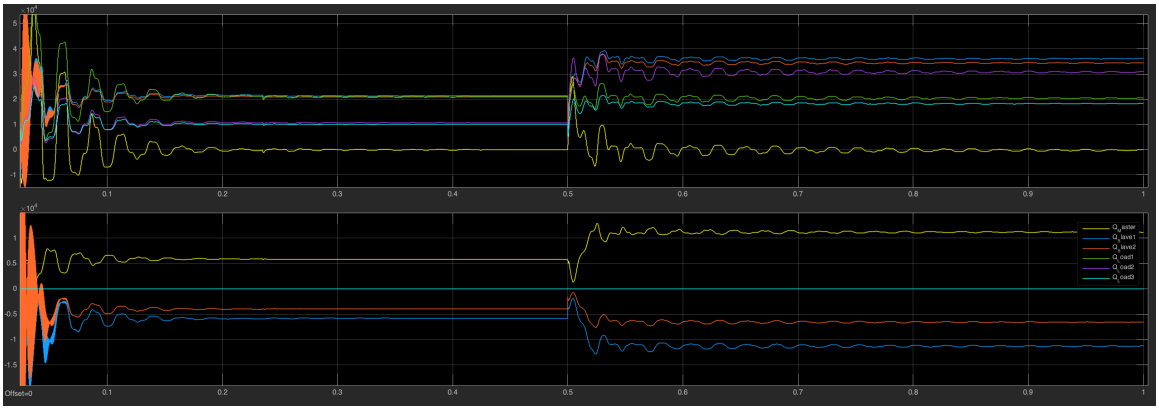

Figure 3.18: Representation of the (re)active power consumption/generation during the simulation: yellow= master, blue = slave1, ref = slave2, green = load1, purple = load2, cyan = load3

Another test has been made changing the length proportion of the microgrid ($\overline{AB} = 800m; \overline{BC} = 400m; \overline{CD} = 400m$), i.e. removing the reference node from central position. Results show more balanced voltage deviations between load 1 and 3 with $\Delta V_{L1} = 35V$, $\Delta V_{L3} = 40V$. This new disposition allows greater line distances (total of 1.6 km) without exceeding allowed voltage gaps.

Configuration	**Result**
100 % of total load - central reference node	1 km
80 % of total load - central reference node	1.3 km
100 % of total load - modified disposition	1.6 km

2.4 Robustness: loss of a generation unit

For this section, the lengths of the system are back to the initial ones ($\overline{AB}$: 55m; $\overline{BC}$: 55m; $\overline{CD}$: 110m).
The idea is to acknowledge the system reaction when confronted to the loss of one of the slave generation units. This situation should be critical for the system as slaves only inject active power to the system (reminder: phase of the slave is adapted to obtain $cos(\phi_M) \approx 0, cos(\phi_S) \approx 1$).

The simulation here lasts 1.5 seconds and initial ratings for the loads are:

$$P_{L1} = 12kW \qquad P_{L2} = 8kW \qquad P_{L3} = 7kW$$

• $\mathbf{t \leq 0.5\ s}$: System is established with loads described above, the two slaves are operational
• $\mathbf{0.5s \leq t \leq 1\ s}$: One of the slaves is cut off, while the loads remain unchanged
• $\mathbf{1s \leq t \leq 1.5s}$: Load 2 increases and jumps to $17kW$, the system tries to handle this load change

Results are shown below, with complementary representations in Appendix B. The observations are the following:
At t= 0s, initialisation of the system in a classical configuration. Total load current $I_{load|tot}$ (in amplitude) is computed and shared among the two operating slaves.
At t= 0.5s, as one of the slaves is removed, the central control unit adapts his command and assigns the whole load current to the remaining slave, as it appears on the first and second graphs of the dedicated section in Appendix B, with the blue and red curve matching each other from that very moment, with a slightly different phase though. The phase of the slaves current is adapted to match power generation criteria. The master current is impacted by a jump in its phase and a rise in the RMS value (to nearly 40 A) as the master, once again, compensates on short time transition while new command is computed for the remaining slave. Current in the mentioned slave obviously rises up to around 70 A and is thus still within the acceptable limit.
Theoretically, slave unit number 2 is still injecting a really low current into the grid (1 A), represented by the green sinusoidal on illustrations.

The second load is increased at t=1s to 17 kW. The buffering effect of the master compensating this load change is still observable. Total load current jumps to 85 A, not recoverable by a single slave unit. The total power it has to deliver is above expectations ($P_{slave1} > P_{max|slave1}$).
Load 3 is here disconnected for $I_{Load|tot}$ to reduce and leading to an acceptable current in the unique slave.

Current distribution are, in term of norms, measured for the different time slots, as (after stabilization):

	0 to 0.5s	0.5s to 1s	1 to 1.5s
I_{master} [A]	0.37	1.31	10.72
I_{slave1} [A]	28.74	57.54	72.83
I_{slave2} [A]	28.74	≈ 0	≈ 0
I_{load1} [A]	29.93	29.93	30.03
I_{load2} [A]	17.52	17.52	42.8
I_{load3} [A]	10.02	10.02	0
Phase of I_{slave} [°]	0	5	8

One can observe that the system is robust in case of loss of one generation unit. However, allowed charges are way more limited as only one slave is needed to inject all the active power asked by the loads.
Nevertheless, as each generation source is sitting alongside with a battery storage unit, both are supposed to be well designed, this case ought to be extremely rare.

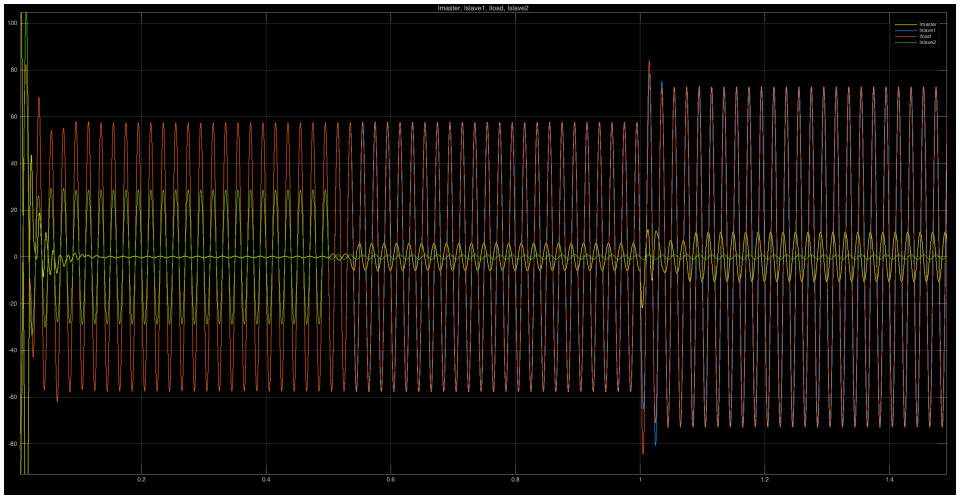

Figure 3.19: Representation of Phase A currents during transition (yellow = master; red= sum of loads; green = slave 1; blue = slave 2)

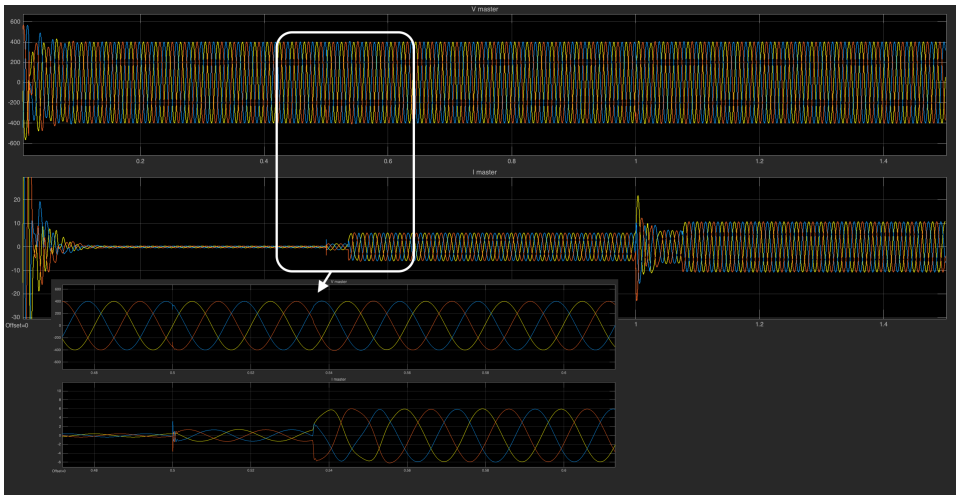

Figure 3.20: Representation of the 3-phase voltage and current for the master

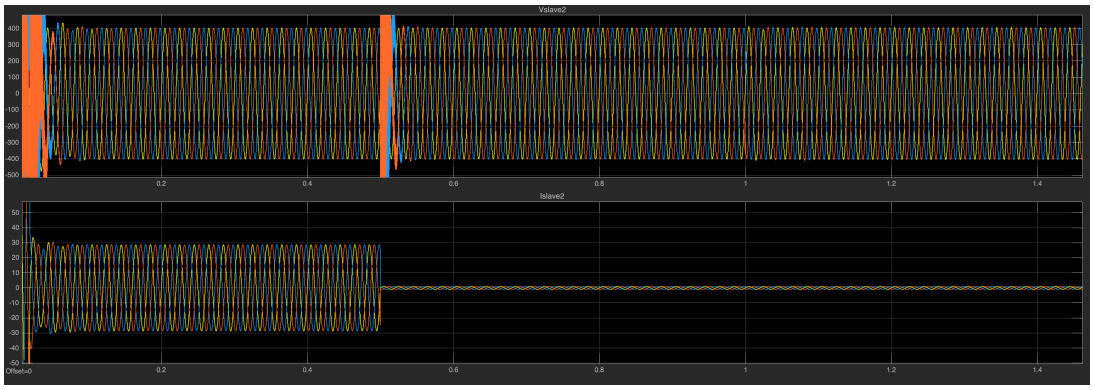

Figure 3.21: Representation of the 3-phase voltage and current for the cut slave

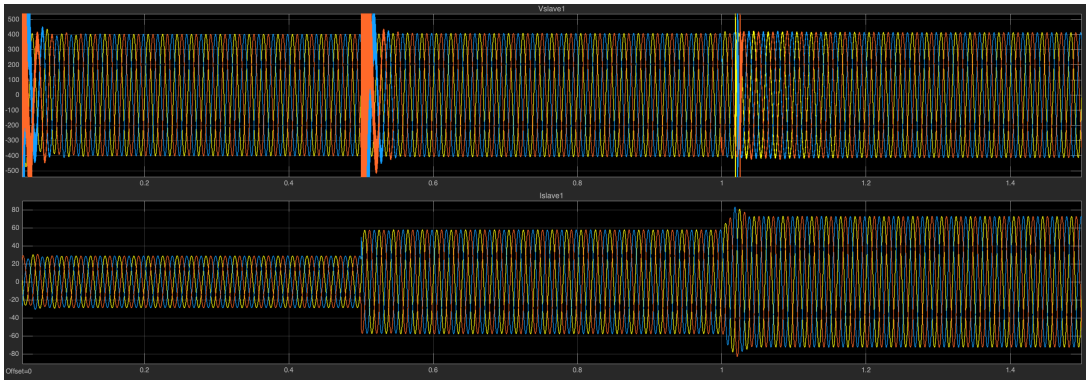

Figure 3.22: Representation of the 3-phase voltage and current for the remaining slave

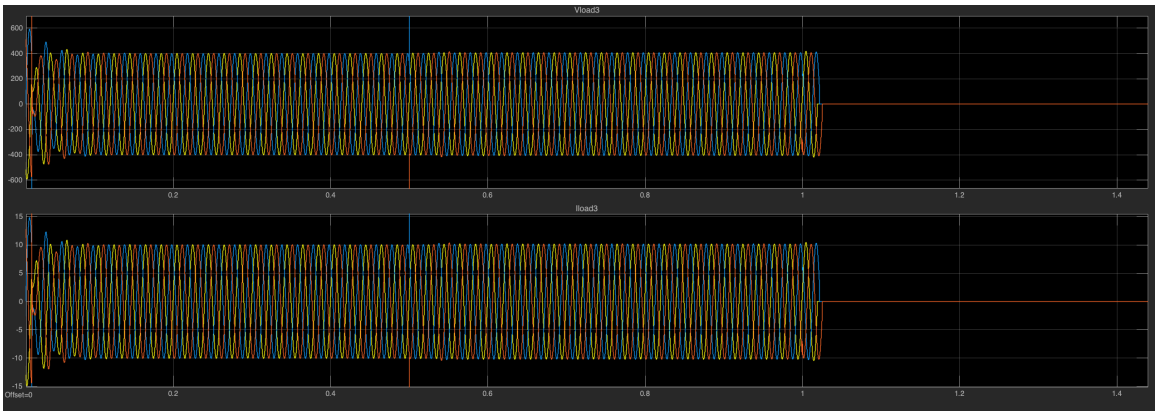

Figure 3.23: Representation of the 3-phase voltage and current for the load3

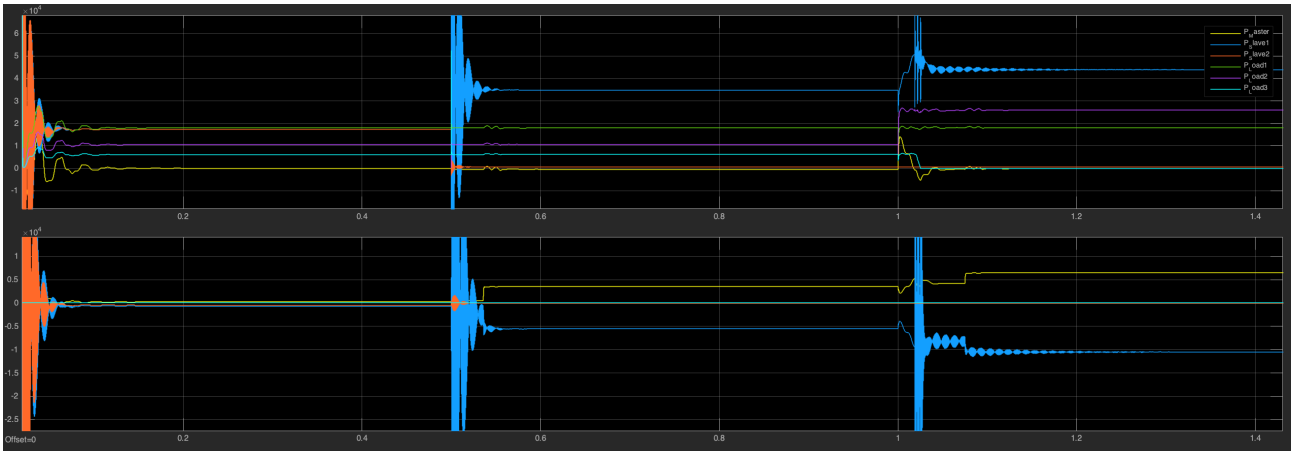

Figure 3.24: Representation of the (re)active power consumption/generation during the simulation: yellow= master, blue = slave1, ref = slave2, green = load1, purple = load2, cyan = load3

2.5 Robustness: capacitive loads

The idea here will be to compare change in the performances with the addition of reactive power consumption in loads. Distances of the microgrid are the same as for the basic simulation and power factor of all consumers may be assumed equal to 0.9, leading. Load ratings are:

-Load 1: (12 kW, 5.8 kVAr) $\xrightarrow{0.5\text{ s}}$ (6 kW, 2.9 kVAr)
-Load 2: (7 kW, 3.39 kVAr) $\xrightarrow{1\text{ s}}$ (17 kW, 8.23 kVAr)
-Load 3: (4 kW, 1.93 kVAr) $\xrightarrow{1\text{ s}}$ (8 kW, 3.86 kVAr)

Simulation time is 1.5 seconds, results are given in Figures 3.25, 3.26, 3.27 and 3.28 with additional ones in Appendix B.
As it was the case for previous simulations, the phase of master voltage source is taken as the reference and remains constant during the whole time, while the phase of the slaves current sources is constantly adjusted to obtain the desired power factor at DGs.

A glance at the power consumption of the system shows even small active power consumption for the master resulting in a slightly smaller than 0 power factor there. Noisy shape at each transition is explained by the voltage regulation process, which takes less than 0.1 second to stabilise the voltage across loads. It is clearly demonstrated and easily deduced at t=0.5s that, once again, master compensates for the abrupt active power consumption changes before finding back its initial generation after the command for the slaves is recomputed.

The phase shift of the voltage phase at the master is clearly observed for both the voltage and the current on master plot, at t=1 s for example. This phase shift is logically reverberated on the different load signals. In terms of voltage deviations and current amplitude, the following values are observed:

$|\Delta V|$

	$0s \rightarrow 0.5s$	$0.5s \rightarrow 1s$	$1s \rightarrow 1.5s$
Master	22	30.5	30
Load 1	1.8	2.8	2.2
Load 2	5.2	6.8	9.9
Load 3	10	12.9	19.7

Table 3.3: Voltage deviation to 400 V

Globally, voltage deviations are way greater compared to the pure resistive loads case, even if the limit for voltage quality issues is not exceeded at any time.

	$\|I\|$		
	$0s \rightarrow 0.5s$	$0.5s \rightarrow 1s$	$1s \rightarrow 1.5s$
Master	35.4	26.01	49.1
Slave	32.4	23.9	44.2
Load 1	33.5	16.7	16.7
Load 2	19.7	19.7	48.3
Load 3	13.4	13.3	23.3

Table 3.4: Current amplitude

Bigger current amplitudes are also observed overall, especially for the master unit.

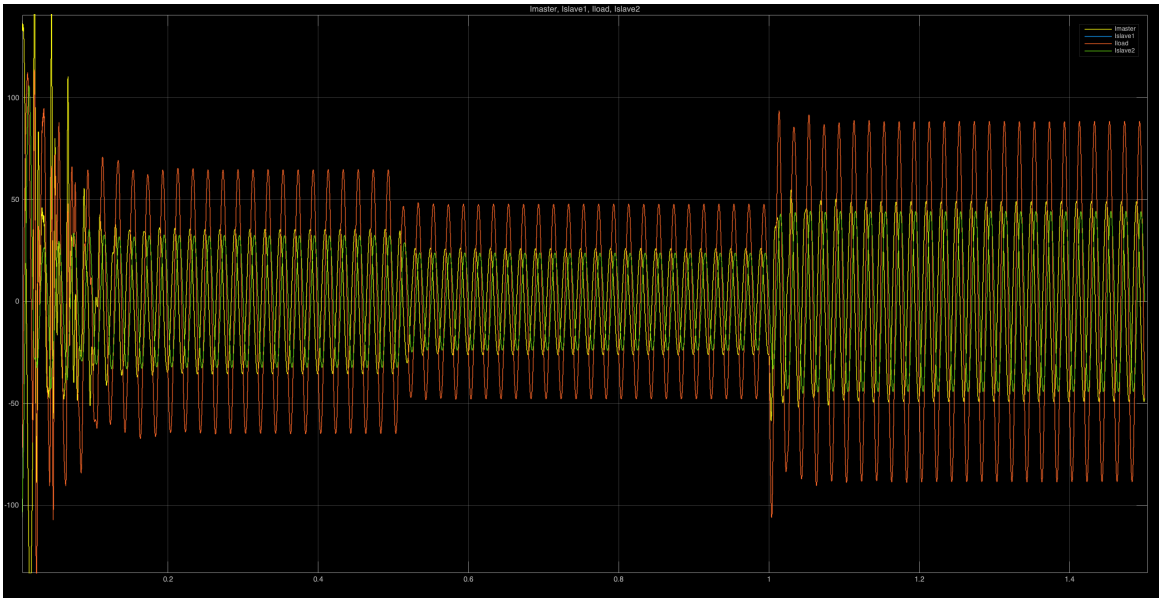

Figure 3.25: Representation of Phase A currents during transition (yellow = master; red= sum of loads; green = slave 1; blue = slave 2)

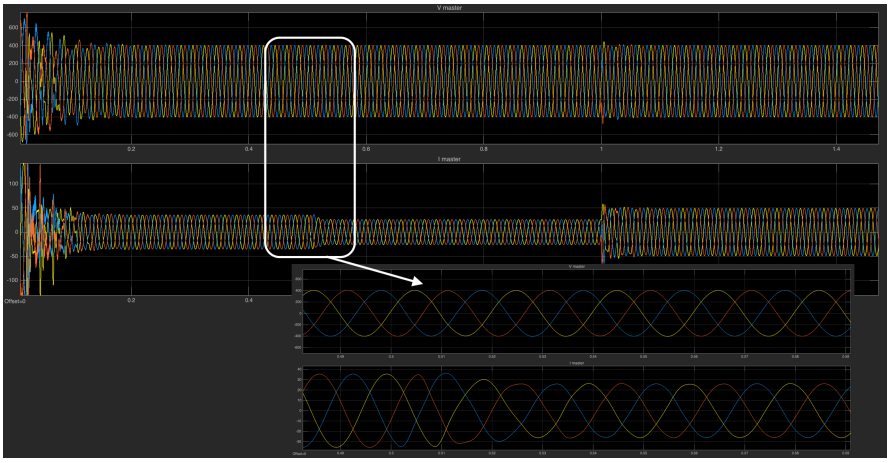

Figure 3.26: Representation of the 3-phase voltage and current for the master

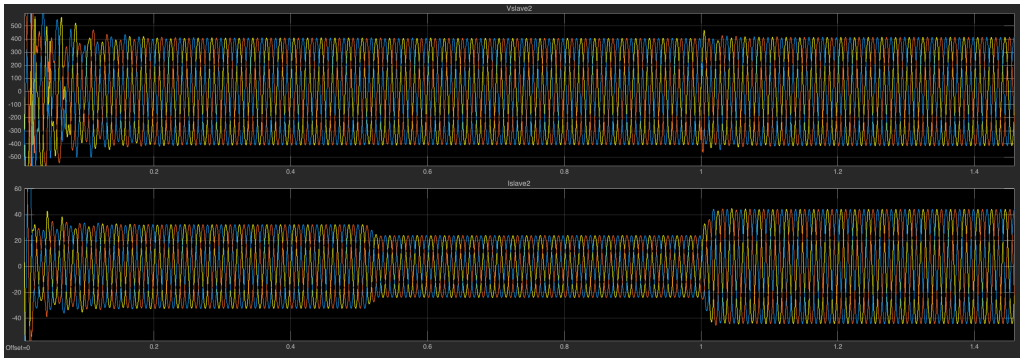

Figure 3.27: Representation of the 3-phase voltage and current for the slave

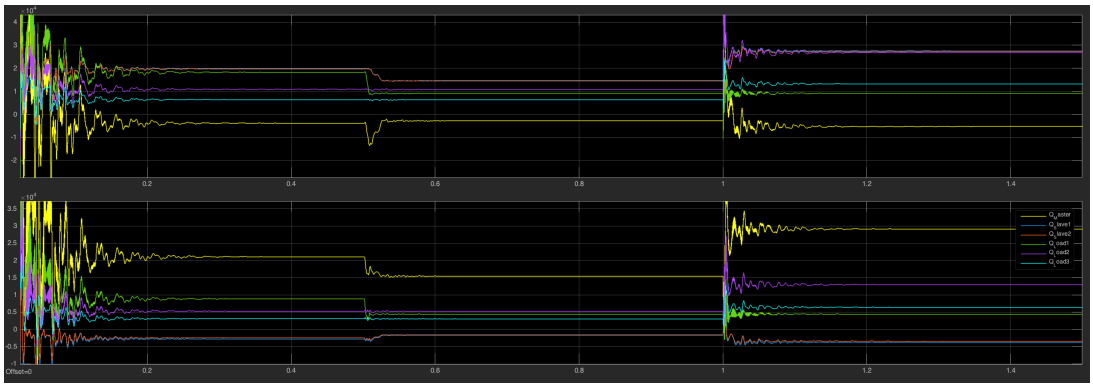

Figure 3.28: Representation of the (re)active power consumption/generation during the simulation: yellow= master, blue = slave1, ref = slave2, green = load1, purple = load2, cyan = load3

2.6 Robustness: inductive loads

For the last case including partly inductive loads (0.9 power factor, lagging this time), control on the slaves current phase turned out to be even more important than for previous simulations. Indeed, change in the phase brought a vertical offset between phases of the current at the master, with repercussions on the loads. Even with the right settlement, big load changes (such as the one observed in t=1s) seem to generate this vertical offset, however attenuated after a 1 second timescale, as proven on plots below (for load 1, 2 and 3 voltage and current evolution, consult Appendix B).

$|V|$

	$0s \rightarrow 0.5s$	$0.5s \rightarrow 1s$	$1s \rightarrow 2s$
Master	433	425.3	439.8
Load 1	395.6	398.4	399.3
Load 2	388.9	391.6	386.7
Load 3	380.9	384.6	377

Table 3.5: Voltage across different modules

$|I|$

	$0s \rightarrow 0.5s$	$0.5s \rightarrow 1s$	$1s \rightarrow 2s$
Master	56.05	41.6	63.11
Slave	31.32	23.16	41.61
Load 1	32.96	16.6	16.64
Load 2	18.91	19.03	45.67
Load 3	10.58	10.68	20.03

Table 3.6: Current amplitude

Contrarily to previous cases, voltage at loads is lower than the reference values. The main cause is that, contrarily to capacitors, inductors consume reactive powers. To counterbalance this, the master is now injecting negative reactive power and injects voltage greater than 400V as reference for the system. Voltage deviations are inside the limits with the greatest one during the last observation period, at load 3, with $\Delta V_{L3} = 23V$ made possible by a 433 V imposed voltage by the master. A slightly oscillating power is observed for the master and each loads due to previously announced offset, but the effect is damped after less than 1 second.

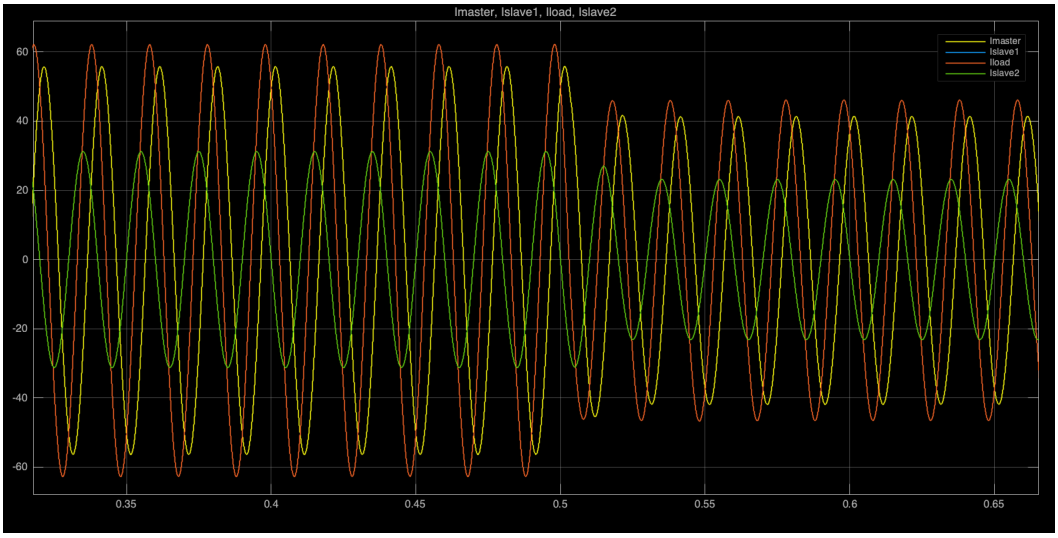

Figure 3.29: Representation of Phase A currents during transition (yellow = master; red= sum of loads; green = slave 1; blue = slave 2)

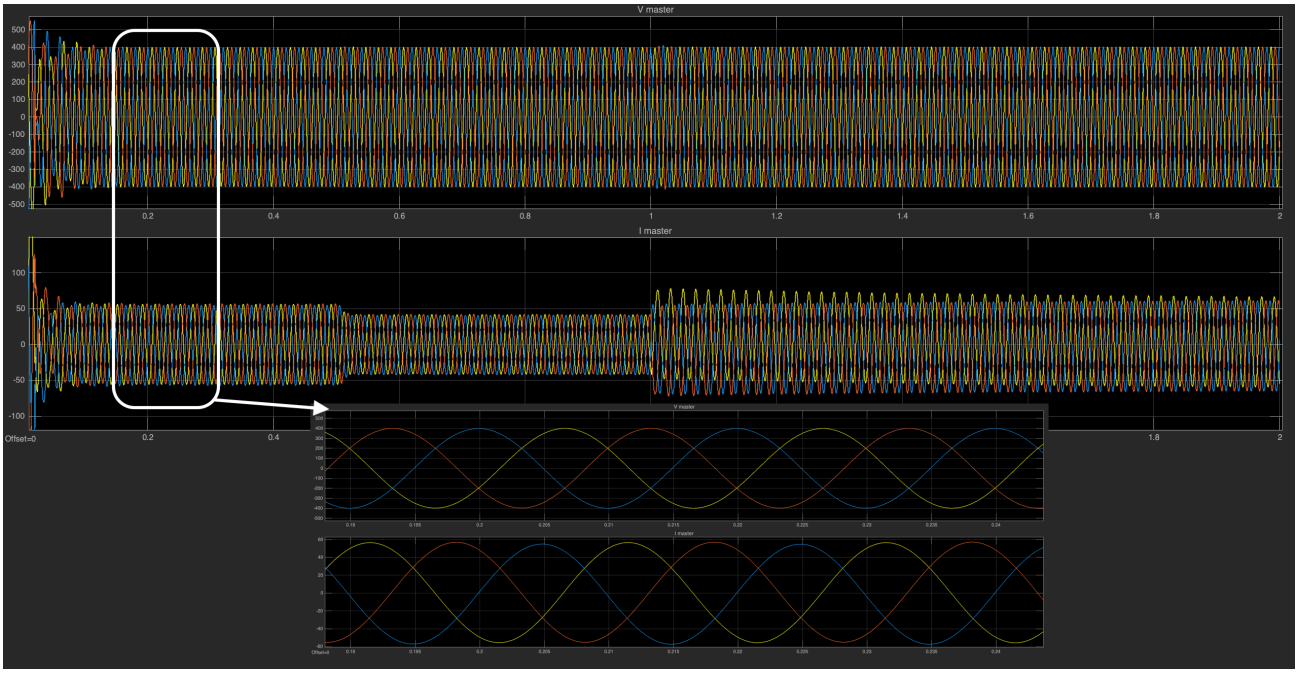

Figure 3.30: Representation of the 3-phase voltage and current for the master

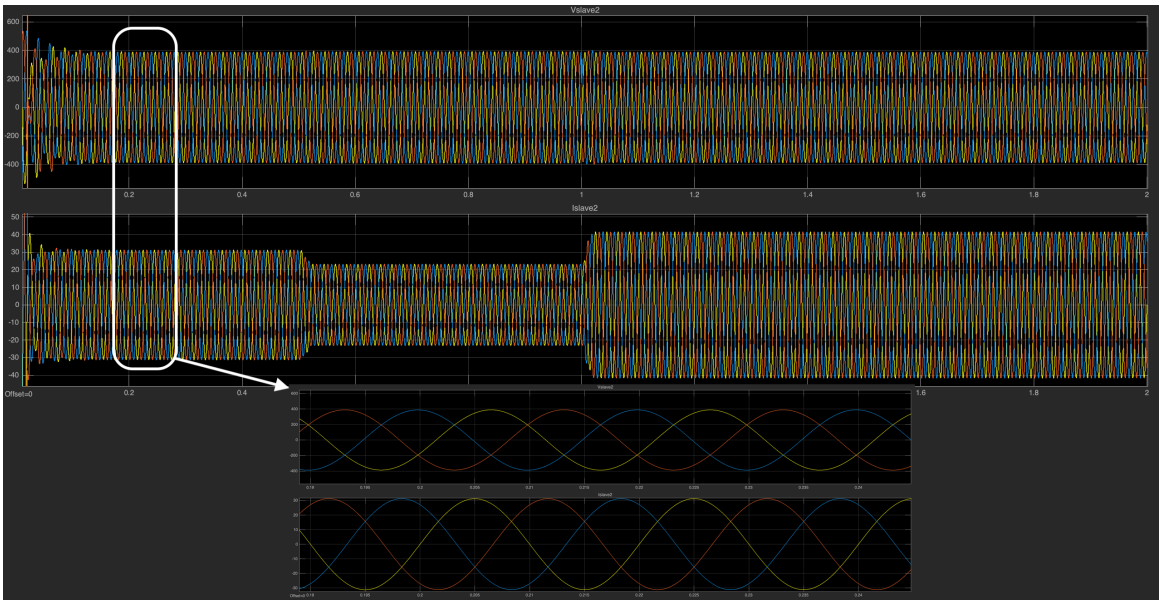

Figure 3.31: Representation of the 3-phase voltage and current for the slave

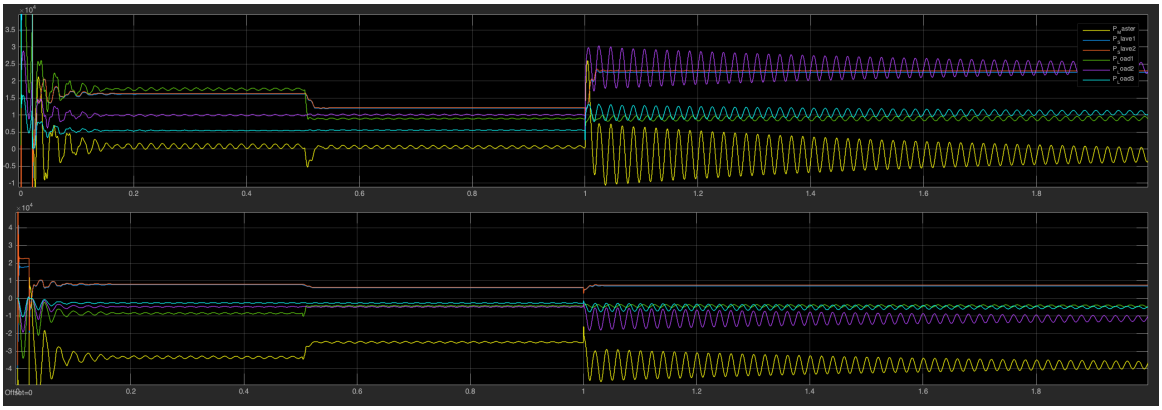

Figure 3.32: Representation of the (re)active power consumption/generation during the simulation: yellow= master, blue = slave1, ref = slave2, green = load1, purple = load2, cyan = load3

2.7 Sizing of DGs

With the simulations now being performed, the power DERs should be able to deliver can be determined. The voltage regulating master will produce reactive power and active power during load transition times, while slaves cover active power generation.

Performed simulations have demonstrated that, for the considered load, the maximum current norms obtained in the master and the slaves are respectively $I_{Master|max} = 85A$ and $I_{Master|max} = 65A$.

Considering the apparent power expression:[31]

$$S = \sqrt{3} U_L I_L$$

$$\Leftrightarrow S_{max} = \sqrt{3} U_{L|max} I_{L|max}$$

In order to deliver quality power, line voltage is expected to variate by $\pm 10\%$ of the rated voltage of the network (in other words, $|\frac{\Delta U}{U}| \in 0.1$) according to European norm NF EN 50160.

With $U_{Ln} = 400V$, the voltage value is expected to range between 360 V and 440 V. Considering these values, one obtains:

$$\left| \begin{array}{l} S_{Master|max} \approx 64 \text{ kVA} \\ S_{Slave|max} \approx 50 \text{ kVA} \end{array} \right.$$

Two installations of 60 kW are considered for slave units, one made out of PVs, the other represented by a small-scale windturbine. Possibilities for the master unit will be discussed further on.
However, these are the values that will need to be provided at the output. The global efficiency of the generation units needs be considered: 0.45 for the WT, 0.25 for the PV installation.

Finally, it is important to note that the master has been "completely oversized" to make it able to deal with extreme cases; the value considered for $I_{Master|max} = 85A$ ought to be rarely reached. It should only be observed in the specific case of transient operation with inductive loads pushed towards their limits. In other words, master production should stay way below the apparent power of 64 kVA, except in the case where it has to cover simultaneously both the reactive power consumption and the active power change during a load transition.

3 Droop control

As already explained in subsection 5.2, the Droop control method is based on measurements taken at the output of the inverter itself, with no need of communication lines. So every controller acts as a controlled voltage source (VSI) [32] and behaves both like a P/V and a Q/f controller at the same time. One unit has a grid-forming role, the others are grid-supporting. [33]
The general symbolic circuit implementing droop control is shown in Figure 3.33.

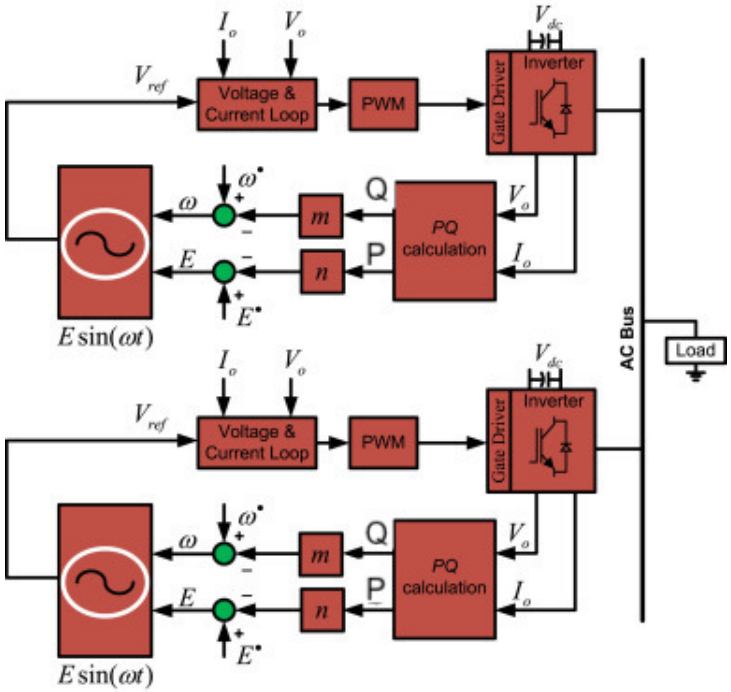

Figure 3.33: Representation of the general circuit of droop control [34]

• **Global droop control:** The general scheme of a controller is depicted in Figure C.3, and its operation mode is described as follows: the current and voltage are measured at the output of the controller and form the input data ($V_{abc|inv1}$ and $I_{abc|inv1}$ in the scheme) in order to compute the active and reactive power. These two influence the new value by applying the droop control itself as illustrated in Figures C.1 and C.2. The new reference values for the frequency and voltage are then compared with the previous ones, initially of 50Hz and 400V. The consequent error is minimised by passing through a PI controller; the corrected value forms the command sent to the generation unit, as shown on Figure C.4.

• **Droop control on active power:** The droop control on the active power P is illustrated on Figure C.1, where the measured value of the active power is

multiplied by the droop coefficient. According to the information found in the article [35], the value for this coefficient is taken as the inverse proportional to the amount of power the controller is designed to deliver.
This result is finally compared with the reference frequency of 50Hz, integrated and directly used to generate the signal frequency.

• **Droop control on reactive power:** Concerning voltage control, the reactive power Q is multiplied by another droop coefficient, which is here a function of a tenth of the rated power of the inverter. The result is compared with the reference voltage of 400V and then passed through a PI controller before being sent to the signal generation unit. This process is depicted on Figure C.2.

• **Signal generation:** With the updated value for the electric voltage and frequency, as shown in Figure C.4, a signal is created, compared with the reference voltage and then sent to the controlled voltage source.

The module $1/z$ is used to induce a step delay, necessary in the simulation to prevent an algebraic loop, as the value measured is used to calculate the following one.

3.1 Simulation procedure

As previously, the simulation is realised using MATLAB/Simulink for a duration of 1.5 seconds with a variation of load ratings every 0.5 second, allowing to observe the behaviour of the grid using droop control method. Load changes are the same as for the master/slave control (as the goal will be to compare both control methods in the next chapter).

Illustrations

The voltage and current measured at the output of the inverters and the loads are depicted in Figure 3.34 and 3.35, respectively. Their power consumption/generation is shown on Figures 3.36 and 3.37.

Now, the average voltage measured at the output of the inverters are presented on Figure 3.38.

Afterwards, the frequency of each inverter is provided on Figure 3.39.

Finally, the RMS voltage recorded at each loads is exposed on Figure 3.40.

Figure 3.34: Voltage and current of the three inverters

Figure 3.35: Voltage and current of the three loads

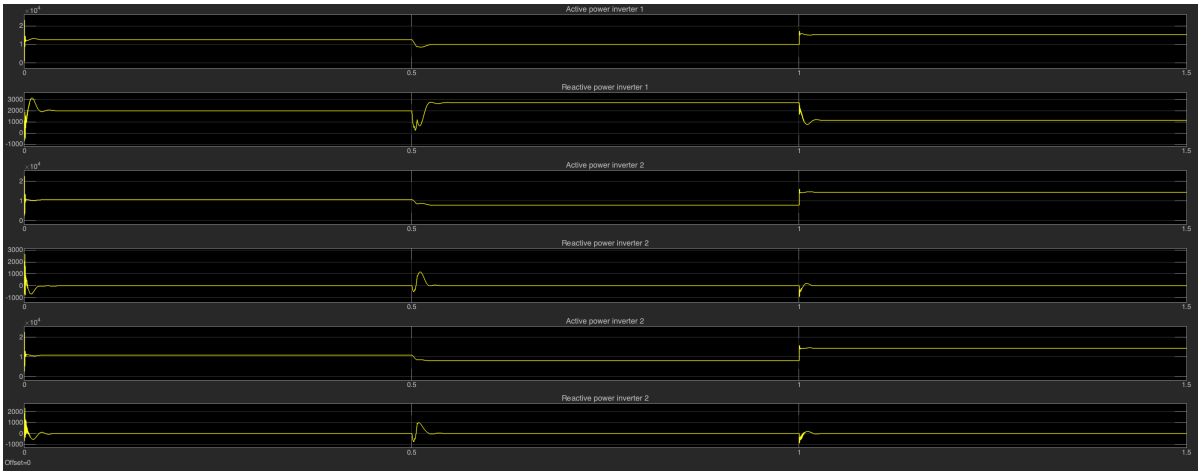

Figure 3.36: Power of the three inverters

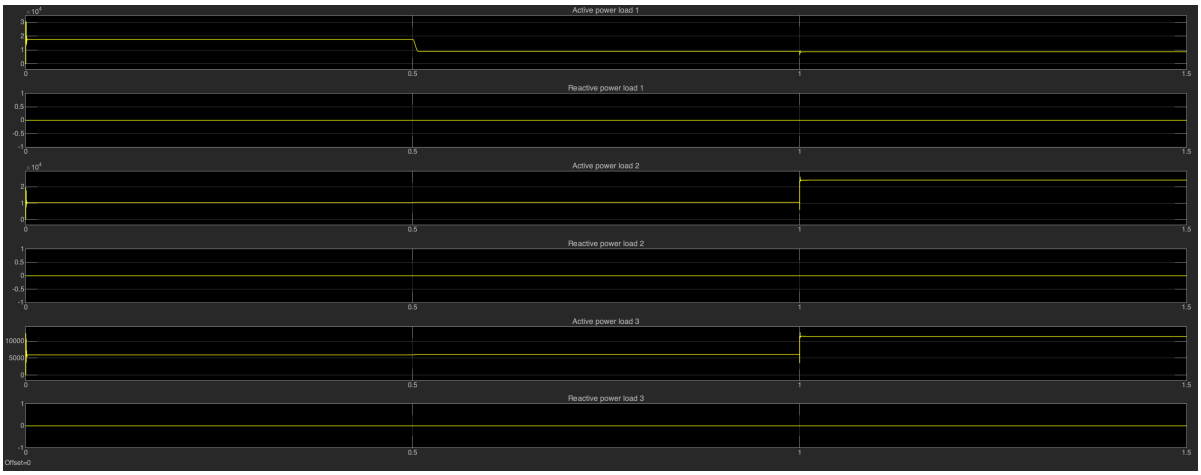

Figure 3.37: Power of the three loads

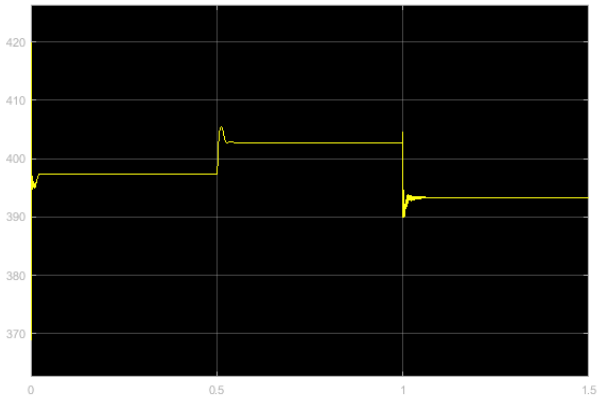

((a)) Average voltage at inverter 1

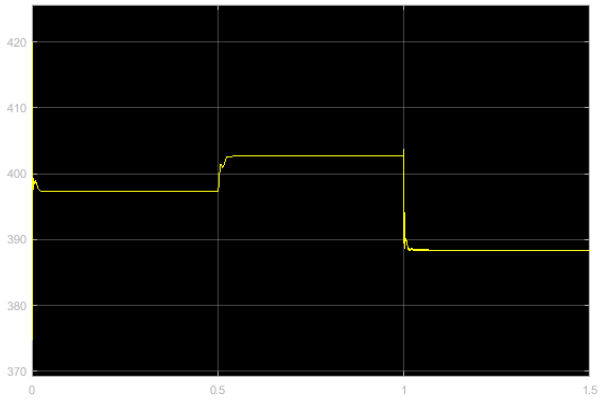

((b)) Average voltage at inverter 2

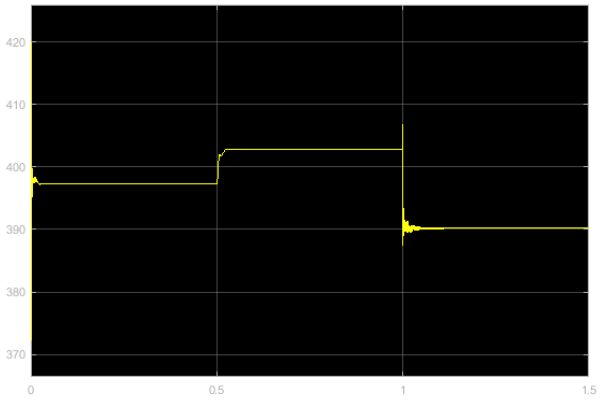

((c)) Average voltage at inverter 3

Figure 3.38

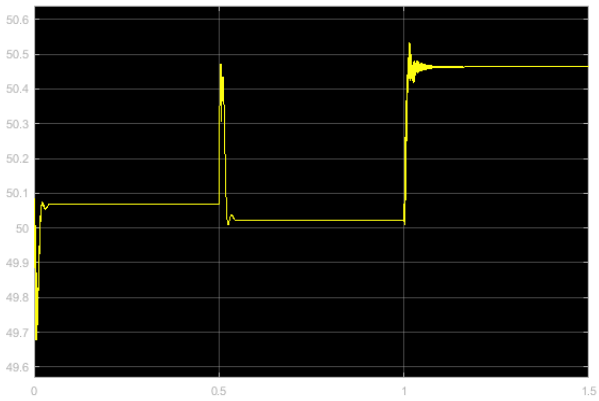

((a)) Frequency at inverter 1

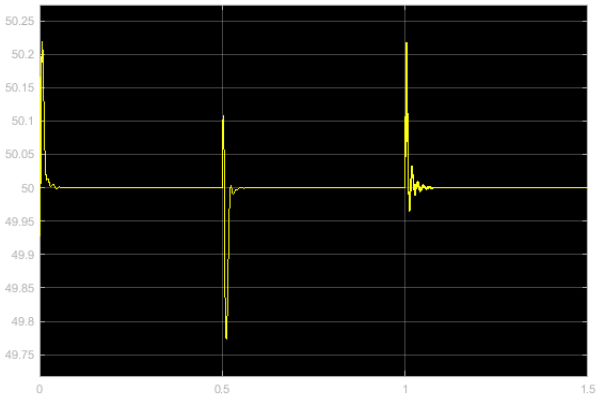

((b)) Frequency at inverter 2

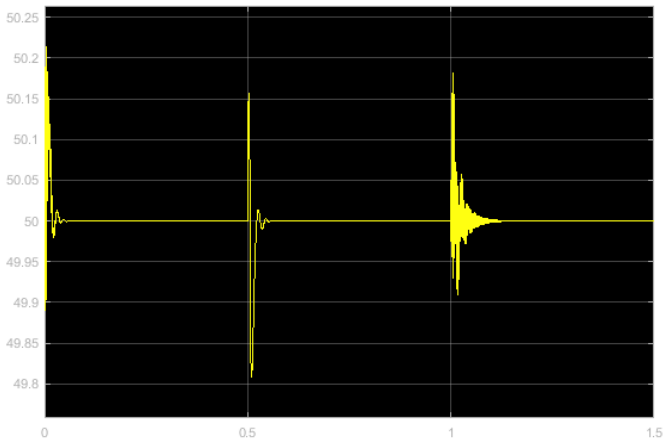

((c)) Frequency at inverter 3

Figure 3.39

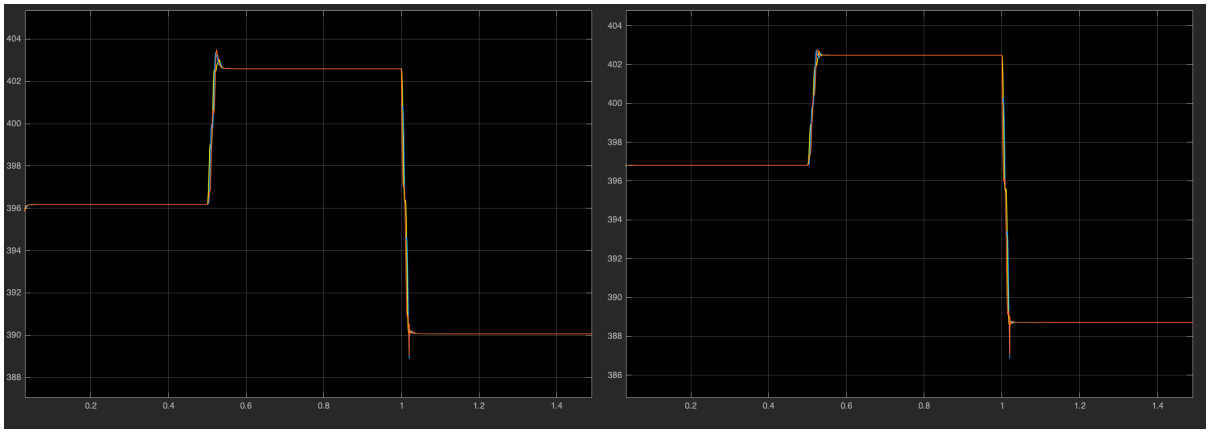

((a)) RMS voltage load 1

((b)) RMS voltage load 2

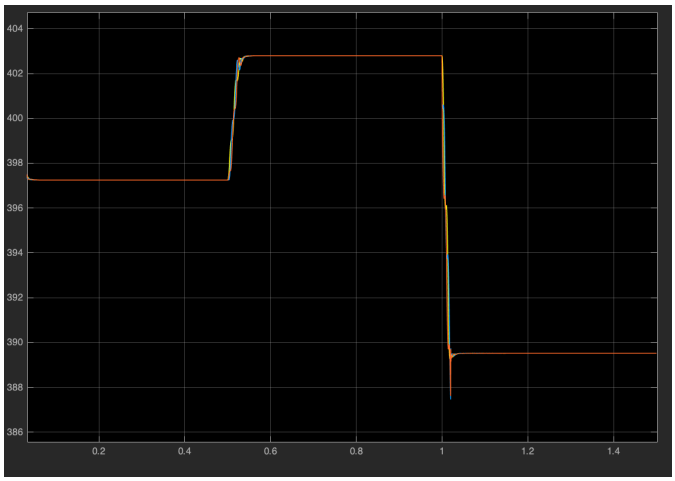

((c)) RMS voltage load 3

Figure 3.40

3.2 Results analysis

Only the case of balanced and purely resistive loads is considered here at first (a reactive part is included in the lines though).

Firstly, the phase shift between the three voltages and currents remains constant. As one can observe in Figure 3.34, the voltage and current at inverters are well synchronised. One should also observe a legit current decrease at 0.5 second of simulation and the right increase at 1 second, according to the demand of power due to the load variation on the grid.
Secondly, in Figure 3.35, the voltages and currents remain well balanced; same observation can be made for the loads. The current and voltage norms are the ones expected.

But the most interesting part is to examine the ability of the droop control technique to handle the variation of the loads. The mean voltage is depicted on Figure 3.38 for each inverter, while the frequency is shown in Figure 3.39.
As observed, the variation of voltage is not the same for each controller. For the first perturbation, all of them seem to show the same increase of voltage, while for the second one the inverter 1 is the less affected, compared to inverter 2 and inverter 3. An explanation could be the distance between the variation point and the source, which is obviously larger for the inverter 1. In every situation, the voltage is satisfying the standard margins, what demonstrates a good control of the voltage.

Concerning the variation of frequency, one can observe a peak caused by the variation of the loads, followed by an equally fast return to the tracked frequency (less than 0.1s). Inverter 1 is the only one exhibiting a significant increase after the second variation, as depicted in Figure 3.39(a). As long as the peak of frequency remains small compared to 50Hz, one can deduce an appropriated control of the frequency by the droop control method.

For the evolution of the active and reactive power, a non zero reactive power produced by the inverters is observed. This production is explained by the presence of a reactive part in the impedance of the line. In the period of transition, the inverter has to support a consequent variation of power (especially reactive). In fact, it has been demonstrated that the smoothness of the power curves is function of the tuning of the droop coefficients.

One last phenomenon to observe is the voltage gap encountered at the loads due to their variation, as demonstrated on Figure 3.40. They are summarised in the following table:

	V		
	$0s \rightarrow 0.5s$	$0.5s \rightarrow 1s$	$1s \rightarrow 1.5s$
Load 1	396	403	390
Load 2	397	403	389
Load 3	398	404	390

Table 3.7: Voltage measured at the loads

As expected, the voltage at the loads remain within the imposed boundaries.

3.3 Robustness: loss of a generation unit

In this case, the loss of one generation unit is considered. The inverter 2 is switched off at 0.5s, which can be induced by several phenomena such as a fault on the grid or a predicted disconnection (needed to implement maintenance for instance). At 1 second of simulation time, load 3 is increased from 7kW to 17kW and the system needs to cope with this situation.

The Figure 3.41 depicts the average voltage at the loads with DG loss, the lowest voltage observed at the loads is 365V in the worst case. The system is able to stay within the margins and to cope with the loss of a source.

As shown on Figure 3.42, the loss of an inverter induces a big drop in inverter 1 mean voltage (the furthest from the lost DG), while inverter 3, closer from the failure, undergoes a smaller increase of mean voltage. Once again, the system is capable to stay within the voltage limits; the voltage norm ranges between 375 Volts and 420 Volts everywhere on the grid.

Only controller 2 is switched off (however not disconnected), so the lowest remaining voltage of 365 Volts is observed at its output.

	V		
	$0s \rightarrow 0.5s$	$0.5s \rightarrow 1s$	$1s \rightarrow 1.5s$
Inverter 1	394	384	374
Inverter 2	395	420	420
Inverter 3	395	385	375

Table 3.8: Voltage measured at the loads with loss of DG

A glance at Figure 3.43 illustrating frequency evolution shows an important variation of about 1.5Hz, which is relatively significant. The transient duration

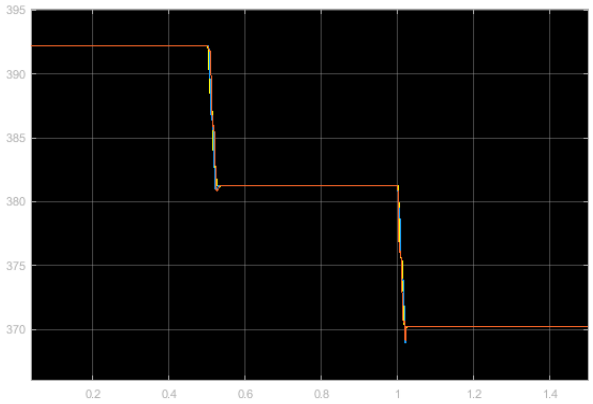

((a)) Load 1

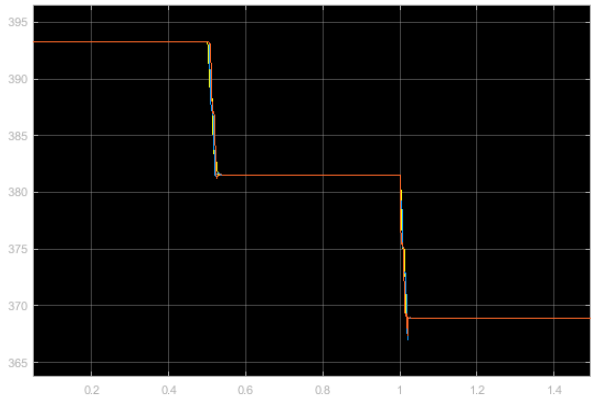

((b)) Load 2

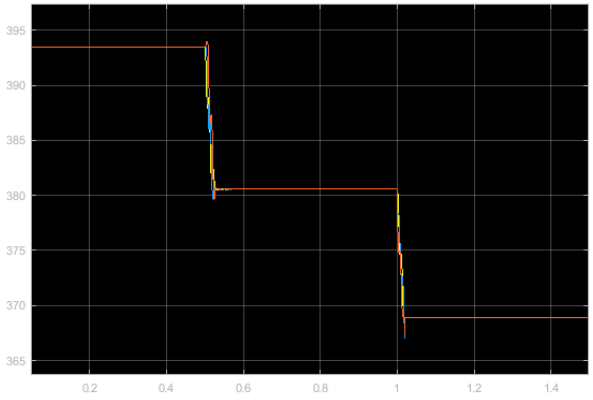

((c)) Load 3

Figure 3.41: Average voltage at the loads with DG loss

remains lower than 0.1s though, which is small enough. This can be explained by the fact that the droop control is based on a Q/f relation, the loss of the inverter 2 has thus a big impact on the total quantity of reactive power received by the

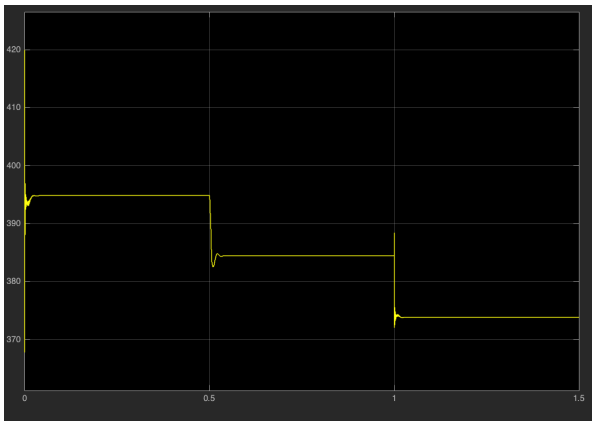

((a)) Inverter 1

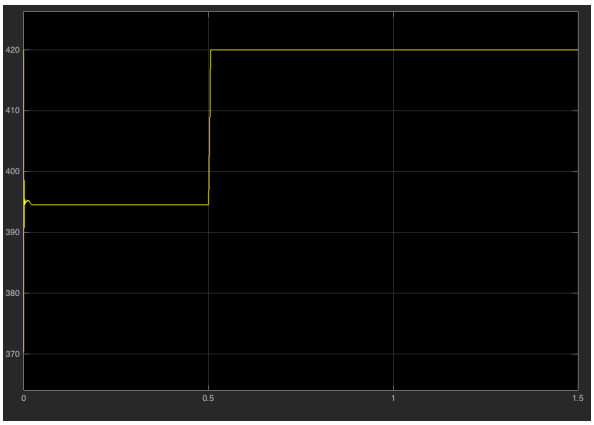

((b)) Inverter 2

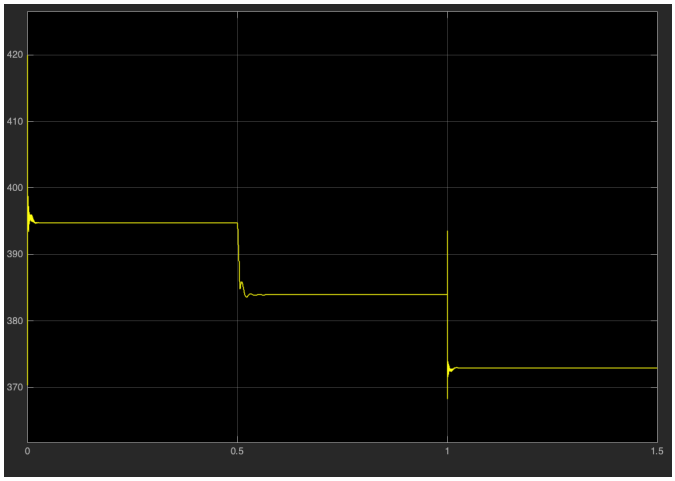

((c)) Inverter 3

Figure 3.42: Average voltage at the inverters with DG loss

grid and its loss forces the frequency to be controlled only by the two remaining

controllers. It induces a non negligible deviation in amplitude and impacts the dynamic of the control.

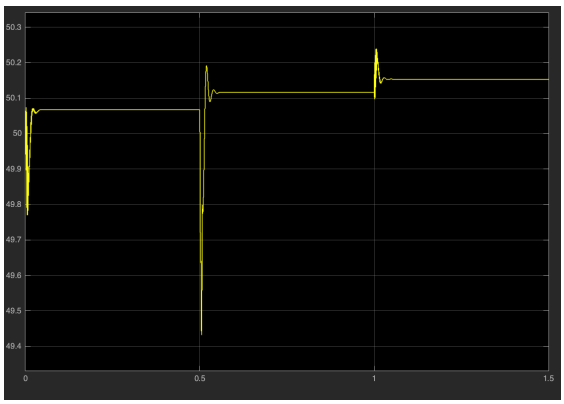

((a)) Inverter 1

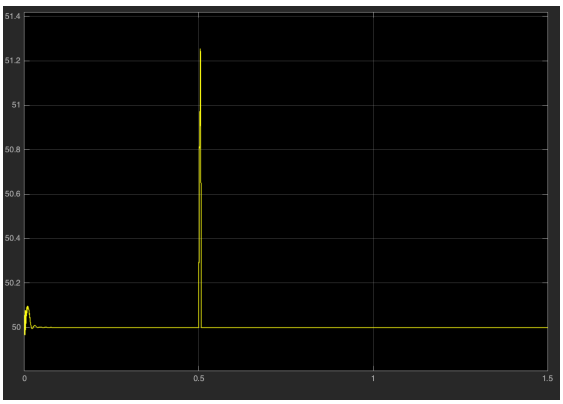

((b)) Inverter 2

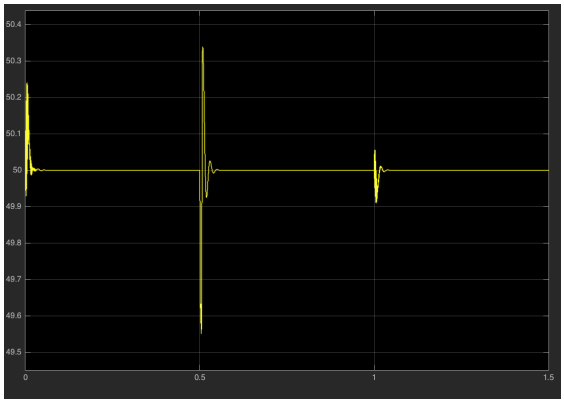

((c)) Inverter 3

Figure 3.43: Frequency at the inverter with DG loss

Besides, the two inverters are able to provide enough power to supply the three loads; no load disconnection is needed using the droop control method which is a main advantage. The power delivered by each inverters is shown in Figure 3.44.

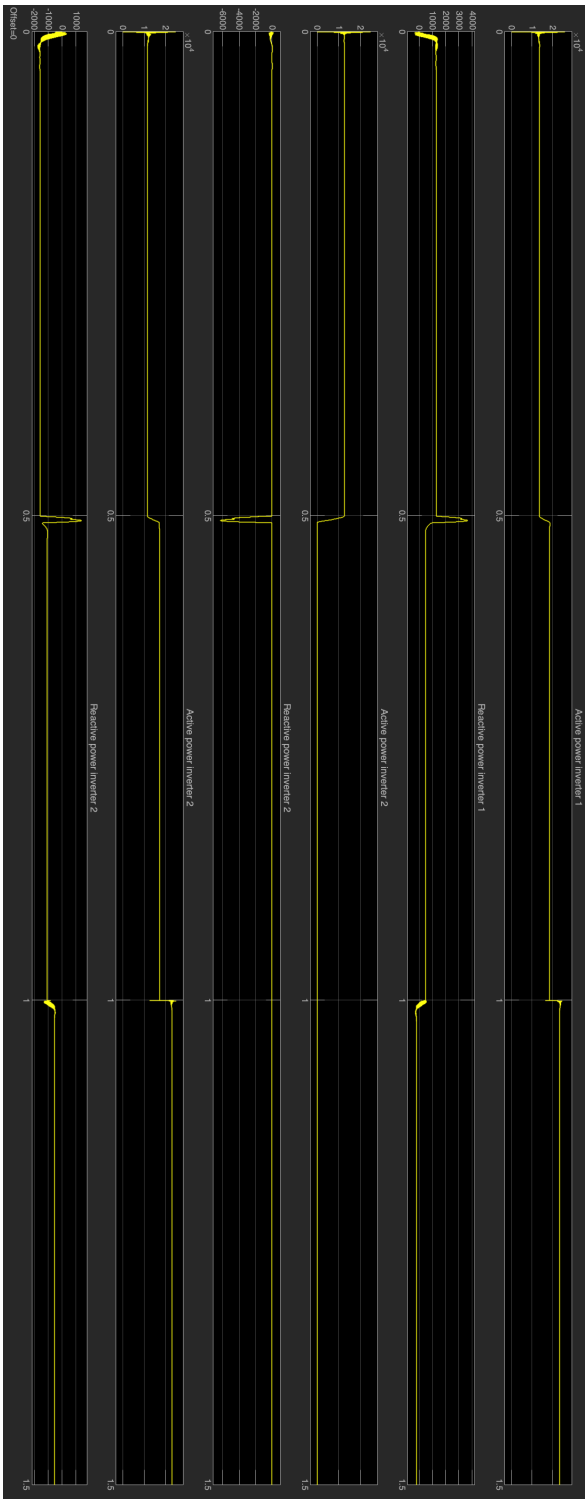

Figure 3.44: Power delivered by the inverters in case of the loss of inverter 2

3.4 Robustness: distance

In this section, as depicted in the appendix D, the line distances are progressively increased to 1km, keeping the same proportion to match what has been simulated for MS control, meaning:

$$\overline{AB} : 55m \rightarrow 250m \qquad \overline{BC} : 55m \rightarrow 250m \qquad \overline{CD} : 110m \rightarrow 500m$$

For this simulation, the duration time is 1 second with only one load variation taken into account. Initially, loads 1, 2 and 3 are connected to the microgrid with the following ratings: $P_{L1} = 15kW$, $P_{L2} = 6kW$, $P_{L3} = 7kW$. Then at t = 0.5 s, each load is pushed to its limits with $P_{L1} = 15kW$, $P_{L2} = 10kW$, $P_{L3} = 20kW$.

The lowest voltage observed at the output of an inverter is greater than 370V, so staying into the standard margins. For the frequency, variations do not exceed 1 Hz (staying between 49.6 and 50.5Hz), what is acceptable, as shorts.

Afterwards, the distance is boosted to 2km and even further to 5km. According to the results, the grid behaviour is sensibly the same as the one for a 1km distance. As it is limited to the case of a microgrid, the size of the electrical network is restrained to 10km. As one can see, the voltage never drops below 365V, and never rises above 410V. The frequency can reach almost 51Hz, which still remains acceptable considering the distance.

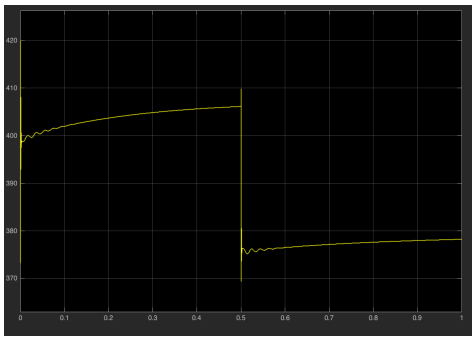

((a)) Voltage

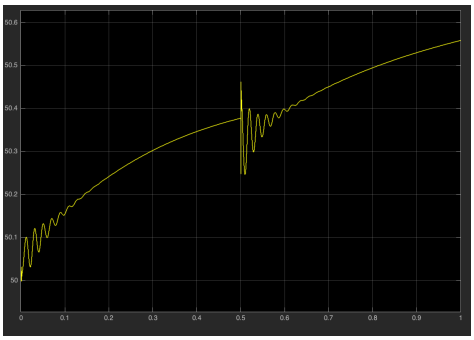

((b)) Frequency

Figure 3.45: Variations at inverter 2 with a 10km distance

One thing to notice, as illustrated on Figure 3.45, is the impact of the distance on the dynamic of the control method: the greater the lines distances, the slower the microgrid response. Thus although a correct response is observed for a grid up to 10km, a slow ability for the grid to reach its tracked set points is expected, causing instabilities.

3.5 Robustness: capacitive load

Now, let's get back to the initial distances and introduce capacitive loads with an assumed power factor equal to 0.9 (leading). The idea is to ensure the quality of the power delivered even when a not purely resistive load is connected to the network.

Simulation time is 1.5 seconds, some results are given on Figures 3.48,3.47, 3.46 with additional ones in Appendix D.

The evolution of the loads is as follows:
-Load 1: (12 kW, 5.8 kVAr) $\xrightarrow{0.5\text{ s}}$ (6 kW, 2.9 kVAr)
-Load 2: (7 kW, 3.39 kVAr) $\xrightarrow{1\text{ s}}$ (17 kW, 8.23 kVAr)
-Load 3: (4 kW, 1.93 kVAr) $\xrightarrow{1\text{ s}}$ (8 kW, 3.86 kVAr)

The voltage measurements are summarised in the tabular 3.9.

	V		
	$0s \rightarrow 0.5s$	$0.5s \rightarrow 1s$	$1s \rightarrow 1.5s$
Inverter 1	401	395	392
Inverter 2	402	408	397
Inverter 3	405	409	402

Table 3.9: Voltage measured at the loads with capacitive loads

The Figure 3.48 shows the power supplied by the inverters. As expected, reactive power is produced, even though the transitions due to load variations are usually smooth. Taking a closer look to the reactive power of the inverter 2, noisy shape at each transition is observed, especially at t=1sec. It is explained by a quite big pic in the voltage variation, as observed in figure 3.47.

The power received by the loads is illustrated on Figure 3.46 and appears to have smooth transition when load variations arise.

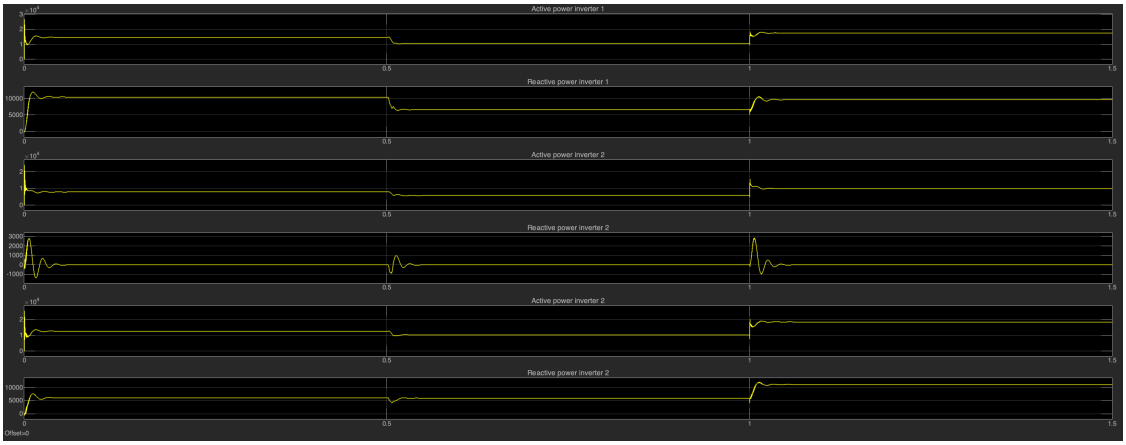

Figure 3.46: Power at the inverter with capacitive loads

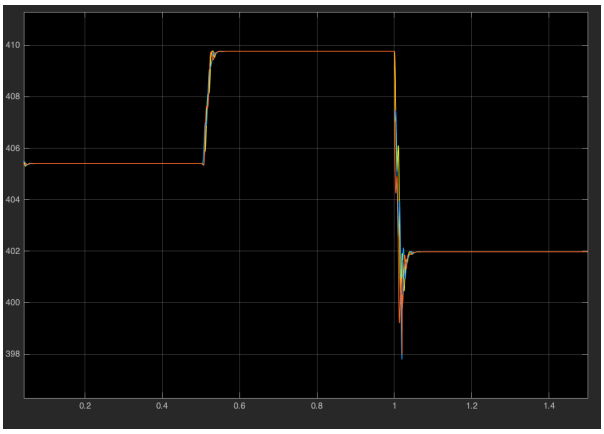

Figure 3.47: Average voltage at the inverter 3 with capacitive loads

3.6 Robustness: inductive load

This last case includes partly inductive loads (0.9 power factor, lagging this time).

As depicted in Figure 3.49, voltage variations at loads are quite limited (within a 10V gap) and satisfy the allowed standard deviation. Frequency deviations do not exceed 0.5 Hz (see Appendix D).

But one thing to notice is the voltage at loads is always lower than the reference values. The explanation is the fact that inductors consume reactive powers. To compensate this, as depicted in Figure 3.51, the inverters are now injecting negative reactive power.

In this case, the control dynamic is fast, allowing a rapid adaptation of the

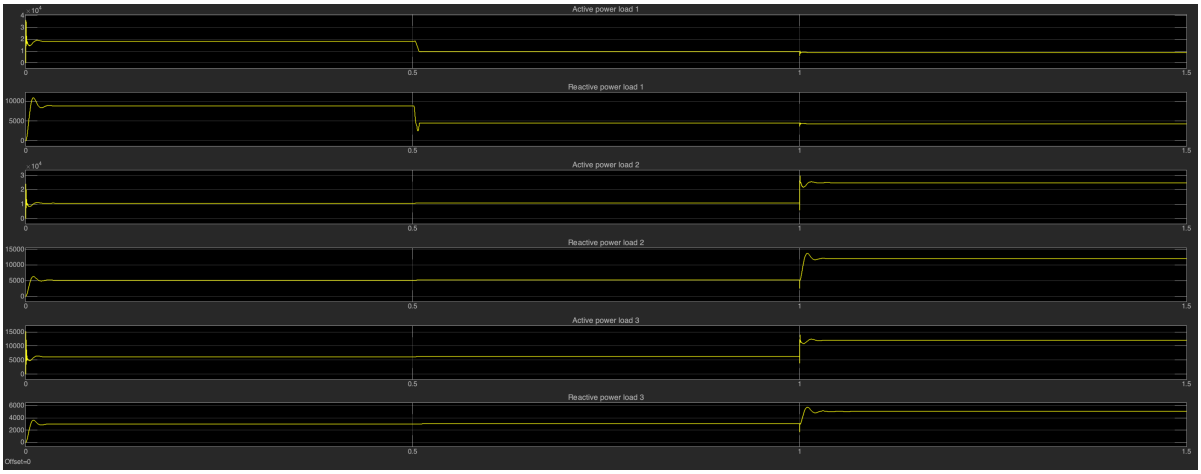

Figure 3.48: Power at the loads with capacitive loads

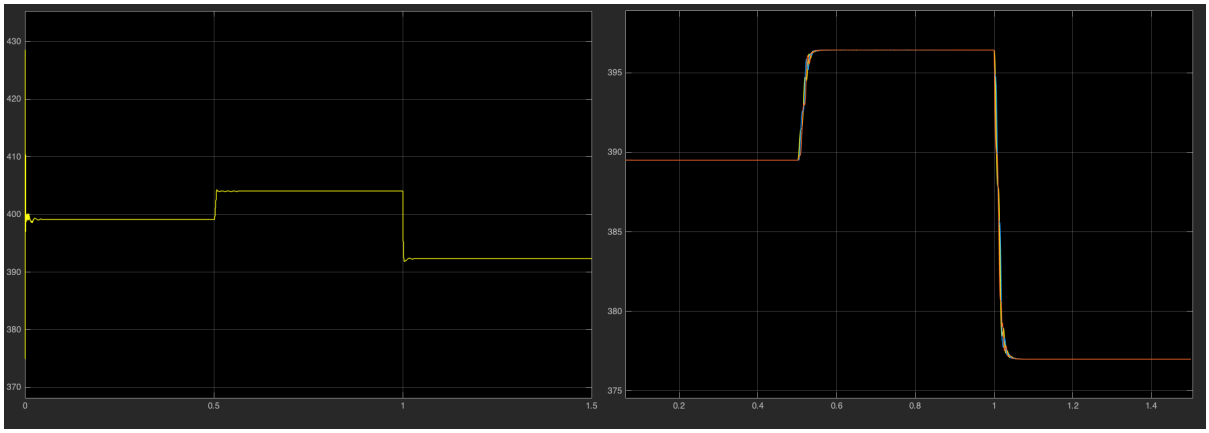

((a)) Inverter 3 ((b)) Load 3

Figure 3.49: Average voltage at the inverter 3 and load 3 with inductive loads

voltage and frequency and proving a well controlled grid.

One can ask himself about the comparison with the mainly inductive lines (R « X) encountered in a classic HV grid. The case of inductive line controlled with a droop method is not taken into account in the present report.

	V		
	$0s \rightarrow 0.5s$	$0.5s \rightarrow 1s$	$1s \rightarrow 1.5s$
Inverter 1	391	399	388
Inverter 2	391	398	381
Inverter 3	389	397	377

Table 3.10: Voltage measured at the loads with inductive loads

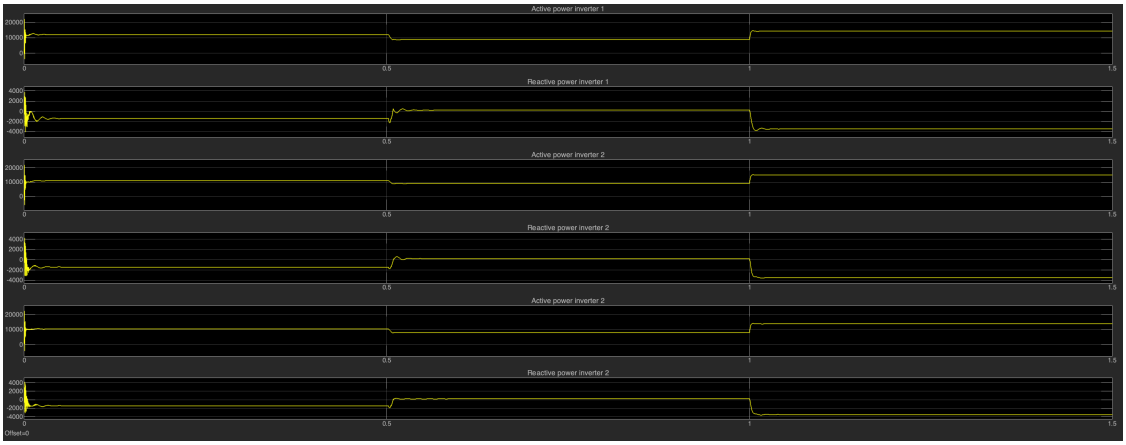

Figure 3.50: Power at the inverter with inductive loads

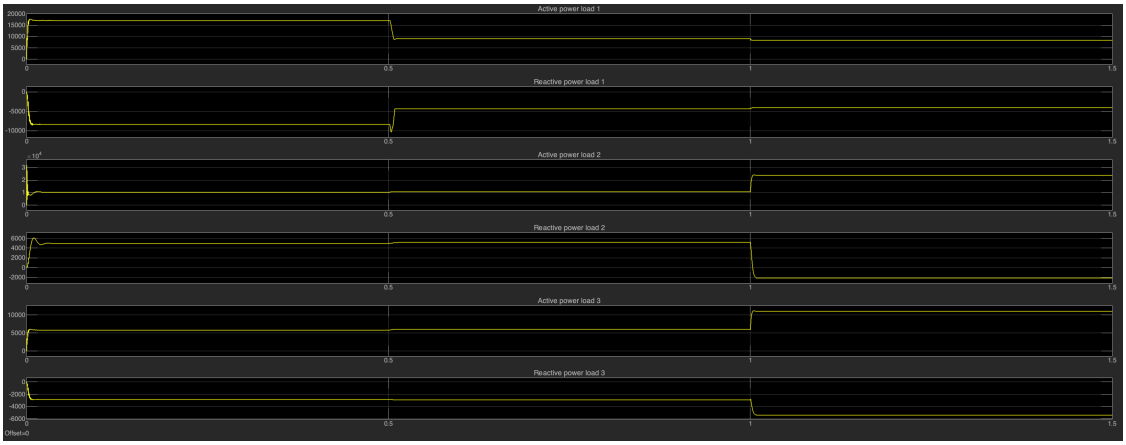

Figure 3.51: Power at the loads with inductive loads

Finally, the comparison between the deviation from the reference voltage of $400V$ for capacitive and inductive loads is established in table 3.11.

As observed, the inductive loads have a stronger impact on the voltage variations compared to capacitive ones, as it was the case previously with the master/slave

		$\lvert\Delta V\rvert$		
		$0s \rightarrow 0.5s$	$0.5s \rightarrow 1s$	$1s \rightarrow 1.5s$
Capacitive loads	Inverter 1	1	5	8
	Inverter 2	2	8	3
	Inverter 3	5	9	2
Inductive loads	Inverter 1	9	1	12
	Inverter 2	9	2	19
	Inverter 3	11	3	23

Table 3.11: Voltage measured at the loads with capacitive loads

control method.

3.7 Sizing of DGs

According to the simulation results presented earlier in the report, maximum currents produced by each inverters can be inferred.

$$\begin{cases} I_{Inverter1|max} \approx 28 \text{ A} \\ I_{Inverter2|max} \approx 25 \text{ A} \\ I_{Inverter3|max} \approx 26 \text{ A} \end{cases}$$

Remembering the apparent power expression: [31]

$$S = \sqrt{3} U_L I_L$$

$$\Leftrightarrow S_{max} = \sqrt{3} U_{L|max} I_{L|max}$$

In order to satisfy the European standard and stay in the $\pm 10\%$ range of variation in the voltage, in other words within $360V$ and $440V$, the following values of maximum power:

$$\begin{cases} S_{Inverter1|max} \approx 22 \text{ kVA} \\ S_{Inverter2|max} \approx 19 \text{ kVA} \\ S_{Inverter2|max} \approx 20 \text{ kVA} \end{cases}$$

Rounding up those values implies that the inverters have ratings of 30 kVA each, leading to a total power of 90 kVA deliverable to the grid.

Chapter 4

Comparison of results

In the last two chapters, the master/slave and droop methods of control were deeply developed, now it is interesting to compare one from another and emphasize in which situation one method control is more suited for.

At first, due to the absence of communication links in the droop method, the measurements available for control are the ones at the output of each inverter (local control). However, for the MS technique, data can be collected in every point of the grid, allowing a more precise voltage regulation thanks to the use made of a reference node central to the grid, for the basic case at least (short lines, resistive loads). This precision has a huge cost though: communications channels must be implemented in the network, making it vulnerable to faults and introducing communication delays.

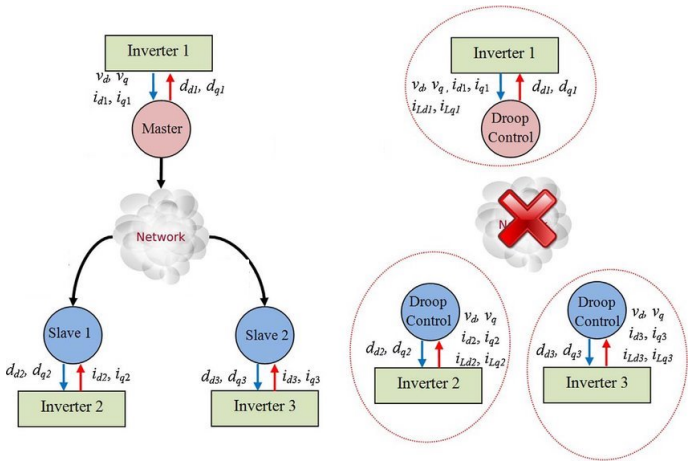

Figure 4.1: Comparison between the global scheme of the two methods [36]

By applying a suited power sharing between the slaves, the frequency imposed by the master does not need to be controlled in the MS, implying deviations of less than 0.5Hz from the tracked one, during an extremely small period of time. This control is, however, essential to the droop control and needs to be realised as accurately as possible by tuning the value of the droop coefficients according to the grid size and components.

A parameter well handled by the droop is the phase shift: it remains constant with either capacitive or inductive loads connected to the grid. It is not the case for the MS where the phase shift needs to be adjusted to ensure good performances in power injection. Poor phase regulation leads to deterioration of slaves power factor.
Besides, the power factor is limited to 0 at the master to allow the one of slaves to reach 1, what is a limitation of the simplified model used in this report. On the other side, power factor is approximated at 1 in major part of the simulations for the droop control method.

In the case of the loss of one inverter, the master/slave sometimes needs to disconnect one load due to higher active power required than the sum of the rated power inverters can actually offer. It is not the case for the droop control; thanks to an active power generation distributed among each of the three power suppliers. The reason is that in MS, the master is only made liable of imposing the voltage and frequency without generating any relevant active power (slaves units ensure this function). This leads to a systematic smaller number of inverters able to deliver active power in agreement to the control method. The droop control will so always be more reliable in the case of loss of one generating power devices than the MS.

It is important to emphasize that for the MS case, because the master injects only reactive power and regulates voltage, it has a limited impact in the basic simulated case (resistive loads, small line distances). However, it helps dealing with transient conditions in which the master takes care of momentarily generating the necessary active power while a new command for the slaves is computed, leading to high peak currents for I_{master}. It could be the reason why the master unit is probably oversized and ought to rarely reach the 64 kVA it has been designed for. This rating should only be achieved in extreme case of inductive load transition on the grid, where it has to cover both reactive power generation and active power change compensation.

When increasing line distances to test the grid robustness (i.e. finding the maximum distance allowed to stay in the standard requirements), the MS suffers

from its single voltage regulation unit (the master), limiting the size of the grid to almost a tenth of the one supported by the droop control, which allows distances greater than needed for a microgrid ($>$ 10km). The reason is the multiple points of collecting/ regulating data at each inverter output for the droop, ensuring redundancy and reliability against the distance.

From the dynamic point of view, the MS reacts quickly by using a simple algorithm and the transient periods stay under 0.1s. The droop method has a slower dynamic, varying from 0.2s up to 0.5s according to the distance. However, no communication delays have been considered for MS control, and one can assume they range from 0.2s...to 1s in case of a large microgrid!

Another important point to underline, is that even if the voltage is controlled for the two methods, the current is an important part of the MS, while the frequency management is more developed in the droop method.

Finally, what concerns voltage deviations, performances are more convincing for the MS in the basic case (purely resistive loads) and, as mentioned, for small line distances. Nevertheless, when dealing with partly reactive loads, voltage regulation seems to be better handled in droop control case due to local control of the voltage. Anyway, in the two cases the inductive loads have the stronger impact on the control accuracy, allowing voltage deviations of respectively 30V and 25V from the reference in the MS and droop control, which are significant.

Conclusion

In this paper, the stability and the performances of two microgrids control methods have been studied. Master/slave (M/S) and droop control strategies have been presented and simulated on a scalable and robust microgrid architecture comprising DG (association of DERs and energy storage systems) feeding different variable loads. Efficient and reliable operation of the 45 kW microgrid is ensured in various microgrid configurations and operating modes.

The Master/Slave strategy is ruled by a central control unit (CCU) who has the responsibility to determine voltage and current reference (norm & phase) and send them to the various DGs. The master DG makes support of voltage and acts like the voltage source, aiming for voltage regulation. The current references are calculated at each time step following loads changes and are communicated to other DGs (slaves) via communication links. In other words, the master DG always runs in a voltage control mode, while slave DGs operate in a current control mode. As enumerated, in this method a communication infrastructure is needed.
In case master DG fails, voltage stability is lost and microgrid may fail to continue its operation. Despite the need for a communication system between the nodes, M/S method demonstrated low computational complexity for good power sharing. In terms of distribution efficiency, voltage stability and power quality are ensured even during severe dynamic transitions. The master DG traces load fluctuation, and therefore, its power output has to be controllable, the DG should be able to respond fast enough to load fluctuation. On the other hand, slave DGs remain under P/Q control. Finally, with M/S, frequency control is not an issue but can be improved by adjusting set points of LCU. [37]

Some other drawbacks are noticeable for the M/S. First, with the master DG acting following a U/f control, its voltage output is constant. Instantaneous load fluctuations are usually first balanced by the master DG, and therefore need to have a certain adjustable capacity. Secondly, as the system relies on the master DG and a CCU to coordinate and control all slave DGs, once the master DG fails, the whole microgrid will collapse. [38]

Pros	Drawbacks
Simple control algorithm	High communication requirement
Good power sharing	Difficult to expand
	Low reliability

Table 4.1: Major pros/cons of master-slave control strategy

Droop power sharing is mainly dedicated to voltage and frequency regulation of microgrids. In this mode, active and reactive powers are regulated through a feedback loop adjusted by droop coefficients adapted on frequency and voltage values.
Actually, the primary control aims to adjust the amplitude and frequency of local voltage references, thus avoiding circulation of unwanted currents among DERs.The meaning of secondary control in droop-controlled microgrids is to compensate for the amplitude and frequency deviations caused by droop control.

Pros	Drawbacks
Autonomy of the DGs	Trade-off between accuracy and power sharing
No vulnerable communication link	
plug-and-play connection of DERs	

Table 4.2: Major pros/cons of droop control

This control strategy does not require any communication link and is thus mainly used in MG so as to present several DGs operating individually (DGs are controlled in a decentralised manner).
Local power measurement allows greater reliability for the grid and flexibility in the physical location of the modules. Nevertheless, some downsides limit its application area, such as slow transient response, trade-off between the power-sharing accuracy and the frequency and voltage deviations, unbalance harmonic current sharing, and high dependency on the inverter output impedance[17]. In addition, the line impedance is supposed to be unknown, which can result in reactive power unbalances in the system.

Future research/development

To conclude the report, let's state some further research or developments which are not studied here due to limited time.

First of all, only idealised sources of current or voltage have been considered, with perfect and smooth generation. Inverters may be used in the future to simulate more accurately the behaviour of a physical MG. Loads have been considered ideal as well, neglecting any white noise or unsteady behaviour that could arise in real case situations.
On top of that, in the case of MS, some delay due to the need of communication lines, should have been taken into account; the greater the lines, the more significant it should get. In the present report, for both MS or droop control, the measurement, transmission and updating of the data are supposed to be instantaneous, which is a major idealisation.
Concerning droop control, one could implement an adaptive method to tune the droop coefficients to improve the accuracy of voltage regulation. Moreover, the resistance of the power line is introduce in the model but the coefficients are computed for a fixed layout of MG.

Another improvement could be to combine the two control techniques to implement a hybrid control method which would both have their own benefits. Master/Slave "peer-to-peer" control strategies of microgrid, based on communication, have nowadays been implemented and successfully tested. It is globally based on a local information and modified droop controller.

A last but not least important aspect, one should bear in mind this report only concentrates on researches in the theoretical feasibility by studying and simulating the two methods. The economic dimension of the project, who has not always pleaded for its financial profitability in well electrified regions, is thus not covered in this work.

Appendix A

Master/Slave standard configuration

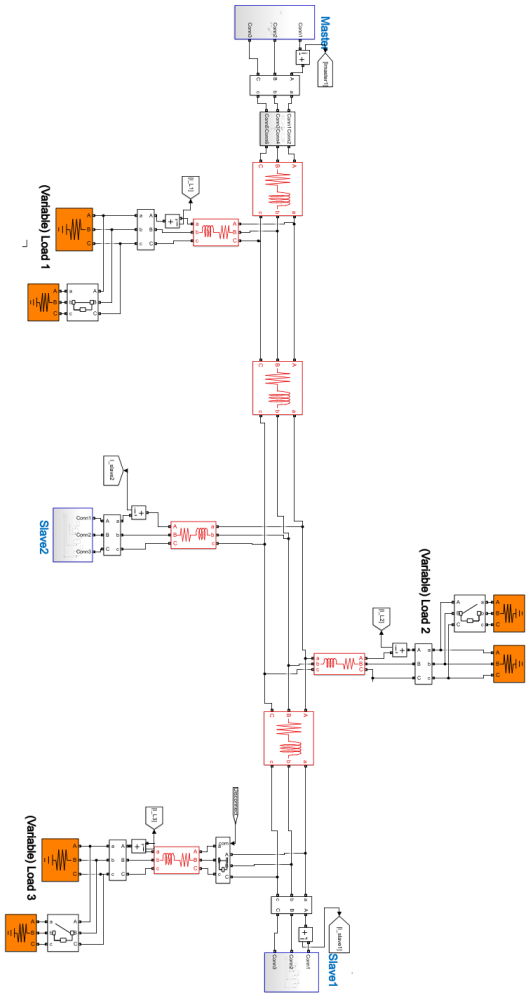

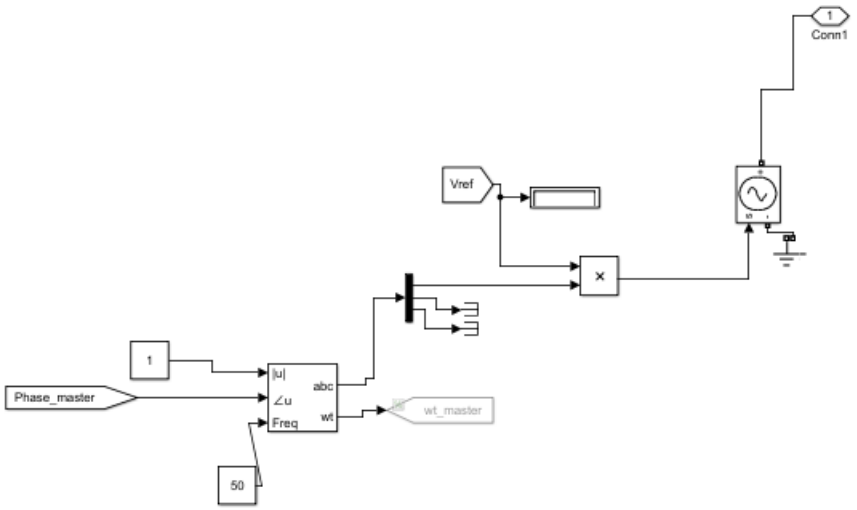

Figure A.1: Voltage generation for one phase (phase A)

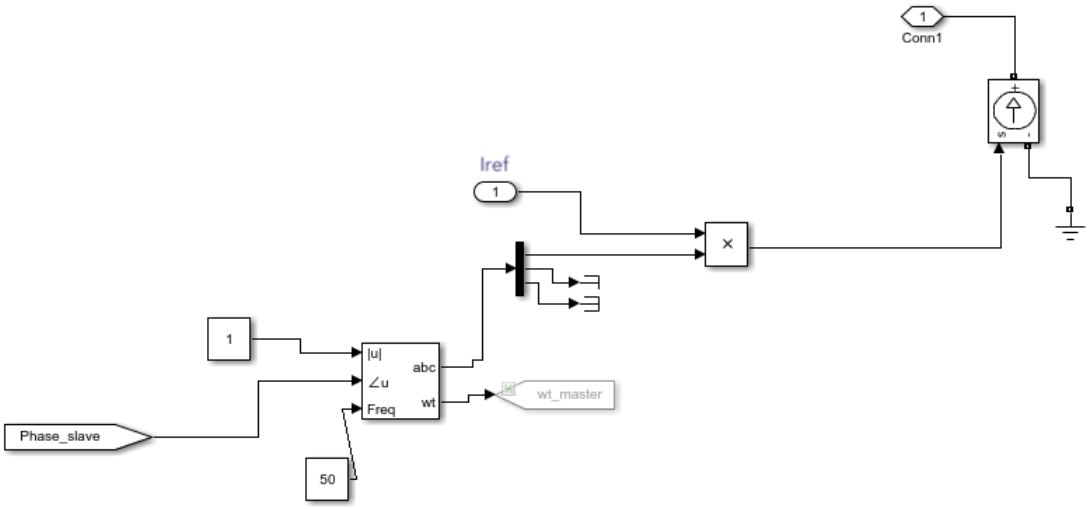

Figure A.2: Current generation for one phase (phase A)

Appendix B

M/S-Robustness: graphic plots

1 On distance

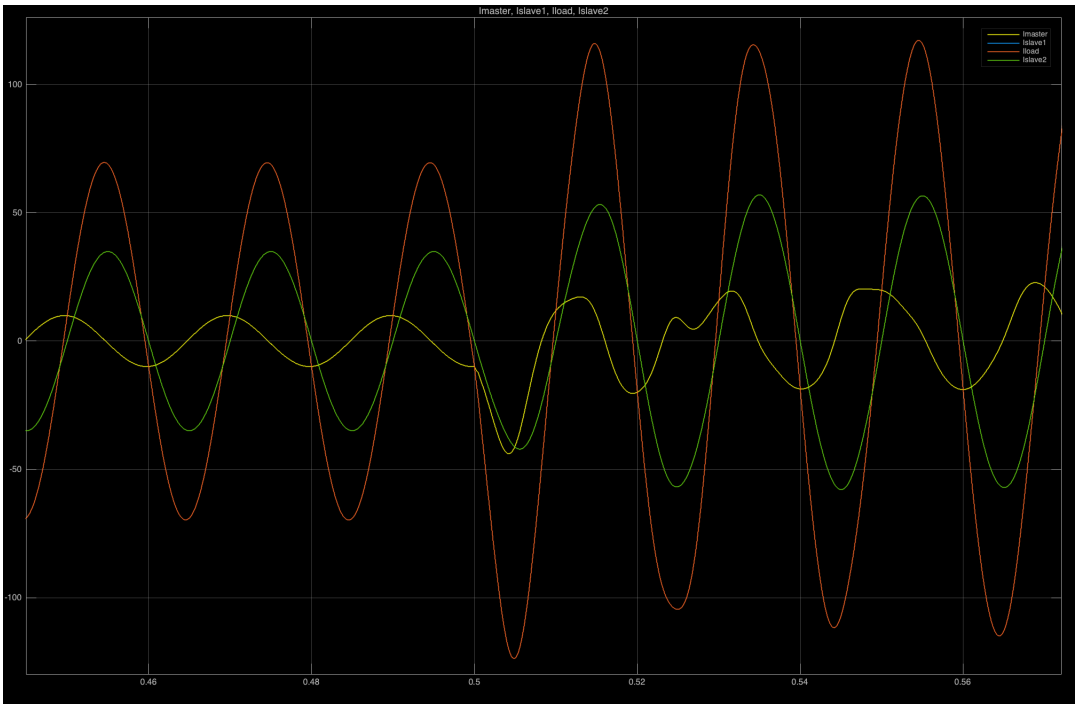

Figure B.1: Representation of Phase A currents during transition (yellow = master; red= sum of loads; green = slave 1; blue = slave 2)

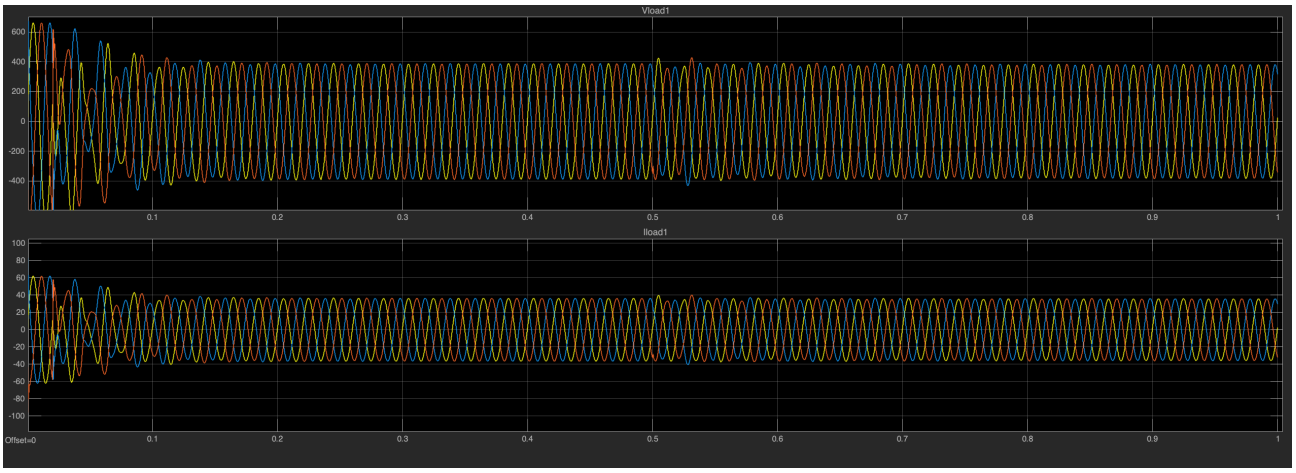

Figure B.2: Representation of the 3-phase voltage and current: load 1

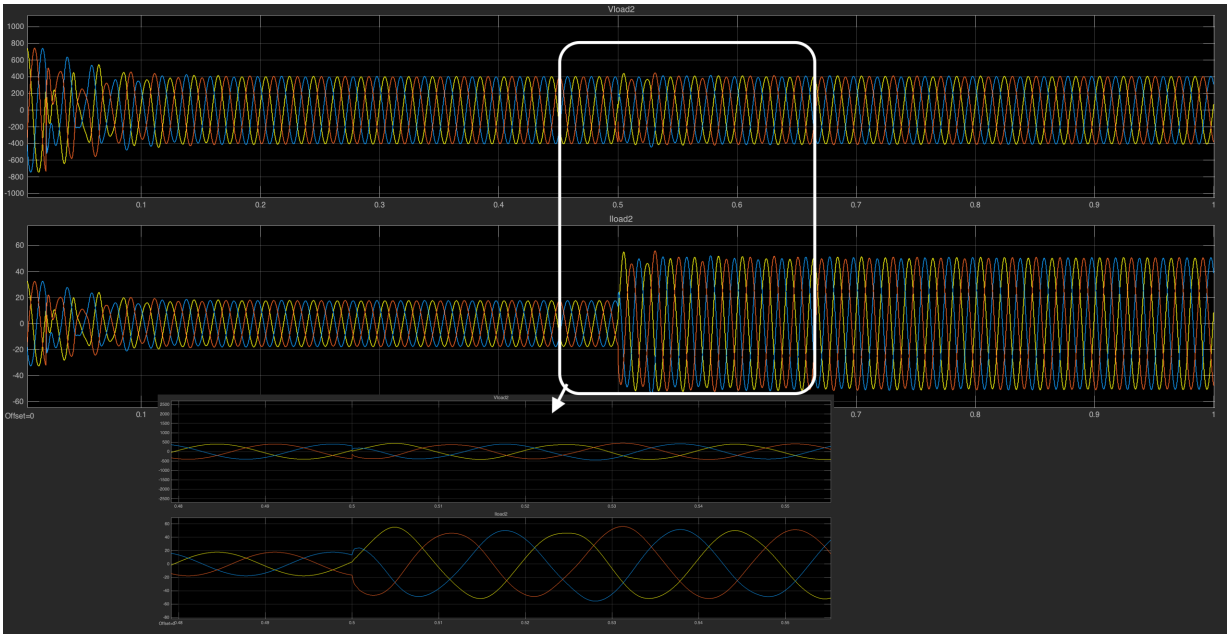

Figure B.3: Representation of the 3-phase voltage and current: load 2

2 Loss of a DG

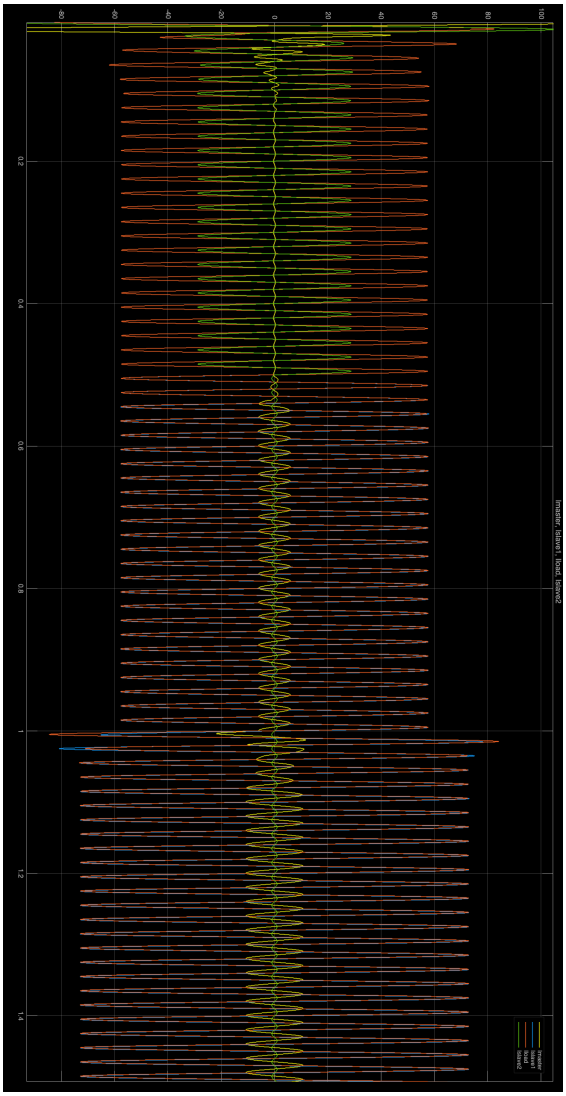

Figure B.4: Representation of Phase A currents during transition (yellow = master; red= sum of loads; green = slave 1; blue = slave 2)

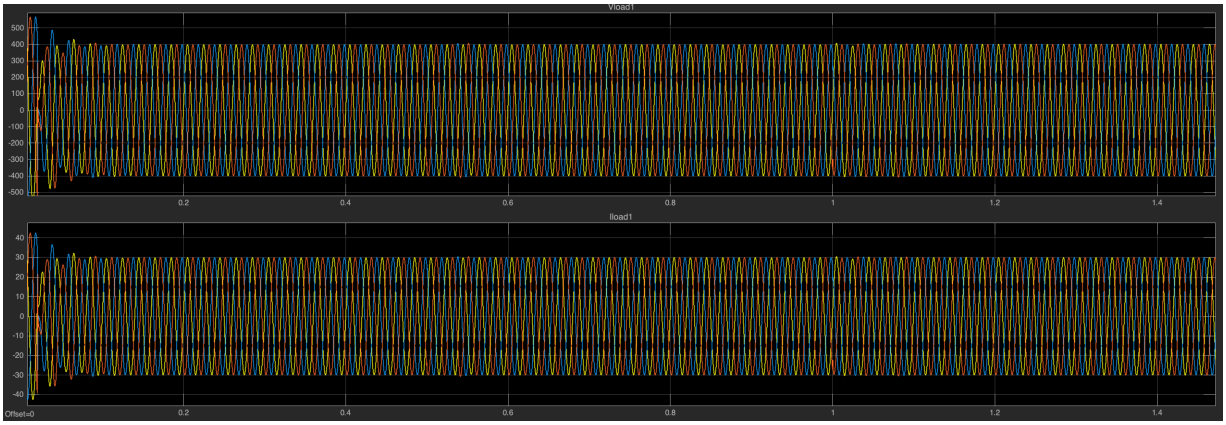

Figure B.5: Representation of the 3-phase voltage and current: load 1

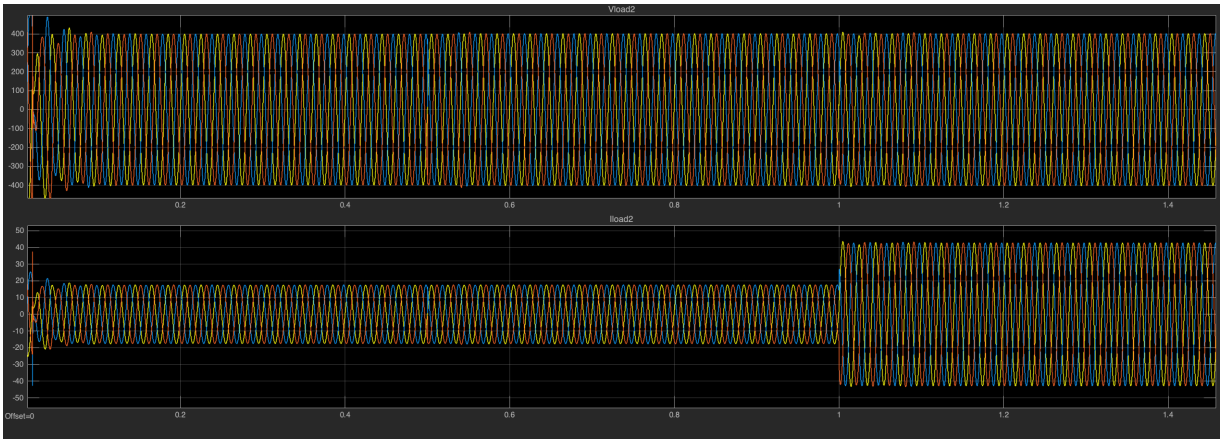

Figure B.6: Representation of 3-phase voltage and current: load 2

3 Capacitive loads

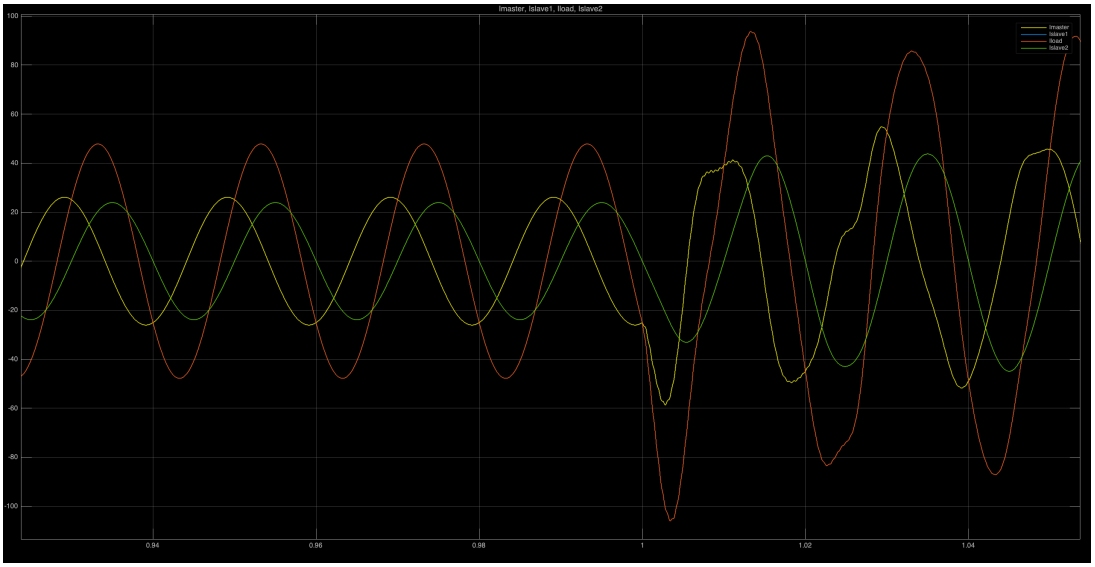

Figure B.7: Representation of Phase A currents during transition (yellow = master; red= sum of loads; green = slave 1; blue = slave 2)

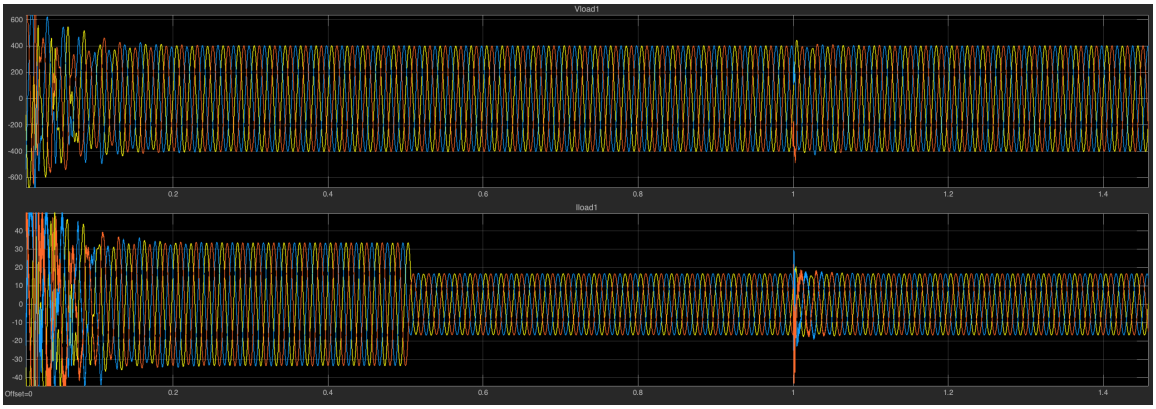

Figure B.8: Representation of the 3-phase voltage and current: load 1

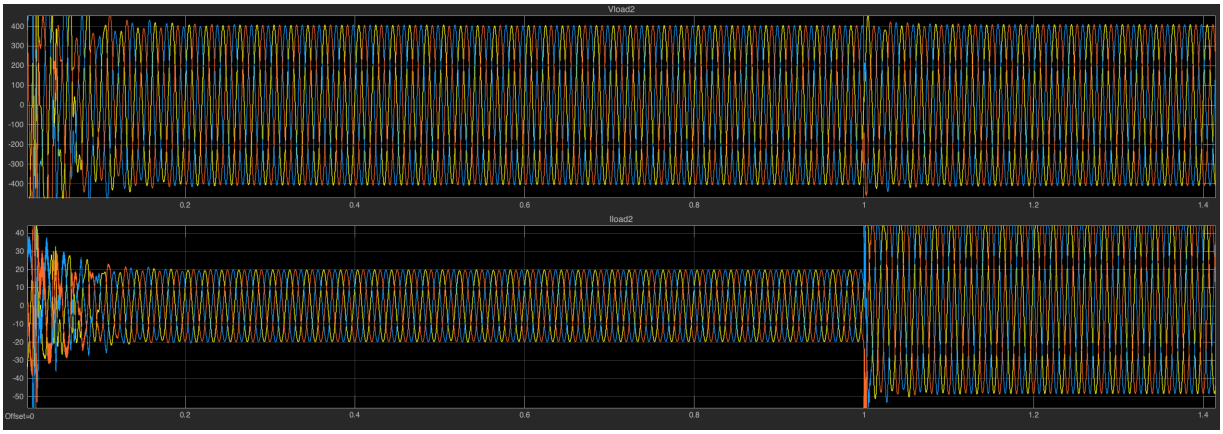

Figure B.9: Representation of the 3-phase voltage and current: load 2

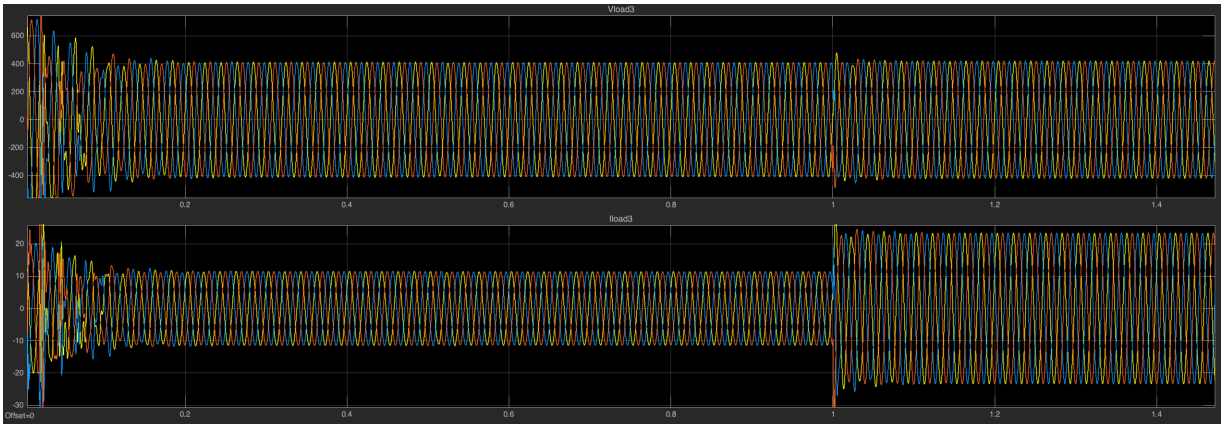

Figure B.10: Representation of the 3-phase voltage and current: load 3

4 Inductive loads

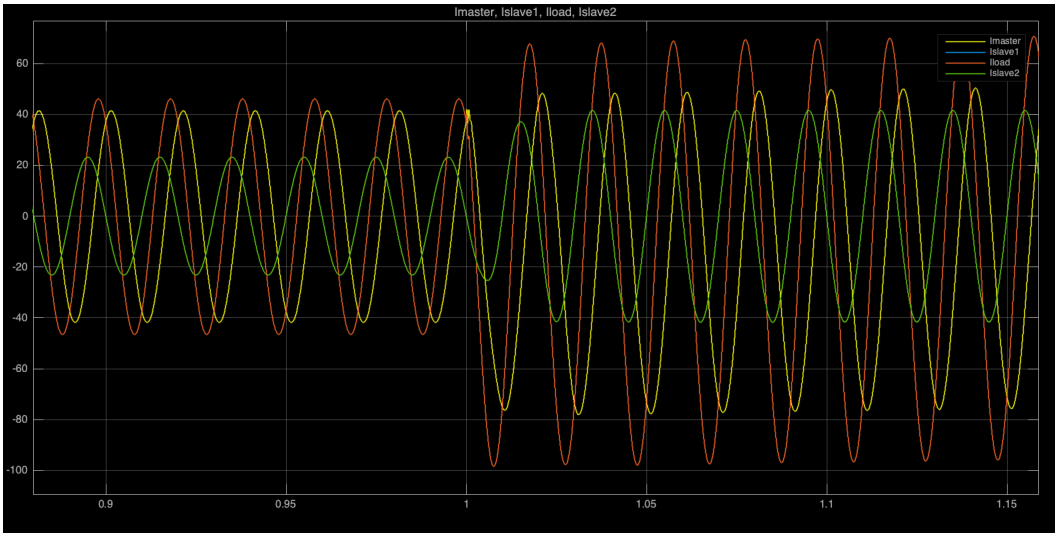

Figure B.11: Representation of Phase A currents during transition (yellow = master; red= sum of loads; green = slave 1; blue = slave 2)

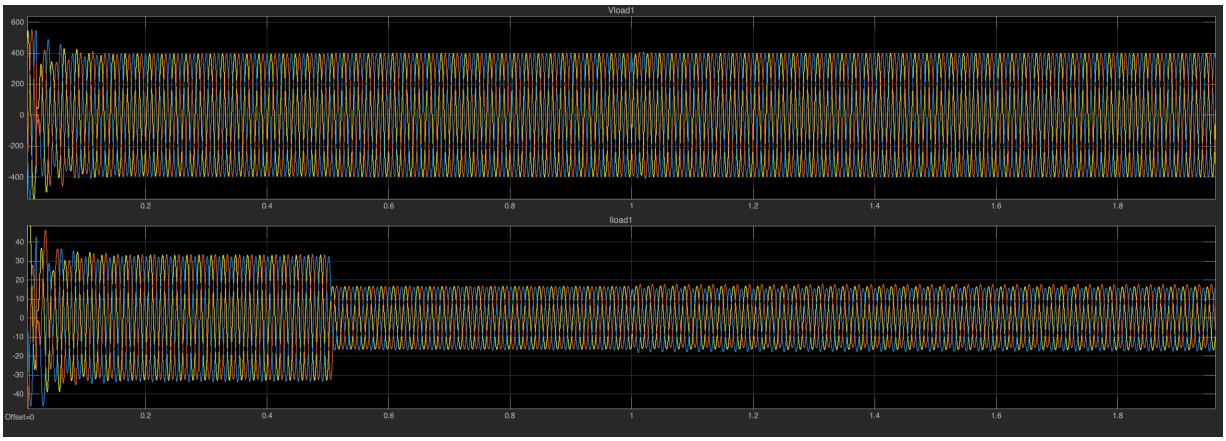

Figure B.12: Representation of the 3-phase voltage and current: load 1

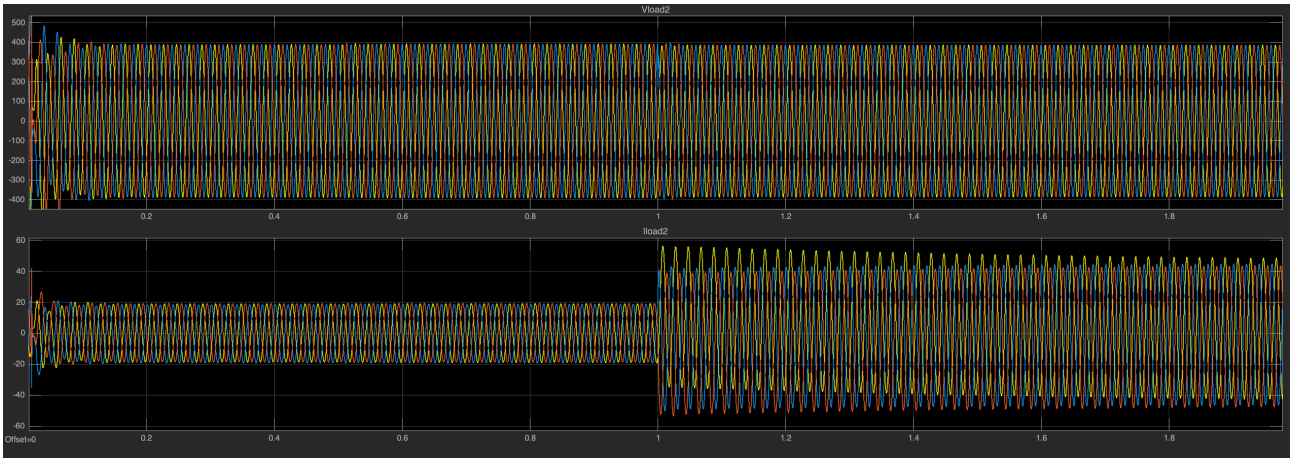

Figure B.13: Representation of the 3-phase voltage and current: load 2

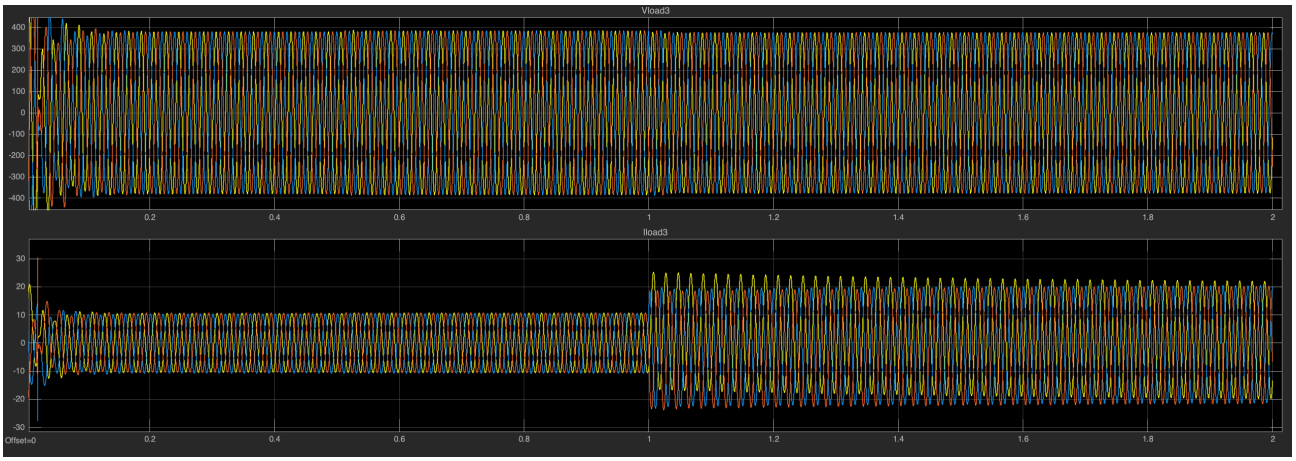

Figure B.14: Representation of the 3-phase voltage and current: load 3

Appendix C

Droop control: simulation layout

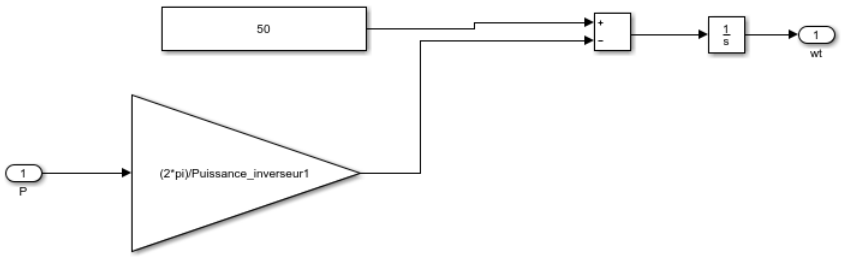

Figure C.1: Droop P

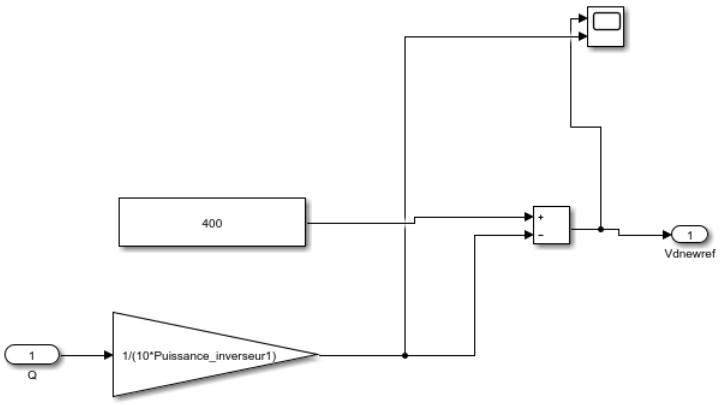

Figure C.2: Droop Q

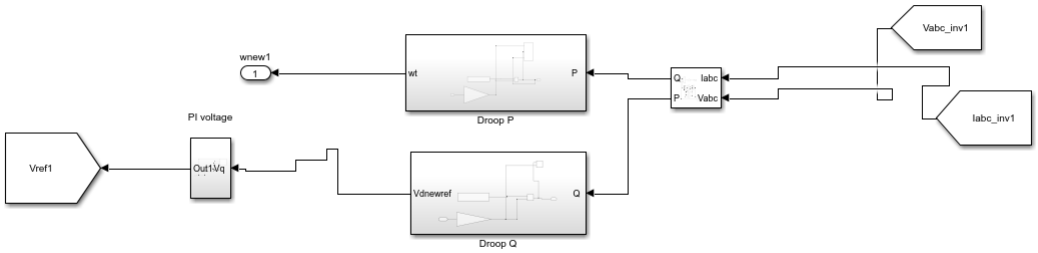

Figure C.3: Circuit of droop control implemented

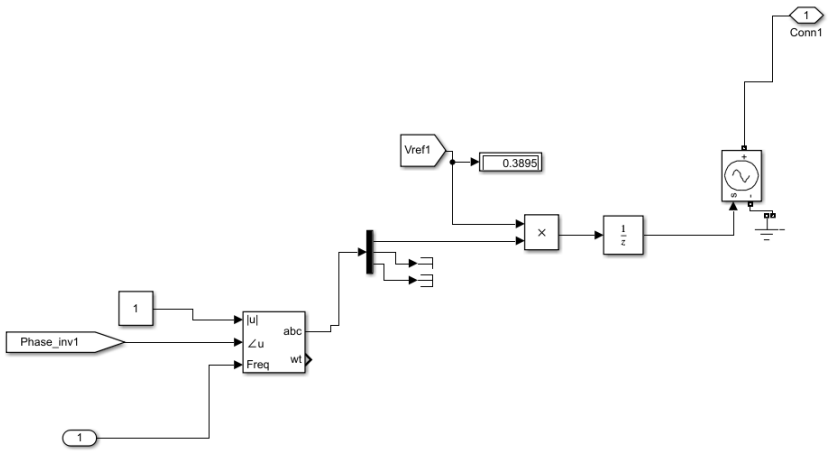

Figure C.4: Signal generation

Appendix D

Droop control-Robustness: graphic plots

1 Loss of a DG

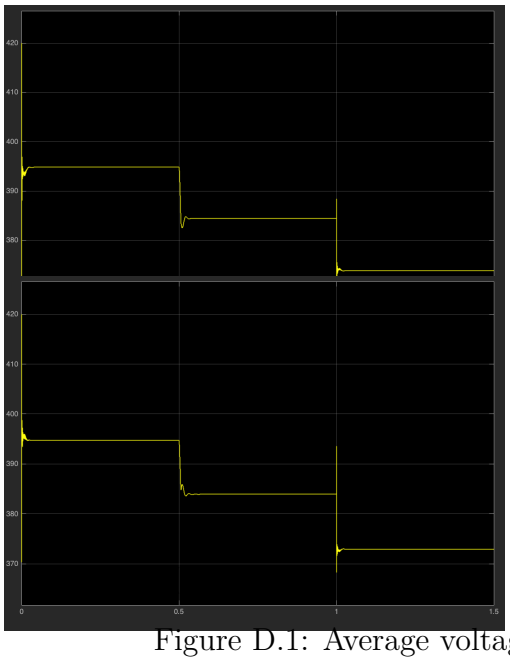

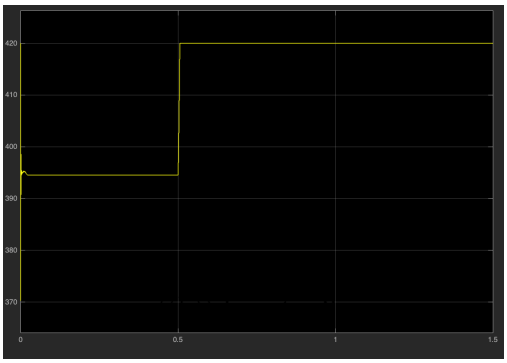

Figure D.1: Average voltage at the inverters with DG loss

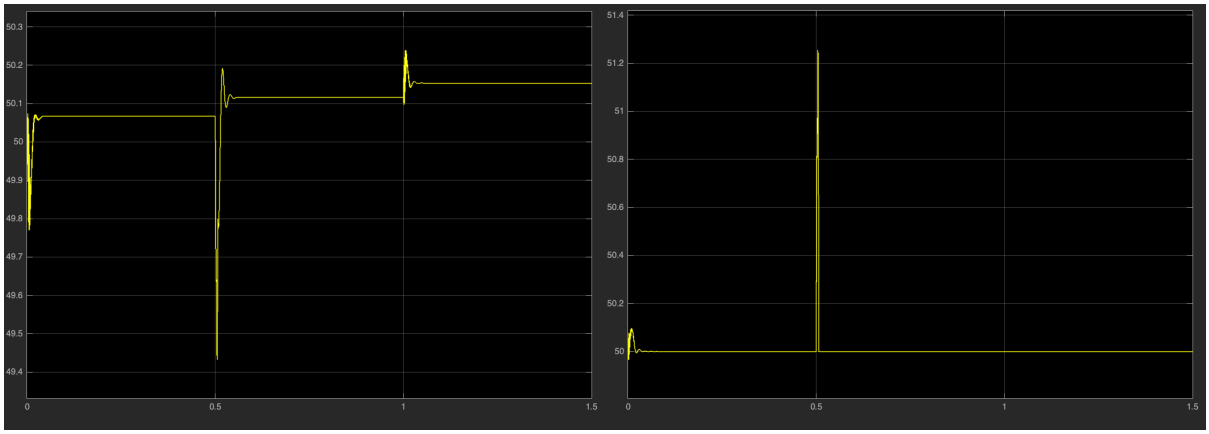

((a)) Inverter 1 ((b)) inverter 2

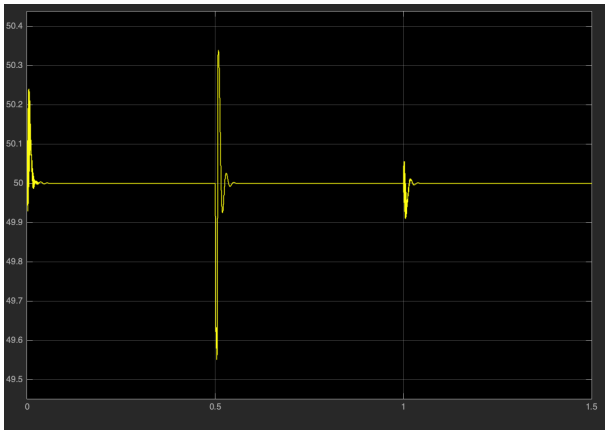

((c)) Inverter 3

Figure D.2: Frequency at the inverter with DG loss

2 On distance

2.1 Distance of 1km

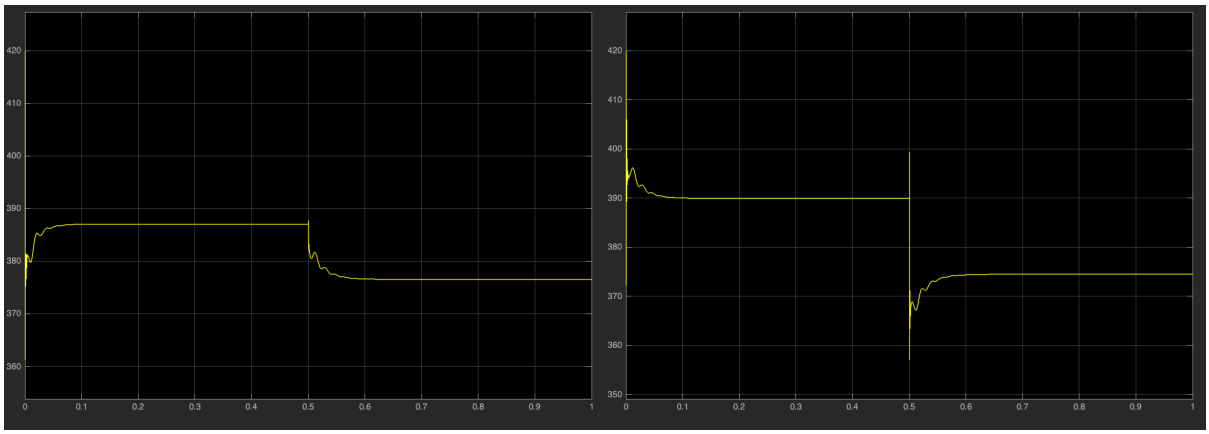

((a)) Inverter 1

((b)) Inverter 2

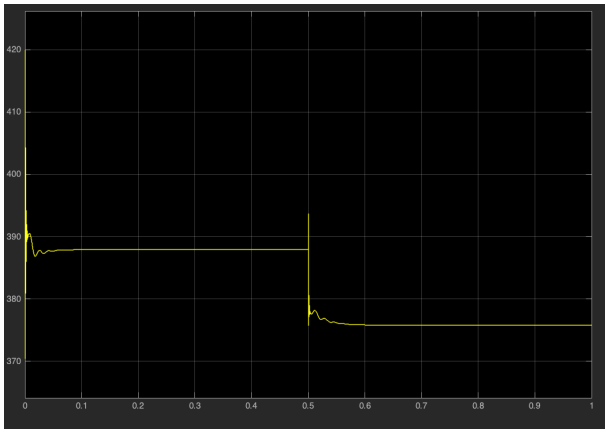

((c)) Inverter 3

Figure D.3: Average voltage at the inverters with a distance of 1km

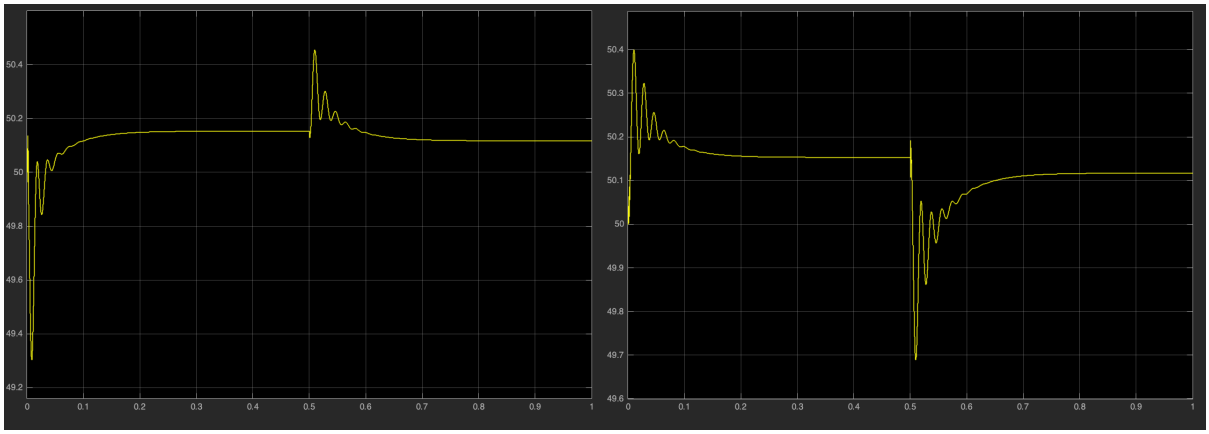

((a)) Inverter 1

((b)) Inverter 2

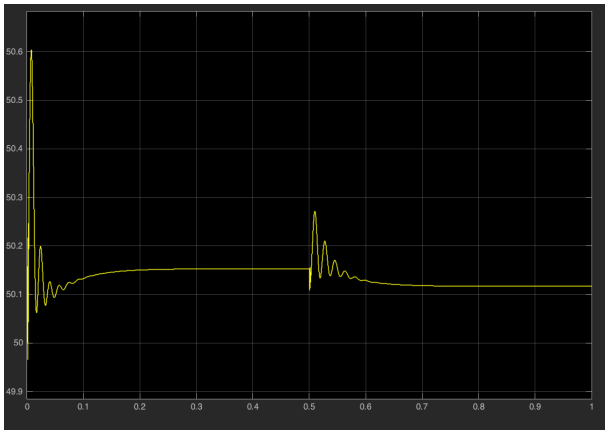

((c)) Inverter 3

Figure D.4: Frequency at the inverters with a distance of 1km

2.2 Distance of 2km

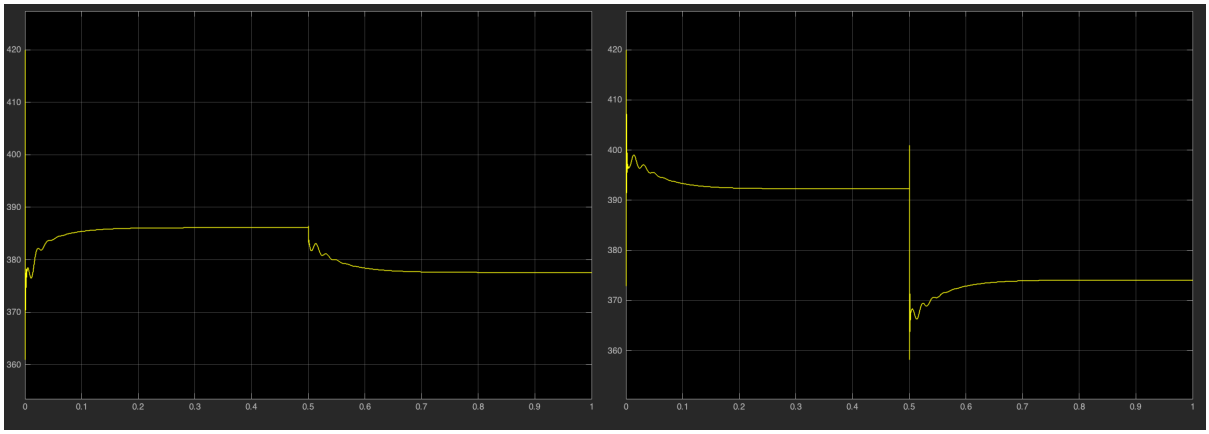

((a)) Inverter 1

((b)) Inverter 2

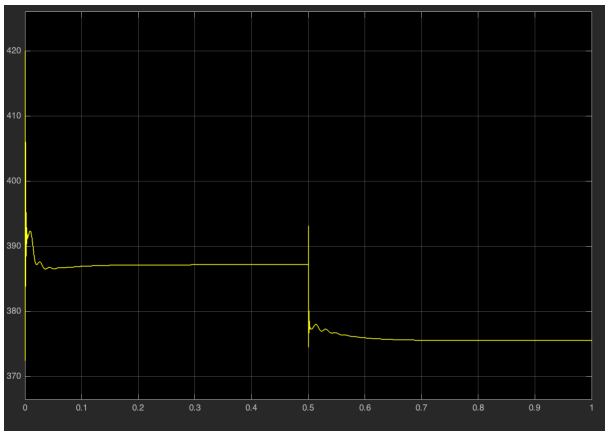

((c)) Inverter 3

Figure D.5: Average voltage at the inverters with a distance of 2km

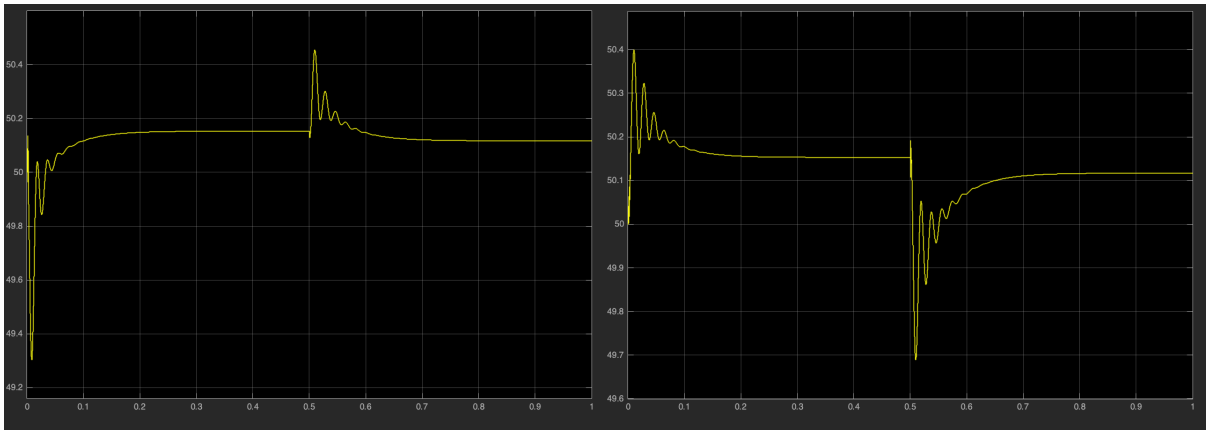

((a)) Inverter 1

((b)) Inverter 2

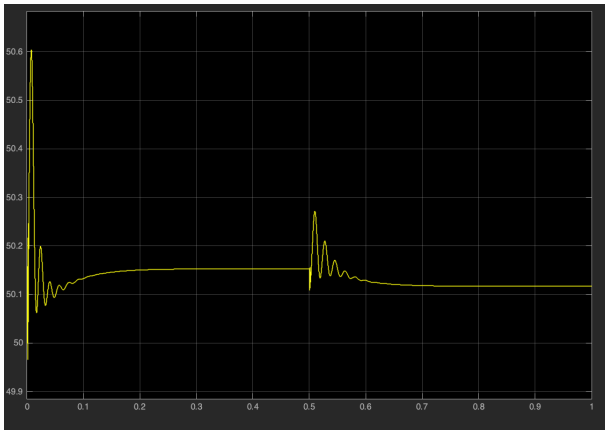

((c)) Inverter 3

Figure D.6: Frequency at the inverters with a distance of 1km

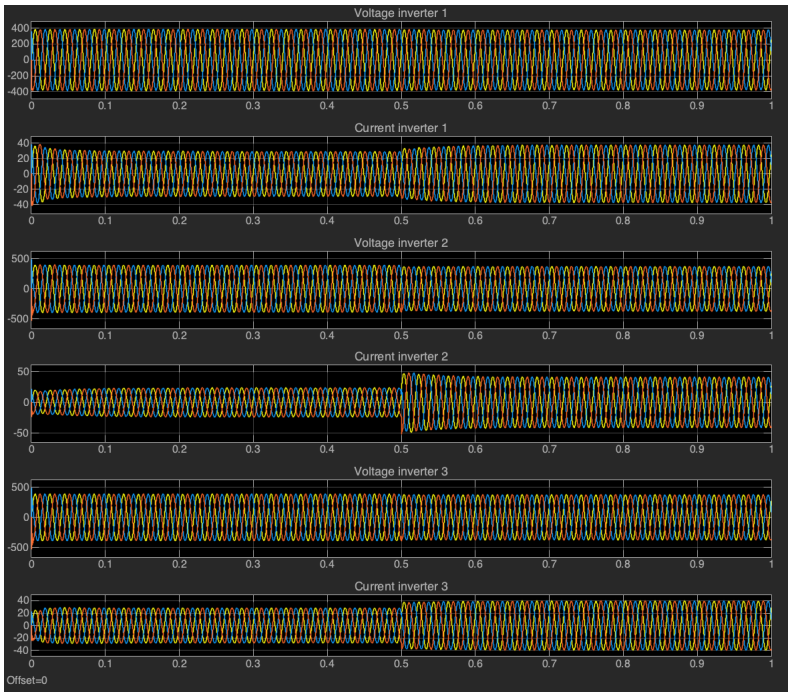

Figure D.7: Voltage and current at the inverters with a distance of 2km

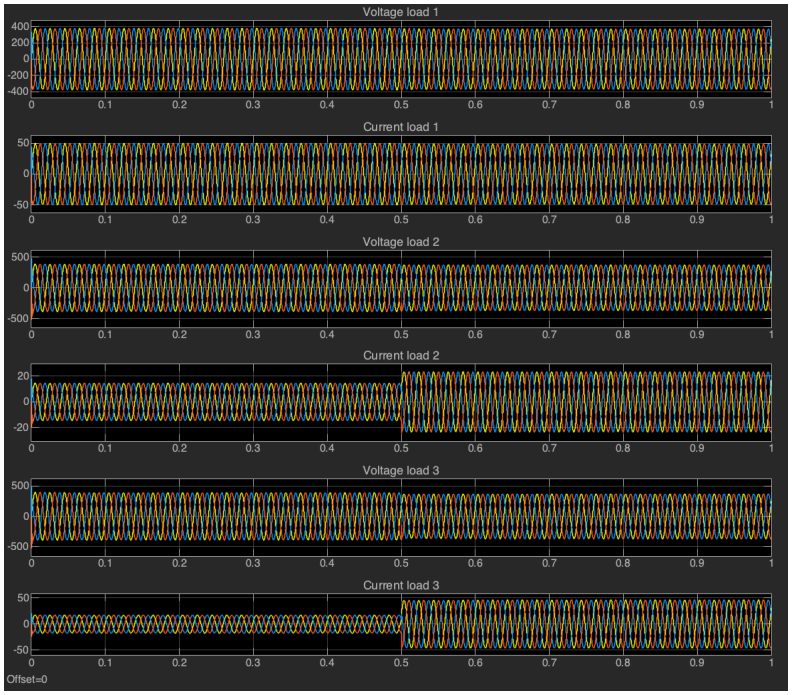

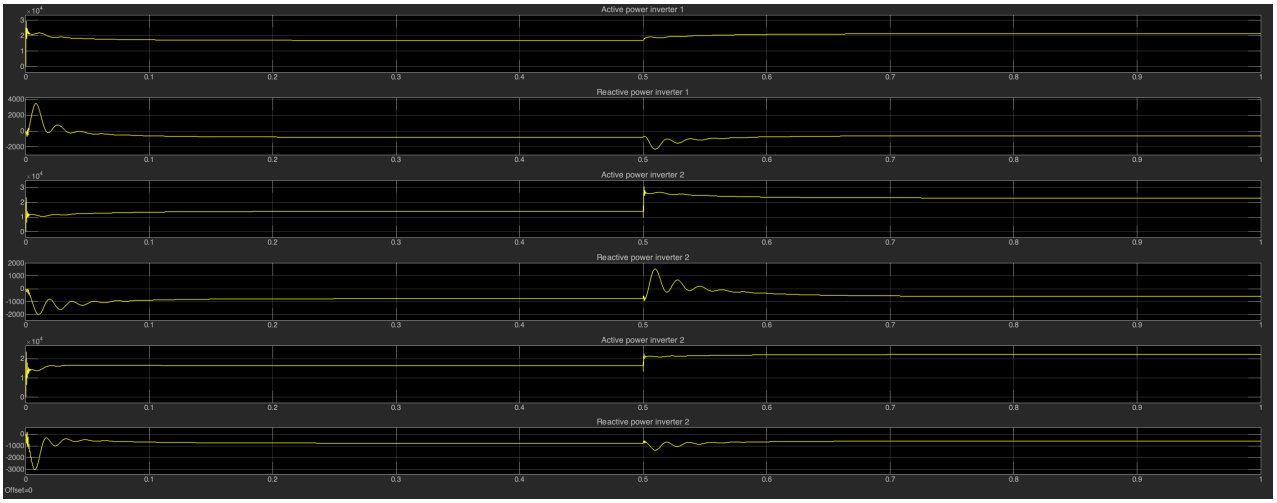

Figure D.8: Power at the inverters with a distance of 2km

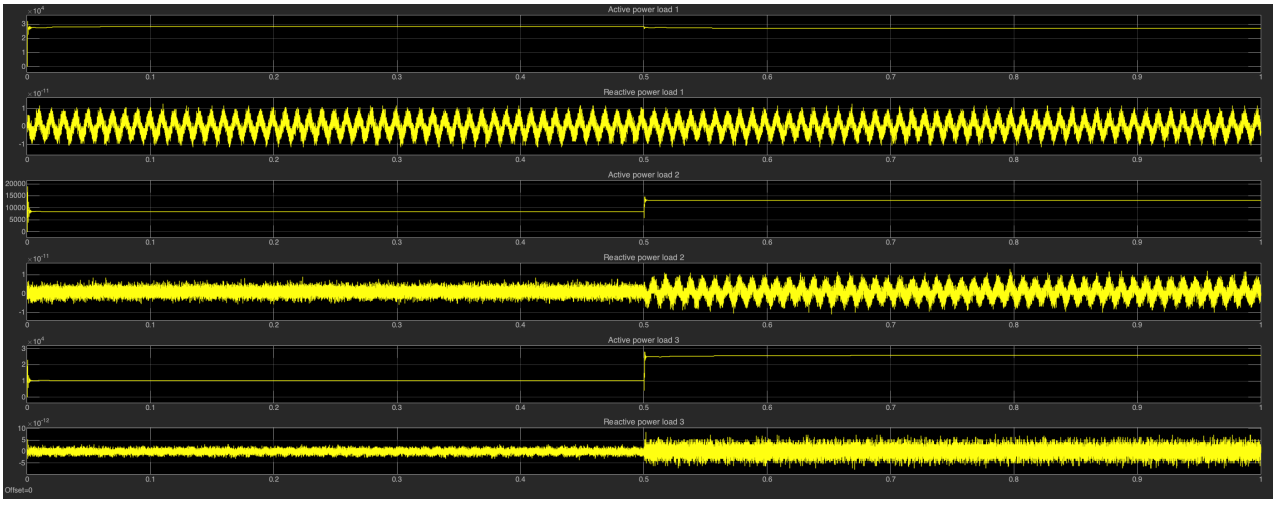

Figure D.9: Power at the loads with a distance of 2km

2.3 Distance of 5km

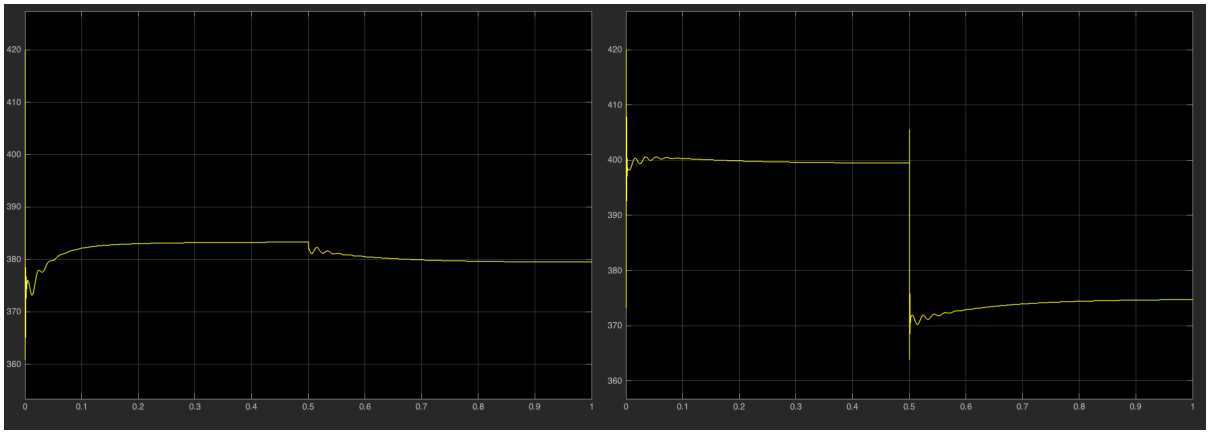

((a)) Inverter 1

((b)) Inverter 2

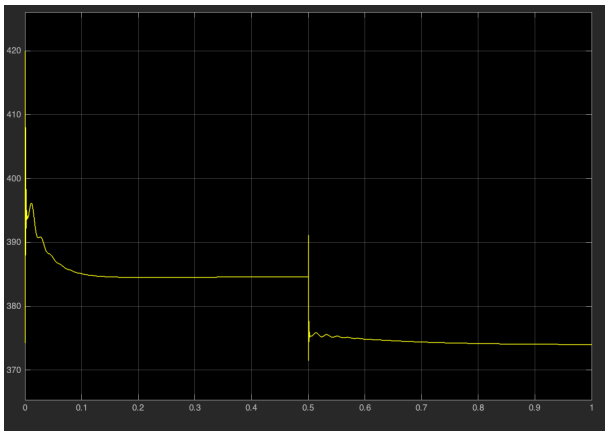

((c)) Inverter 3

Figure D.10: Average voltage at the inverters with a distance of 5km

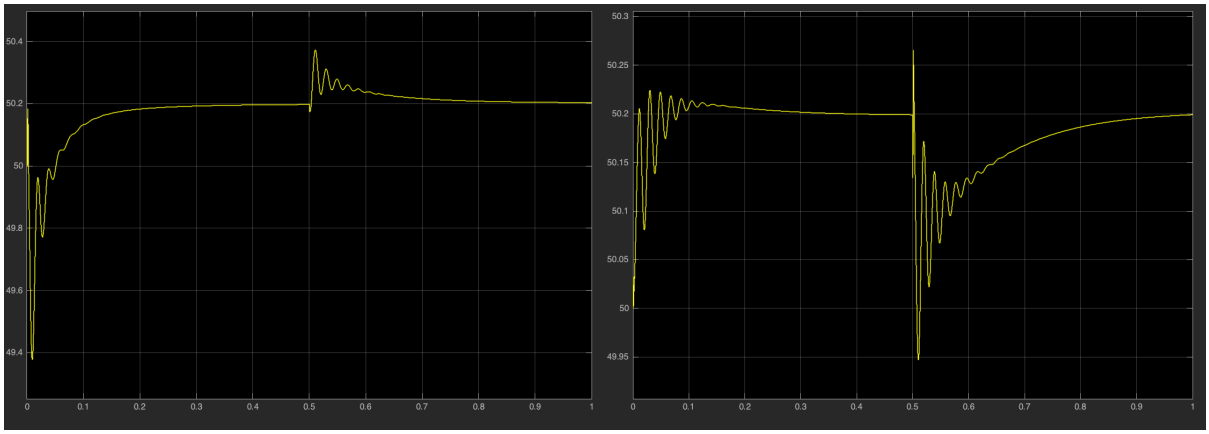

((a)) Inverter 1

((b)) Inverter 2

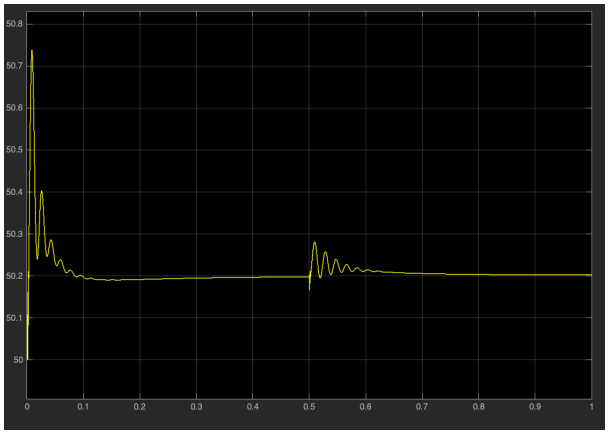

((c)) Inverter 3

Figure D.11: Frequency at the inverters with a distance of 5km

2.4 Distance of 10km

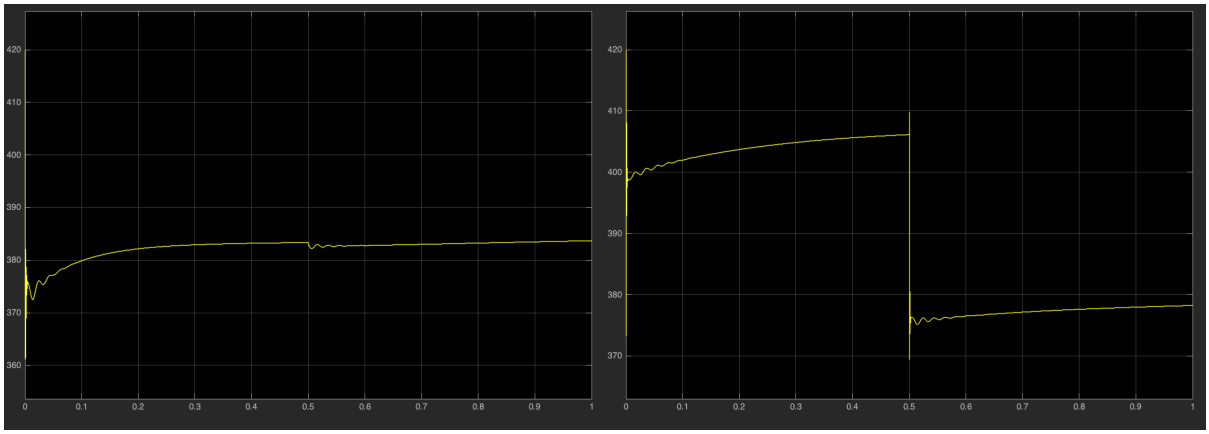

((a)) Inverter 1 ((b)) Inverter 2

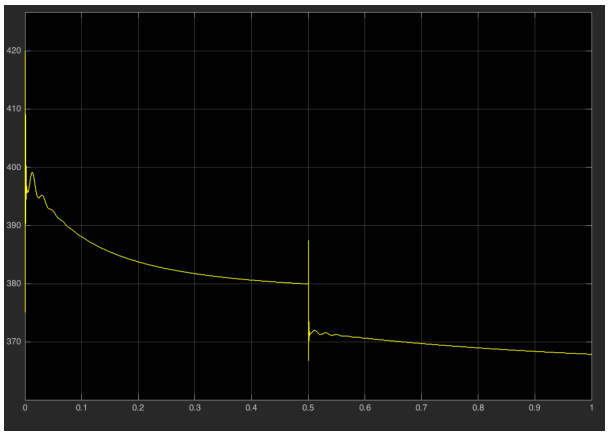

((c)) Inverter 3

Figure D.12: Average voltage at the inverters with a distance of 10km

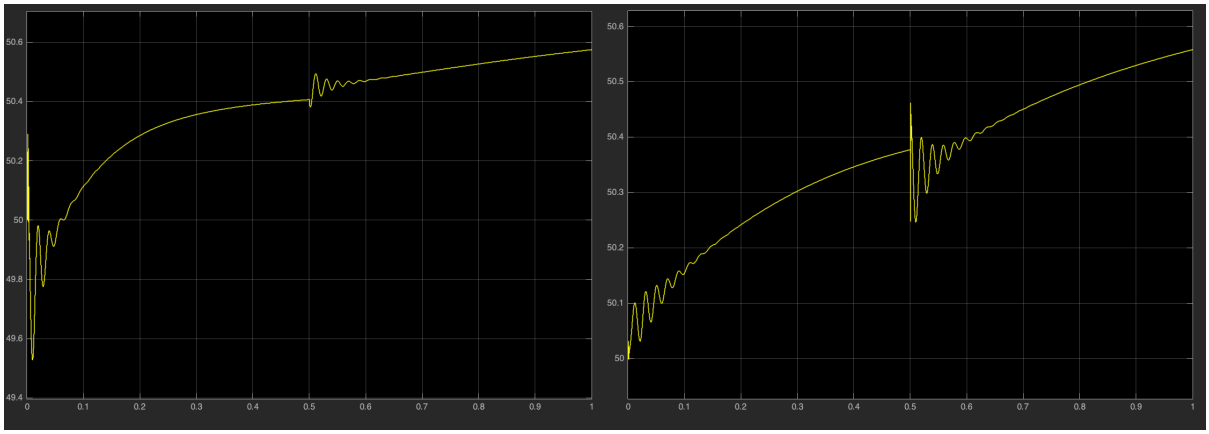

((a)) Inverter 1

((b)) Inverter 2

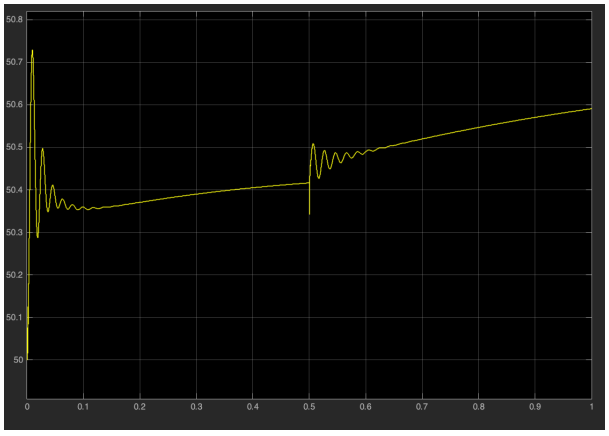

((c)) Inverter 3

Figure D.13: Frequency at the inverters with a distance of 10km

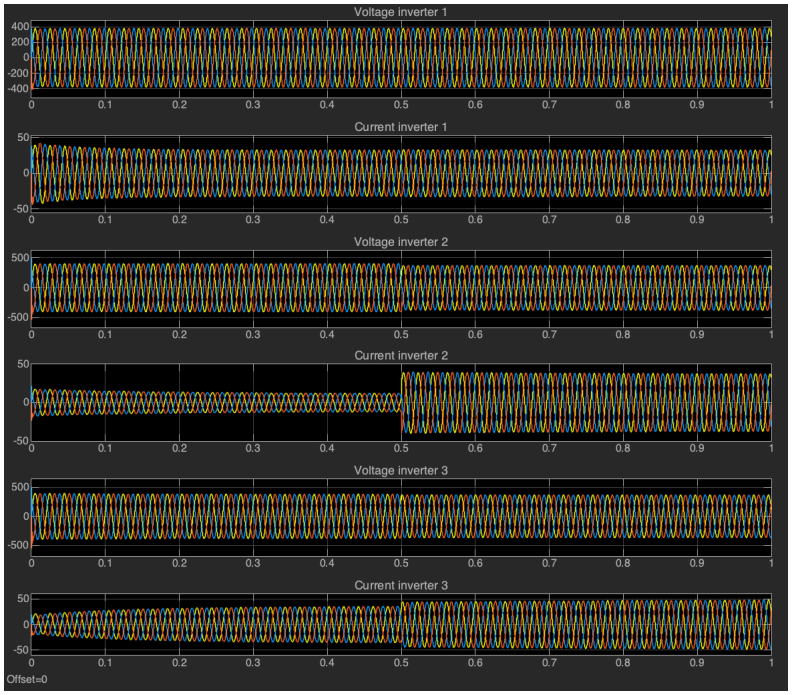

Figure D.14: Voltage and current at inverters with a distance of 10km

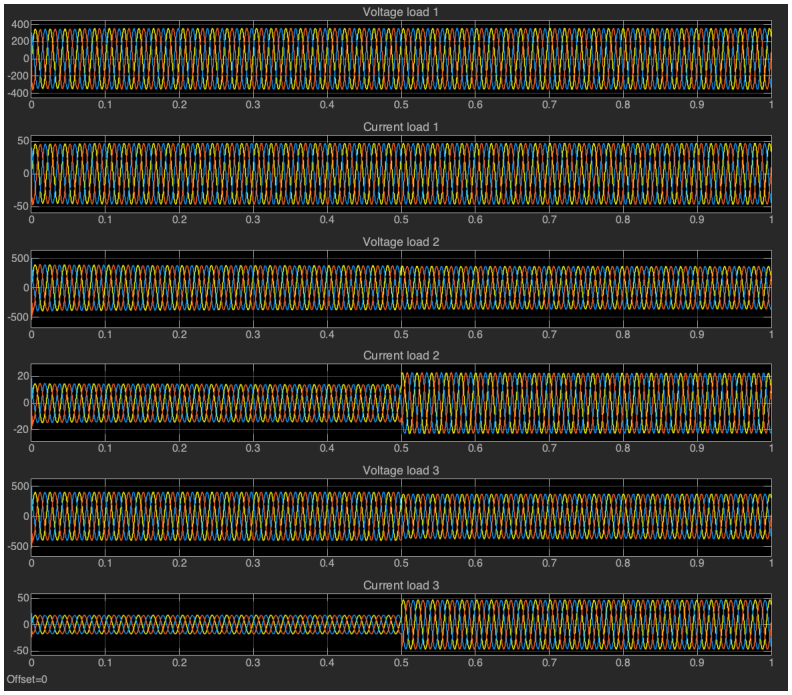

Figure D.15: Voltage and current at loads with a distance of 10km

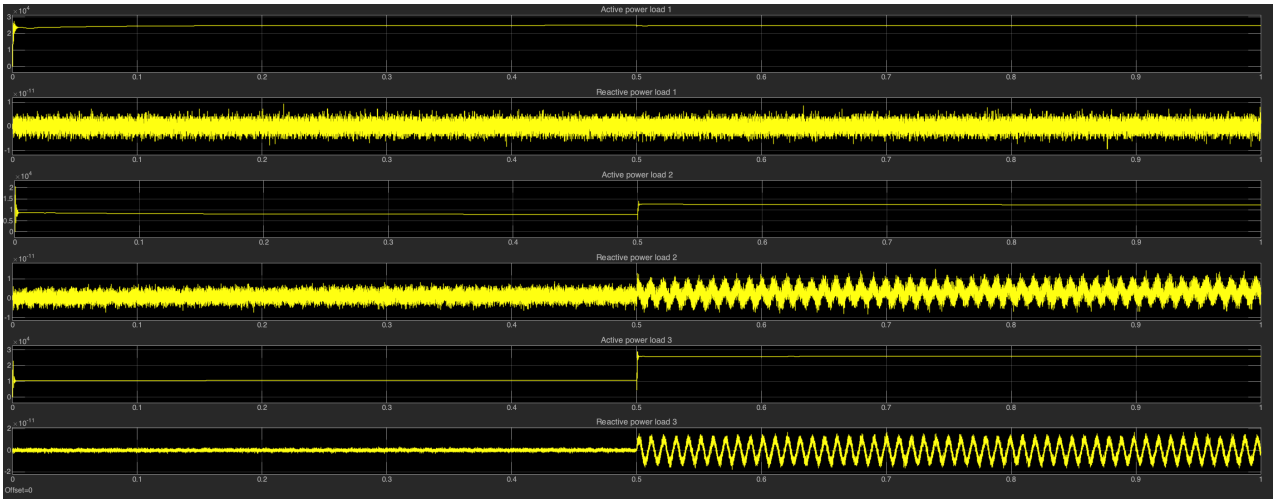

Figure D.16: Power at the inverters with a distance of 10km

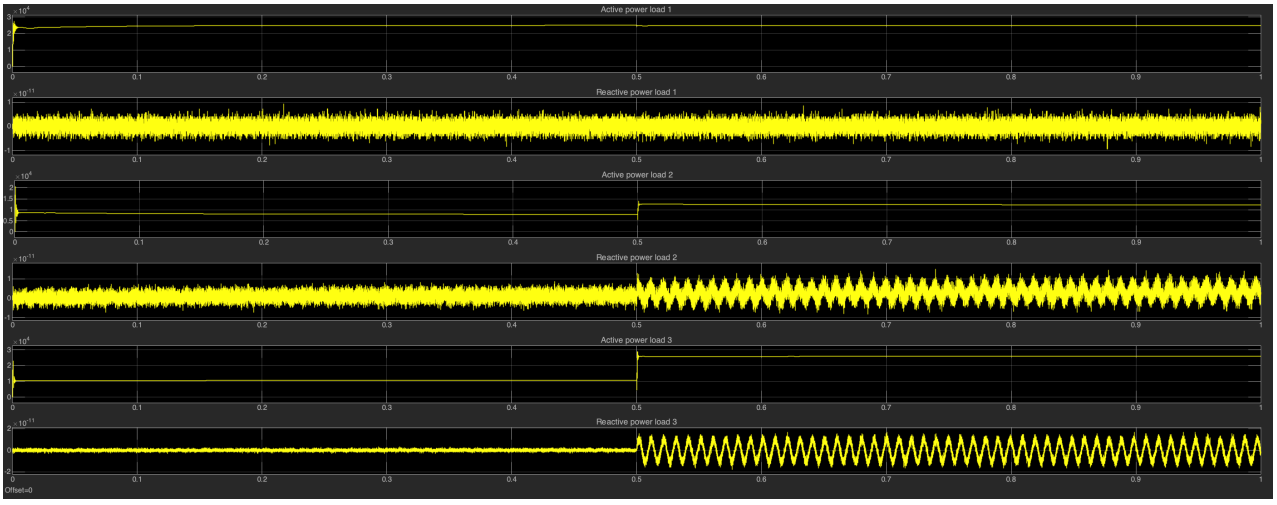

Figure D.17: Power at the loads with a distance of 10km

3 Capacitive loads

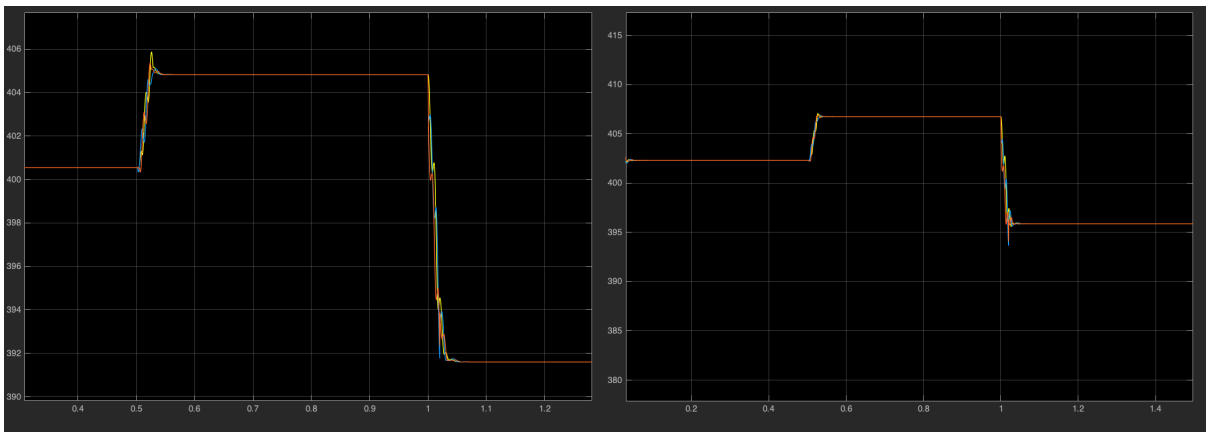

((a)) Inverter 1

((b)) Inverter 2

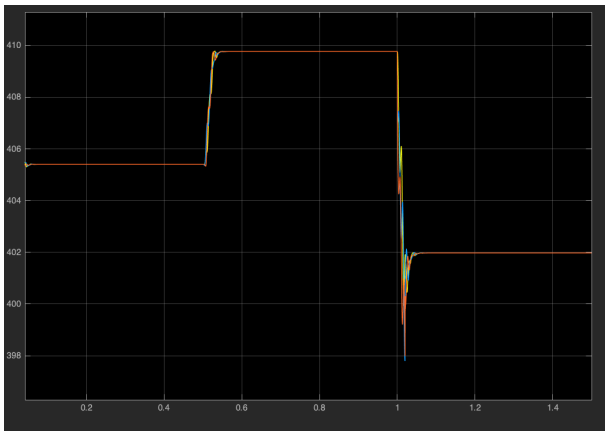

((c)) Inverter 3

Figure D.18: Average voltage at the inverters with capacitive loads

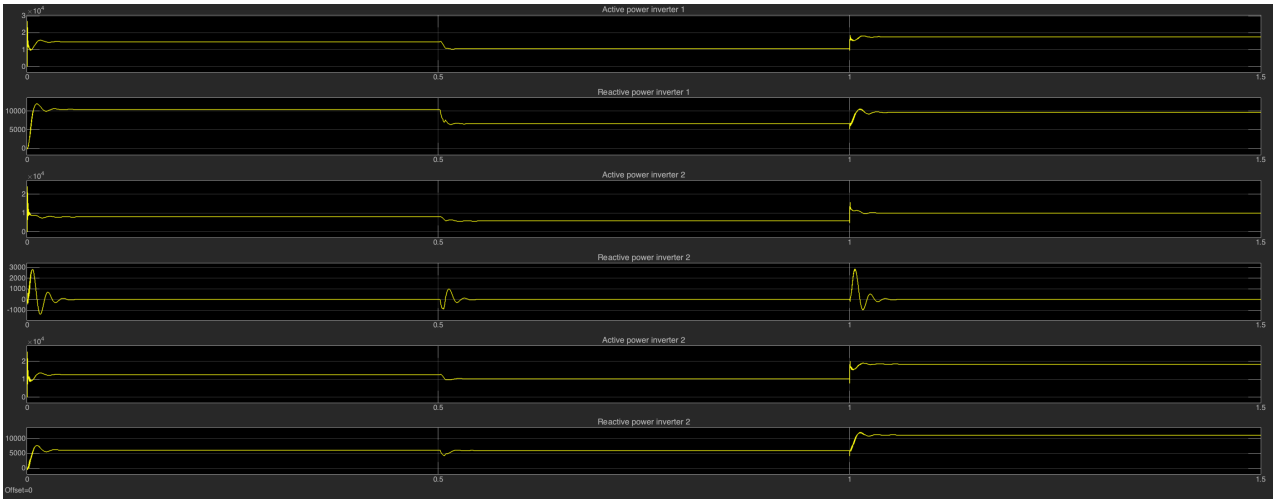

Figure D.19: Power at the inverter in case of capacitive loads

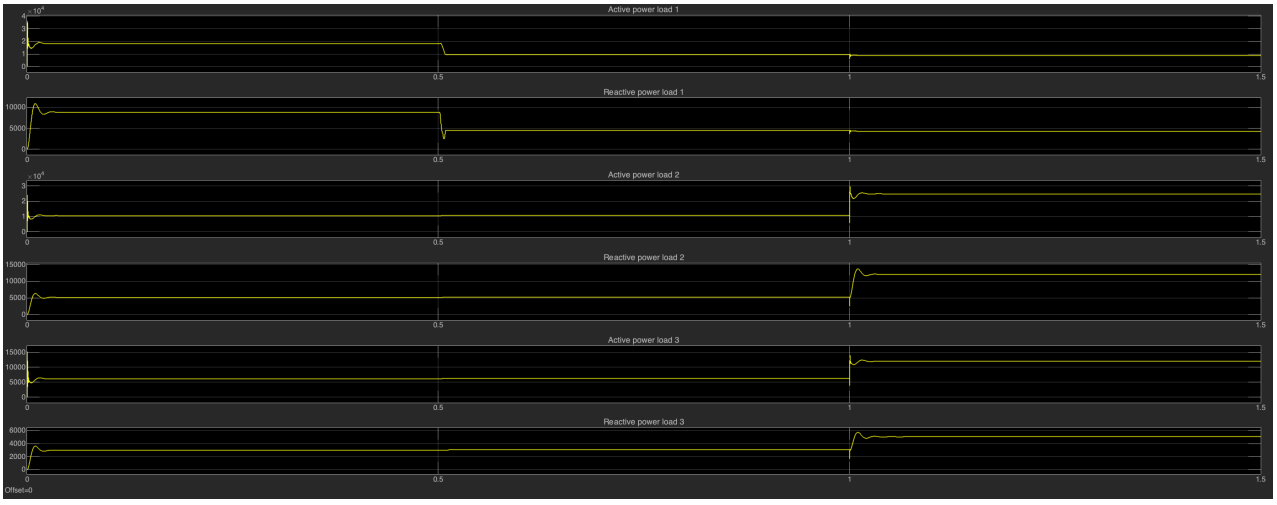

Figure D.20: Power at the capacitive loads

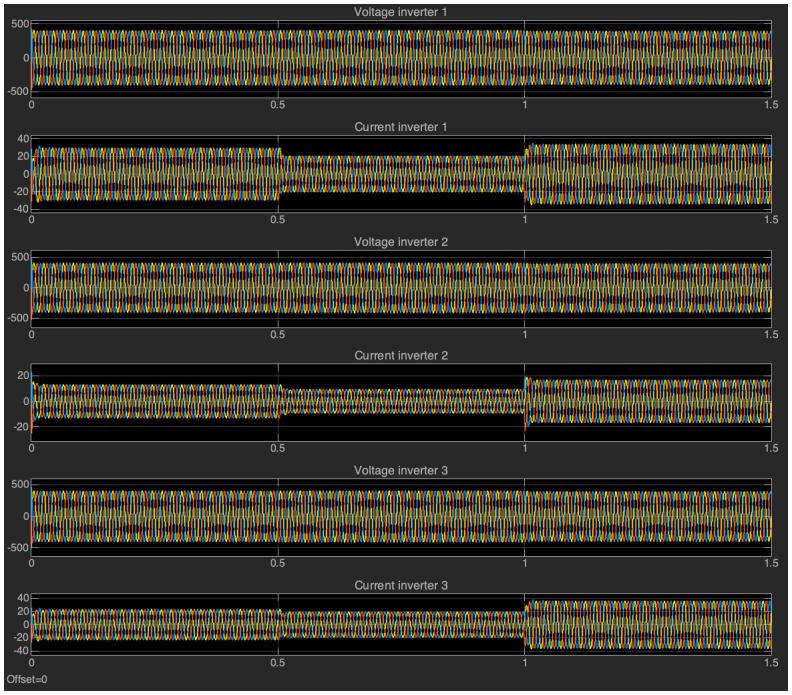

Figure D.21: Voltage and current at inverters with capacitive loads

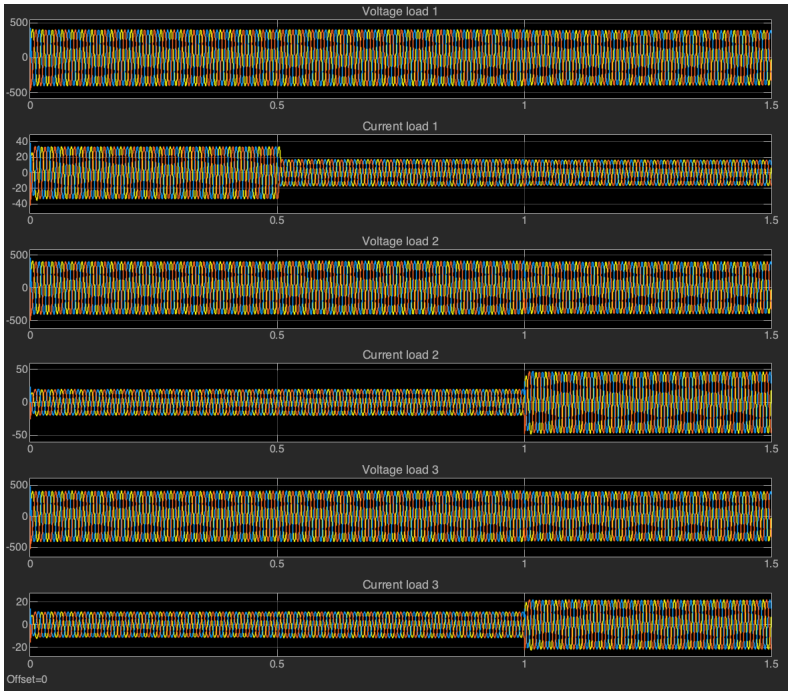

Figure D.22: Voltage and current at loads with capacitive loads

4 Inductive loads

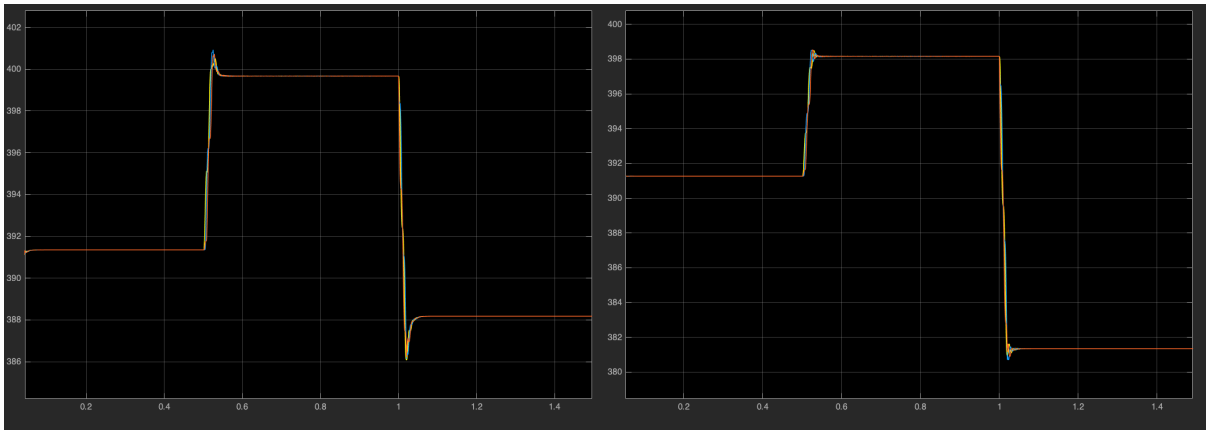

((a)) Inverter 1

((b)) Inverter 2

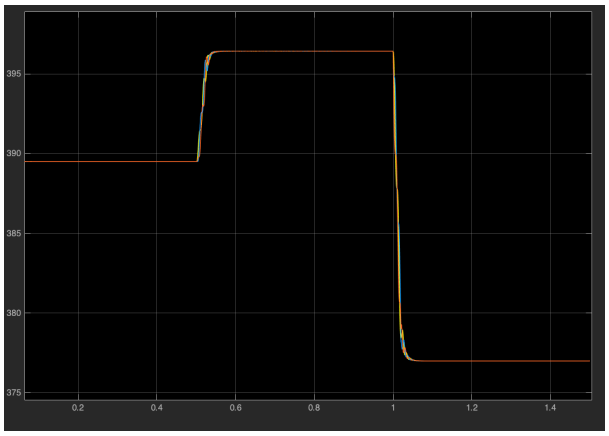

((c)) Inverter 3

Figure D.23: Average voltage at the loads with inductive loads

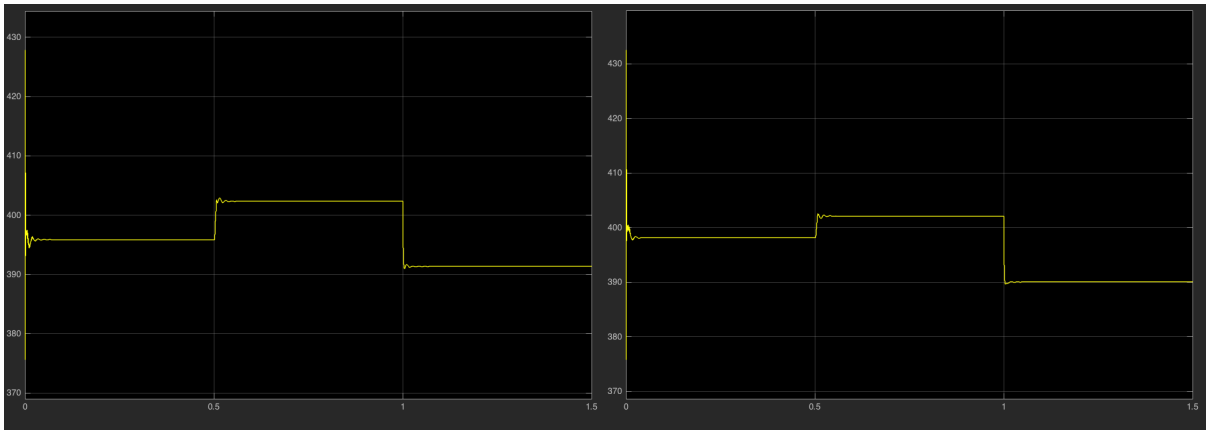

((a)) Inverter 1

((b)) Inverter 2

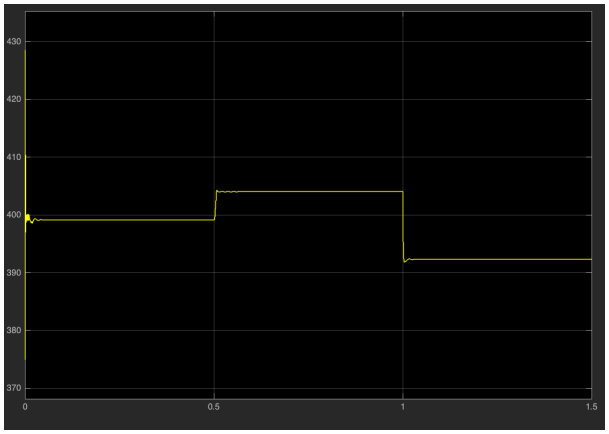

((c)) Inverter 3

Figure D.24: Average voltage at the inverters with inductive loads

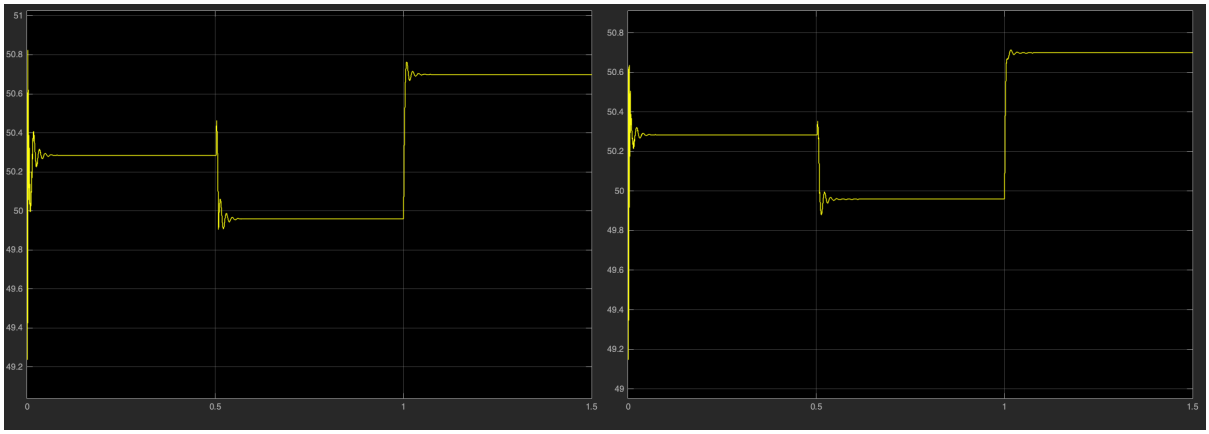

((a)) Inverter 1

((b)) Inverter 2

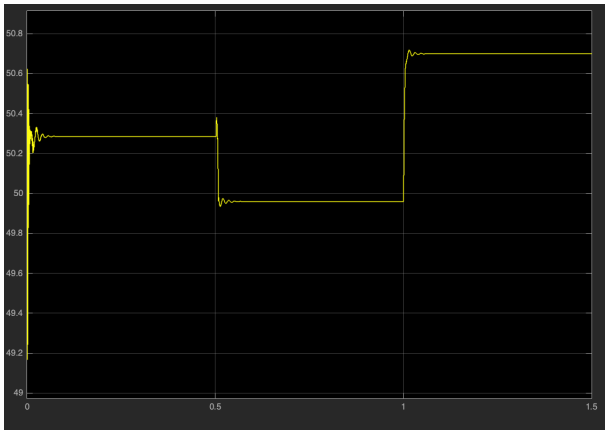

((c)) Inverter 3

Figure D.25: Frequency at the inverters with inductive loads

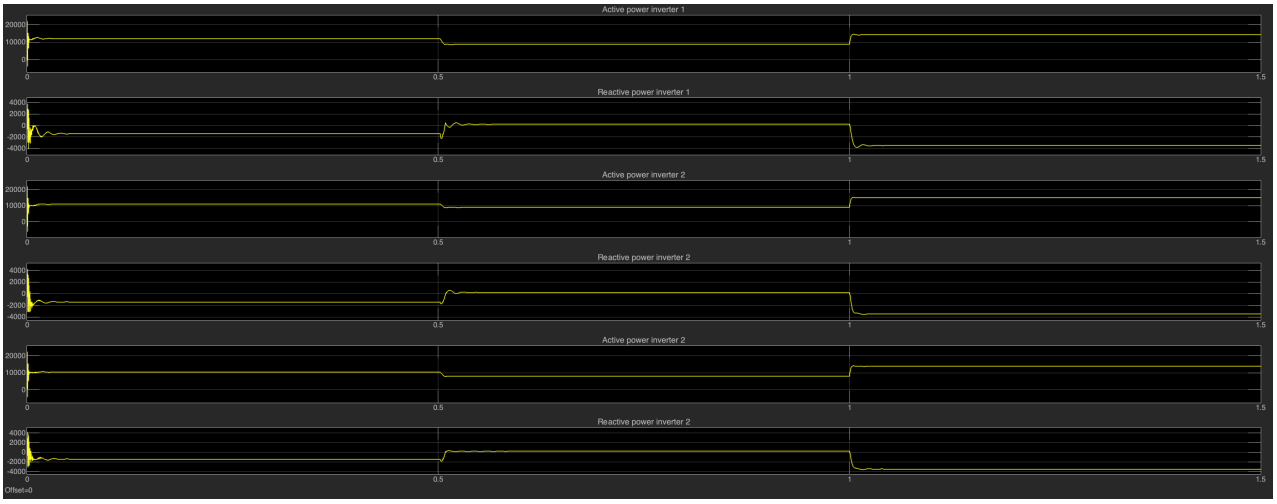

Figure D.26: Power at the inverter with inductive loads

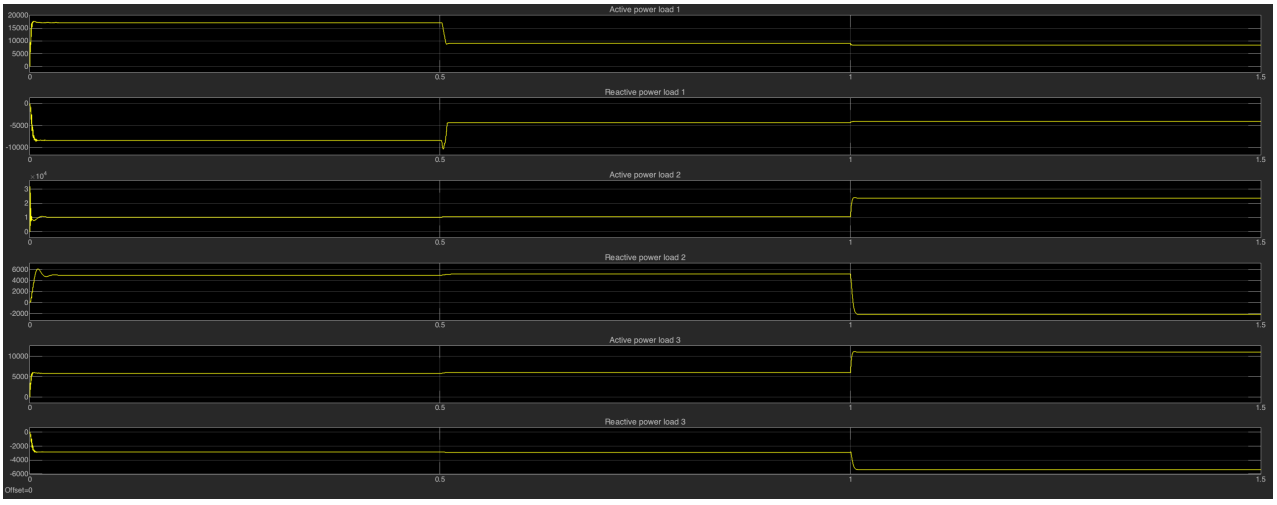

Figure D.27: Power at the loads with inductive loads

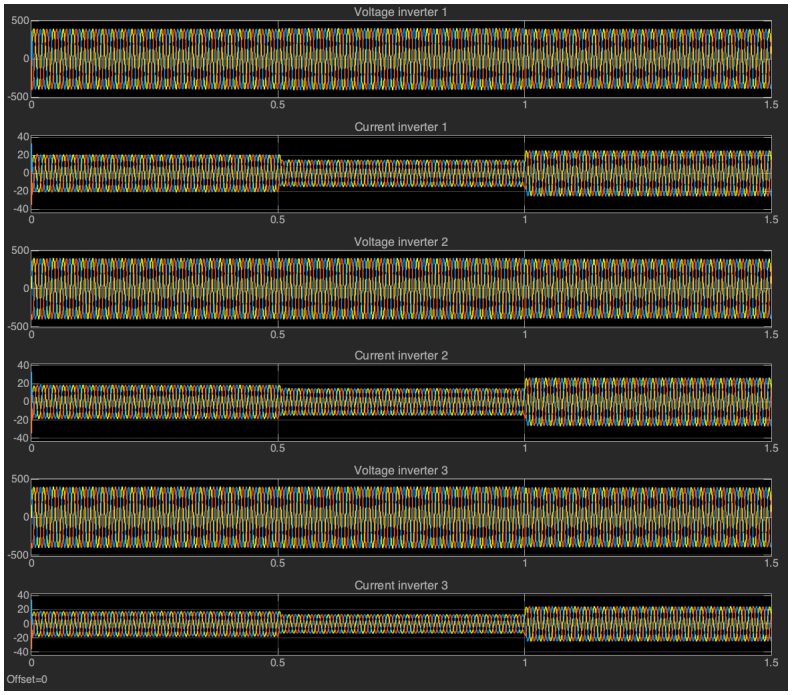

Figure D.28: Voltage and current at inverters with inductive loads

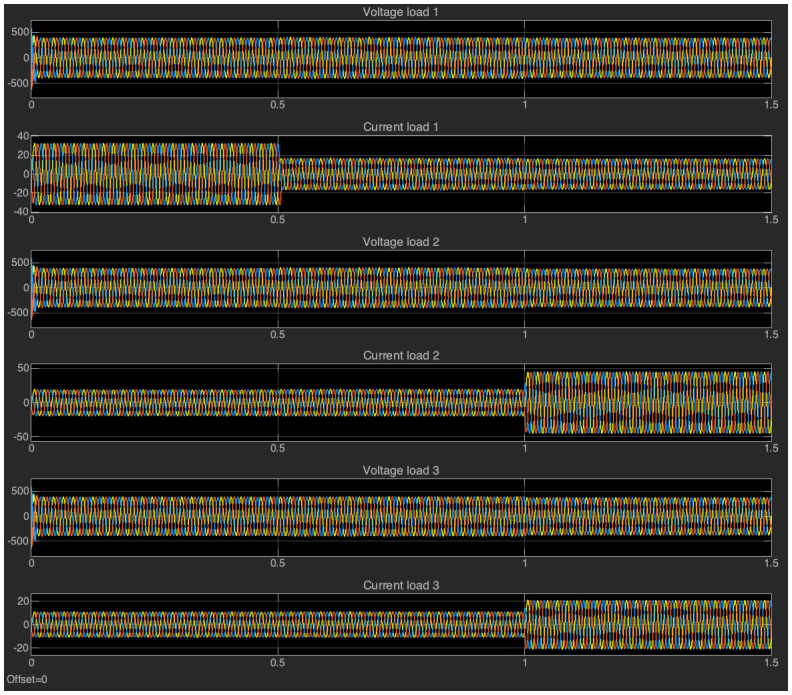

Figure D.29: Voltage and current at loads with inductive loads

Bibliography

[1] "Modeling, control and certification of an electric decentralized microgrid with random exogenous inputs and constrained information.", *Author: Jean DOBROWOLSKI*, May 2016
https://tel.archives-ouvertes.fr/tel-01825302/document

[2] "D'ici à 2040, la demande d'électricité devrait progresser de 60 %", *Author: Jean-Claude Bourbon*, 13/11/2018
https://www.la-croix.com/Economie/Dici-2040-demande-delectricite\-devrait-progresser-60-2018-11-13-1200982846

[3] "Li-ion energy storage takes microgrids to the next level", *Author: Michael Lippert* in Renewable Energy Focus Volume 17, Issue 4, July–August 2016, Pages 159-161
https://www.sciencedirect.com/science/article/pii/S1755008416300692

[4] "Global Market Outlook For Solar Power / 2018 - 2022", *Project manager lead author: Michael Schmela, SolarPower Europe*
http://www.solarpowereurope.org/wp-content/uploads/2018/09/Global-Market-Outlook-2018-2022.pdf

[5] Renewable energy > Integration into the energy system, from Wikipedia, the free encyclopedia for the academic journal, see Renewable Energy (journal).
https://en.wikipedia.org/wiki/Renewable_energy#Integration_into_the_energy_system

[6] "Renewables 2017, Analysis and Forecasts to 2022, executive summary", *Authors: IEA (International Energy Agency)* , 04/10/2017
https://www.iea.org/newsroom/energysnapshots/announced-wind-and-solar-average-auction-prices.html

[7] "Renewables, power and energy use forecast to 2050", *Authors: DNV GL – Energy Department*, 09/2017

http://www.ourenergypolicy.org/wp-content/uploads/2017/09/DNV-GL_-Energy-Transition-Outlook-2017_renewables_lowres-single_0109.pdf

[8] "How Energy Storage Works", *Authors: Union of councerned scientists*, last edited in February 2015
https://www.ucsusa.org/clean-energy/how-energy-storage-works

[9] "Illustrations Smart microgrids", *Authors: Cap interactif*, 2016
https://www.cap-interactif.com/reference/44_saft.html

[10] EDS official website, sharing on their current and coming microgrids projects
https://www.edsoforsmartgrids.eu/policy/eu-steering-initiatives/smart-grids-european-technology-platform/

[11] "Microgrid control: A comprehensive survey", *Authors: Sachidananda Sen, Vishal Kumar* for Annual Reviews in Control Volume 45, 2018, Pages 118-151
https://www.sciencedirect.com/science/article/pii/S1367578818300373

[12] "Microgrids: Non-exhaustive Review of Technical Issues", Powerpoint presentation shared by Emmanuel De Jaeger, March 2017
https://hosting.umons.ac.be/aspnet/journeeores2017/documents/Presentation_Emmanuel_DeJaeger.pdf

[13] "Master-slave control based reliable micro-Grid with back-to-back voltage source converter as master DG", *Authors: Girish G. Talapur ; H. M. Suryawanshi ; Amardeep B. Shitole*, published in December 2017
https://ieeexplore.ieee.org/document/8216056/references#references

[14] "Microgrid Power Converter Control With Smooth Transient Response During The Change Of Connection Mode", *Authors: Gustavo M. S. Azevedo, Marcelo C. Cavalcanti, Francisco A. S. Neves*, published in August 2014
https://www.researchgate.net/publication/326257315_Microgrid_Power_Converter_Control_With_Smooth_Transient_Response_During_The_Change_Of_Connection_Mode

[15] "A survey on control of electric power distributed generation systems for microgrid applications", *Authors: Allal M.Bouzidab Josep M.Guerreroc Ahmed Cheriti* for enewable and Sustainable Energy Reviews, January 2016
https://www.sciencedirect.com/science/article/pii/S136403211500026X

[16] More microgrids: “Advanced Architectures and Control Concepts for More microgrids”, FP6 STREP, Proposal/Contract no.: PL019864. 2006–2009.
http://www.microgrids.eu/documents/670.pdf

[17] "Comparison of Different Power Sharing Methods in AC-and DC-microgrid with Power Electronic Interfaced Distributed Generations", *Authors: Gholamreza Kadkhodaei,Mohsen Hamzeh*, May 2016
https://www.researchgate.net/publication/306097794_Comparison_of_Different_Power_Sharing_Methods_in_AC-and_DC-microgrid_with_Power_Electronic_Interfaced_Distributed_Generations

[18] "Review of primary control strategies for islanded microgrids with power-electronic interfaces", *Author: T.L. Vandoorn J.D.M. De Kooning B.Meersman L.Vandevelde* for Renewable and Sustainable Energy Reviews Volume 19, March 2013, Pages 613-628, May 2012
https://www.sciencedirect.com/science/article/pii/S1364032112006764

[19] "Hierarchical control structure in microgrids with distributed generation: Islandand grid-connected mode." *Authors: Omid Palizban, Kimmo Kauhaniemi*, Available online 28 January 2015
https://www.sciencedirect.com/science/article/pii/S1364032115000180

[20] "Microgrids Operation Based on Master-Slave Cooperative Control", *Authors: Tommaso Caldognetto, P. Tenti* in IEEE Journal of Emerging and Selected Topics in Power Electronics 2(4):1081-1088, December 2014
https://www.researchgate.net/publication/287510140_Microgrids_Operation_Based_on_Master-Slave_Cooperative_Control

[21] "Secondary Droop for Frequency and Voltage Restoration in Microgrids", *Authors: Inam Ullah Nutkani, Wang Peng,Loh Poh Chiang, Frede Blaabjerg*, added online 29 October 2015
https://ieeexplore.ieee.org/document/7309457

[22] "Control techniques of Dispersed Generators to improve the continuity of electricity supply", *Authors: Stefano Barsali, Massimo Ceraolo, Paolo Pelacchi, Member, IEEE, Davide Poli*, February 2002
https://www.researchgate.net/publication/3937124_Control_techniques_of_Dispersed_Generators_to_improve_the_continuity_of_electricity_supply

[23] "Virtual negative impedance droop method for parallel inverters in Microgrids", *Authors: Guolian Hou,Fulin Xing,Yu Yang,Jianhua Zhang*, June 2015
https://www.researchgate.net/publication/308821538_Virtual_negative_impedance_droop_method_for_parallel_inverters_in_microgrids

[24] "Improved Droop Control of Isolated Microgrid with Virtual Impedance", *Authors: Haoming Liu, Yi Chen, Shanshan Li*, added online 25 November 2013
https://ieeexplore.ieee.org/document/6672849

[25] "Conventional and Reverse Droop Control in Islanded Microgrid: Simulation and Experimental Test", *Authors: Alberto Villa, Federico Belloni, Riccardo Chiumeo, Chiara Gandolfi*, added online 01 August 2016
https://https://ieeexplore.ieee.org/document/7526020

[26] "Control and analysis of droop and reverse droop controllers for distributed generations", *Authors: Dan Wu, Fen Tang, Juan C. Vasquez, and Josep M. Guerrero*, September 2014
https://www.researchgate.net/publication/265552736_Control_and_analysis_of_droop_and_reverse_droop_controllers_for_distributed_generations

[27] "Power quality and stability analysis during islanded mode operation in a microgrid based on master-slave configuration", *Authors: R. Garde ; S. Casado ; M. Santamaria ; M. Aguado*, published in 2015 Saudi Arabia Smart Grid (SASG), 2015
https://ieeexplore.ieee.org/stamp/stamp.jsp?tp=&arnumber=7449288

[28] "A Benchmark Low Voltage Microgrid Network", *Authors: Stavros Papathanassiou, Nikos D. Hatziargyriou*, January 2015
https://www.researchgate.net/publication/237305036_A_Benchmark_Low_Voltage_Microgrid_Network

[29] "LCL filter design for photovoltaic grid connected systems", *Authors: A.E.W.H. Kahlane, L. Hassaine and M. Kherchi*, published in 2014
https://www.cder.dz/download/sienr2014_31.pdf

[30] "Modeling and control of master-slave microgrid with communication delay", *Authors: Asma Alfergani, Ashraf Khalil*, added on IEEE xplore on 15 May 2017
https://ieeexplore.ieee.org/document/7926049

[31] "Spellman APPLICATION NOTES - HIGH VOLTAGE POWER SUPPLIES", *Authors: Spellman High Voltage Electronics Corporation*, 01/13/16

https://www.spellmanhv.com/en/Technical-Resources/Application-Notes-HVPS/AN-21

[32] "Defining Control Strategies for MicroGrids Islanded Operation", *Authors: J. A. Peças Lopes, Senior Member, IEEE, C. L. Moreira and A. G. Madureira*, October 2013
https://www.researchgate.net/publication/3267593

[33] "Modified Droop Control for Low Voltage Single Phase Isolated Microgrids", *Authors: Lucas S. Araújo, Dante I. Narváez, Thais G. Siqueira, Marcelo G. Villalva*, October 2016
https://www.researchgate.net/publication/311610357_Modified_droop_control_for_low_voltage_single_phase_isolated_microgrids

[34] "A review of droop control techniques for microgrid", *Authors: Usman Bashir Tayaba, Mohd Azrik Bin Roslana, Leong Jenn Hwaia, Muhammad Kashifa*, 2017
Renewable and Sustainable Energy Reviews 76 (2017) 717-727

[35] "Simulation for parallel operation of inverters with frequency and voltage droop control", *Authors: Kapil Duwadi, Hemanta Bhandari, Pratigya Shrestha, Hari Surya Tiwari*, July 2015
https://www.researchgate.net/publication/280044192

[36] "Networked Control of AC Microgrid", *Authors: Asma Alfergani, Ashraf Khalil,Zakariya Rajab* in Sustainable Cities and Society, January 2018
https://www.researchgate.net/publication/317565117_Networked_Control_of_AC_Microgrid

[37] "Microgrids Operation Based on Master-Slave Cooperative Control", *Authors: Tommaso Caldognetto, P. Tenti* in IEEE Journal of Emerging and Selected Topics in Power Electronics 2(4):1081-1088, December 2014
https://www.researchgate.net/publication/287510140_Microgrids_Operation_Based_on_Master-Slave_Cooperative_Control

[38] "Basic Concepts and Control Architecture of Microgrids", *Authors: David Wenzhong Gao*, published in Energy Storage for Sustainable Microgrid, 2015
https://www.sciencedirect.com/topics/engineering/microgrid-control

UNIVERSITÉ CATHOLIQUE DE LOUVAIN
École polytechnique de Louvain
Rue Archimède, 1 bte L6.11.01, 1348 Louvain-la-Neuve, Belgique | **www.uclouvain.be/epl**